Electrical Stochastic Resonance System

Design of a miniaturised electrical stochastic resonance device

Flinders University
Shannon Deale 213719
October 2018

Submitted to the College of Science and Engineering in partial fulfilment of the requirements for the degree of Bachelor of Engineering (Biomedical) (Honours), Master of Engineering (Biomedical) at Flinders University - Adelaide Australia

Supervised by:
Dr Ben Patritti, Nigel Kelly, Dr Olivia Lockwood & Assoc. Prof Kenneth Pope

Declaration

I certify that this work does not incorporate without acknowledgment any material previously submitted for a degree or diploma in any university; and that to the best of my knowledge and belief it does not contain any material previously published or written by another person except where due reference is made in the text.

Acknowledgments

I wish to express my appreciation and gratitude towards the people who have contributed to and helped me throughout this project.

Dr Ben Patritti from Adelaide's Repatriation Hospital has provided an immense amount of support in all aspects of this project. Spending many days and likely late nights helping me improve my writing and presentation skills. Ben gave more feedback and notes than I believe I've ever seen before and I believe this is a compliment. His commitment to being hands on and helping students improve their academic skills is admirable and greatly appreciated. There was never a moment that Ben was unwilling to help me when I asked and for this and everything you taught me, I will honestly forever be grateful.

Dr Olivia Lockwood of South Australia Biomedical Engineering's state-wide Research and Teaching team for providing encouragement, industry and project advice, direction and the resources to work on this project. I was always made to feel comfortable and welcomed in SA BME and Olivia was always willing to answer my "quick questions" (unfortunately they never really were). Olivia has my thanks for providing such a fantastic experience that I personally feel I learned a great deal from.

Associate Professor Kenneth Pope for the incredible words of wisdom and encouragement every week throughout the course of this project. Kenneth at one-point light heartedly referred to our weekly meetings as "our weekly therapy sessions". Kenneth was a grounding force when I was feeling overwhelmed, stressed or discouraged and he provided ways of thinking or analogies that helped me gain perspective as an engineer. Without Kenneth's contributions this project would not have been the same.

The time, effort and guidance of Nigel Kelley was invaluable. He helped me understand electronics concepts such as electrical isolation or good practices in PCB design in an intuitive way. I will never forget breaking open a capacitor so that we could inspect the physical components and understand how these relate to the mathematics. He was patient with the many questions (especially during your lunch breaks) I asked are greatly appreciated. The real-world experience I learned from him has already made me a better engineer and for that I can't thank Nigel enough.

Abstract

The term stochastic resonance (SR) has been commonly used to describe the positive effect the presence of a level of randomised signal (noise) has on the performance of a non-linear (threshold-based) system. The somatosensory system is a threshold-based system that is essential to everyday life for most people and allows people to independently and effectively traverse or interact with the environment with little conscious effort. The sensitivity of the somatosensory system is known to deteriorate due to advanced age or certain neurological diseases. The objective of this project was to design and develop a prototype system that can deliver a random electrical stimulus (in the form of pseudo-white Gaussian noise) to sites on the body via electrodes to facilitate SR effects in enhancing the sensitivity of the somatosensory system.

This project was undertaken to improve upon a previous prototype device of similar function that was considered too big to be sufficiently portable and did not have high enough voltage output to sufficiently deliver 1mA through typical skin impedance. The project intended to yield a device that had a much higher voltage output as well as being much smaller (increasing wearability). It was determined that a completely new design would best facilitate these improvements. Working towards this aim the objectives of this project involved the development of electronic circuitry that included a high voltage power supply unit (HVPSU), high voltage current pump (HVCP), microcontroller, digital-to-analogue converter, level shifter and a wireless transmitter/receiver. Additionally, the project required using software to develop a graphical user interface (GUI) and signal generation software to produce the pseudo-white Gaussian noise signal.

Several milestones towards the objective of this project have been achieved. The design of the electronic circuitry, including the HVPSU, HVCP and control circuitry, that realises the concept for the device has been completed. Printed circuit boards (PCBs) have been designed for the HVPSU and HVCP based on thorough breadboard testing of the two circuits (the results of which matched data reported for similar circuits documented in literature), making them ready for immediate manufacture. All the components for the PCBs have been identified and budgeted for. The design considerations and testing for the control circuitry has also been completed, ready for the design of a PCB. Finally, the main functional components of the software have also been developed. Significant work has been completed across all the major components within this system. All that remains is to combine them into a functioning prototype. The long-term aim is that the system will be used in a clinical research setting enabling the investigation of potential benefits from prolonged use of SR stimulation, hopefully leading to improved function and quality of life.

Table of Contents

List of Figures

List of Tables

1   Introduction

The term '*noise*' in an engineering context is a general term that typically describes any signal or disturbance that a system is unintentionally sensitive to and which may negatively impact the performance of the system. Under this broad definition noise can constitute a wide variety of phenomena, from electromagnetic interference in circuitry caused by power lines, to muscle activity interfering with an electroencephalogram measurement. Noise may have a repeating pattern or be random. In most engineering contexts noise carries a negative connotation. This is because historically metrics such as a signal to noise ratio (SNR) are used to measure system performance (with noise being considered the detrimental factor to performance). There is evidence, however counterintuitive it seems, that noise can, in certain contexts such as non-linear systems, enhance the system performance. Non-linear systems are common among human physiological systems such as sensory neurons which require the stimulation of threshold-based receptors to transmit information through the nervous. Linear systems have not been observed to receive benefit from noise [1].

One such context in which noise can be beneficial is the phenomenon of stochastic resonance (SR). The term SR has been commonly used to describe the positive effect the presence of a particular, non-zero level of a random signal (noise) has on the performance of a non-linear (threshold-based) system. This is typically characterised by improved processing or transmission of a signal (i.e. information) by the system [2-4]. SR was studied principally by physicists for over 25 years. Recently, this field has seen growing interest among biologists, neurophysiologists and engineers of various disciplines toward understanding and applying it in a range of non-linear systems be they naturally occurring (i.e. biological) or designed (i.e. electric circuitry)[1, 5]. For example, SR effects were first investigated as a plausible explanation for the recurrence of Earth's ice ages [11] but have since been demonstrated in a range of systems including animal physiological systems [6-10], human physiological systems [2-4, 11, 12] and electronic circuitry [13-15].

Most SR effects in different physiological systems have been demonstrated through the addition of external input noise into the system [2-4]. This is pertinent to the current project because it supports the development and efficacy of biomedical devices designed to deliver noisy input signals to enhance the performance of physiological systems within the body [4, 16, 17]. A focus of past and present work has been on using noise to enhance the sensitivity of the body's somatosensory system which conveys information about touch and proprioception [18-20]. Previous work with this focus has achieved SR effects by introducing either mechanical noise via small actuators delivering low level (milliNewton sized) random amplitude vibrations or electrical noise via electrodes delivering low level (microAmperes) random current stimulation [21, 22]. Interestingly, some of this work has demonstrated cross modal effects whereby electrical noise has been shown to enhance the detection of mechanical stimuli [23-25]. This is an important design consideration as mechanical actuators (that produce the vibration noise) are often more expensive and power consuming than electrodes.

Almost all systems to date demonstrating SR effects with somatosensation have been desktop-based systems [2, 6, 7, 16, 19, 21-23, 26-31]. To further investigate the long-term benefits of SR effects achieved via the delivery of electrical noise to the body more portable and wearable systems are necessary. A portable mechanical system in the form of vibrating insoles has been proposed and developed by different researchers [32-34] based on early work by Priplata et al. [16, 21, 35]. Currently there are no reports of a portable system for the application of noisy electrical stimulation. Recent work has outlined design considerations for

elements of the circuitry of such systems [36, 37], however these lacked the integration of a microcontroller, control software and a user interface. As such a complete, portable electrical system for delivering low-level noise input signals has not been documented to date.

A wearable system for home use, delivering low level noisy electrical stimulation could potentially be used by individuals with somatosensory deficits due to aging or certain neurological diseases (e.g. diabetes mellitus, stroke). The deterioration of the somatosensory system can impact fine touch and vibrotactile perception and proprioception (i.e. the sense of limb position). In addition to vision and vestibular inputs these somatosensory inputs are important for the control of balance, so any deterioration in somatosensation can contribute to an increased risk of loss of balance and falls. The potential for a SR device as an adjunct to therapeutic interventions such as balance training is promising but requires further investigation as most studies to date have only demonstrated an acute benefit from SR mediated effects (i.e. enhanced sensation or performance with input noise, with a return to baseline with no input noise). A compact portable system delivering low level noise stimulation that can be used continuously for prolonged periods. This would enable an investigation of potential long-term benefits mediated by SR effects on somatosensory function and associated neuroplastic changes of the nervous system.

2   Project Motivation

According to the Australian Bureau of Statistics, 15% of Australians were aged 65 and over in 2017 [44], and this is predicted to rise to 20% by 2037 [44] (shown in Figure 1). This expected increase in the number of older adults only highlights that any problems associated with age related deficits in function will become an increasing problem for Australia's health system in the future. For example, deterioration in tactile sensation, muscle strength, reaction time, vestibular function, and vision can all occur as a result of ageing [28, 38-40]. These impairments can affect an elderly individual's balance and increase their risk of falling, and the likelihood of sustaining a fall related injury.
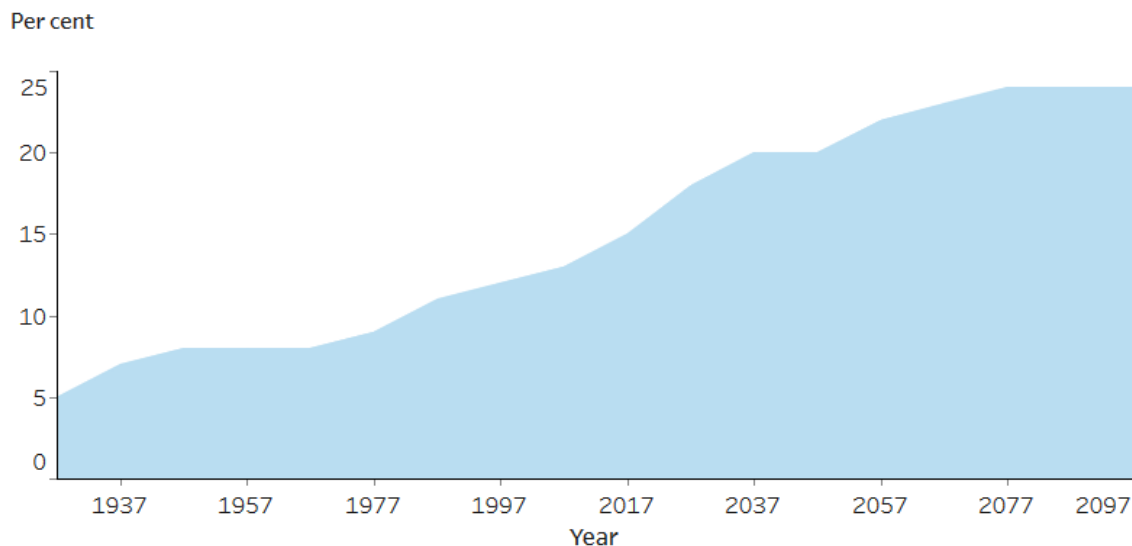
Figure 1 Proportion of the Australian population aged 65 and older over time [44].

It was estimated that between 2009 and 2010 that 83,768 people aged 65 and over were hospitalised in Australia due to injuries associated with falls. Between 2012 and 2013 that number had risen to an estimated 98,704 incidents [41, 42]. During the years of 2006 and 2007 in New South Wales alone it was estimated that the cost of healthcare associated with age related falls was $558.5 million, and it is predicted that by 2051 that cost will increase to $1375 million per annum [43, 44]. With its high incidence and associated cost, it is clear that

this presents a significant issue for the Australian healthcare system. An individual's risk of falling is multifactorial [45, 46]. Sensorimotor, visual, and cognitive impairments and environmental hazards can all contribute to a person's risk of falling [46]. Among the sensorimotor factors is deterioration of the somatosensory system.

The somatosensory system provides feedback to the central nervous system about mechanical stimuli such as touch, vibration, pressure and skin stretch, muscles and connective tissues based on signals from exteroceptors, proprioceptors and interceptors of the body. Each of these combine to form the body's sense of the external environment, limb and body position as well as visceral conditions [47, 48]. The somatosensory system comprises the senses of touch and proprioception that are essential to everyday life for most people and allow people to independently and effectively traverse or interact with the environment with little conscious effort. The sensitivity of somatosensory systems is known to deteriorate due to advanced age or certain neurological diseases [21, 35, 40, 49].

Ageing isn't the only cause of such deficits. Certain neurological conditions such as diabetes mellitus or cerebrovascular accident (stroke) can also impair the structure and function of the somatosensory systems [35, 38, 48, 50-53]. For those unfortunate enough to have suffered a stroke it has been observed that somatosensation declines significantly in 65% of cases [53]. Individuals with diabetes also experience somatosensory deficits due to an increase in sensory thresholds of their mechanoreceptors and changes in the afferent neurons, effecting signals travelling to the central nervous system [35, 48, 52]. This leads to diminished sensory feedback information from the afferent periphery sensory system [53].

With an ageing population in Australia that is predicted to rise in the future as well as the increasing incidence of diabetes mellitus, the number of individuals with impaired somatosensation is likely to only increase [54, 55]. The loss of these senses is a risk factor for increased falls and causes serious detriment to an individual's quality of life in terms of health and independence, making it a serious healthcare problem. The development of a portable, wearable system (or device) which can exploit SR effects in the somatosensory system via the delivery of low-level electrical input noise to the body may offer a solution to this problem.

3   Project Aim

Although stochastic resonance has been studied principally by physicists for over 25 years, there is growing interest among engineers and this field of study stands to gain a great deal from devices such as the one being designed and developed in this project [1]. Devices that enable the safe application of electrical (or mechanical) noise signals to the body with the purpose of enhancing signal processing in various physiological systems such as tactile sensation or balance control [22, 35] may be extremely valuable in the future. Furthermore, such a device that is portable will enable experimental investigations to assess potential benefits from prolonged periods of home use.

The aim of the project was to design and develop a prototype system that was capable of delivering a random electrical stimulus (pseudo-white Gaussian noise) to the body via electrodes. This will facilitate SR effects, subsequently increasing the sensitivity of the somatosensory system. The system needed to allow for the adjustment of the amplitude of the electrical noise stimulus via a user interface and the testing of the stimulus to establish an individual's sensory threshold to the stimulus. Once the desired sub-sensory level of the

noise stimulus was set, the system would need to be able to deliver the noise stimulus for a prolonged period (e.g. up to 8 hours).

The prototype was aimed at proving the concept for use in a research setting from which it could evolve into a commercial product. As the device was intended for use in a research setting it did not need to be listed with the TGA prior to use (nor does it require any TGA approval). However, ethically as the manufacturer it is our responsibility to ensure that the system is safe and suitable for use with human subjects.

This project improved upon a previous prototype device with a similar function which required a redesign to make the system portable (ideally wearable) and improve its performance. The project should yield a device that has superior performance, as well as being much smaller (increasing wearability). Lessons learned from the previous device were used to guide the decision making in this project. Results relating to the previous system were used as a benchmark from which to measure improvements in performance of the newly designed system.

3.1 Identification of Design Requirements and Specifications

The following is from the project specification document (see Appendix X) which was discussed and developed with the client Dr Ben Patritti.
General specifications:

- The stimulation device should be non-invasive, portable, compact and lightweight such that the user can comfortably wear the device in a cuff on their arm or leg.
- The stimulation device should have up to 8 electrodes (4 pairs) and a minimum of 4 electrodes (2 pair)
- The stimulation device should be battery powered and rechargeable with a battery life of 8-10 hours. The device may possibly require a separate charging circuit due to size/ weight constraints.
- Generate and deliver an electrical noise signal (although mechanical noise could be considered and avenues for its later implementation left available)
- The system must enable the user to determine the sensory threshold of noise stimulus for a particular individual (and more specifically a particular site on the body).
- The system should have a graphical user interface (GUI) that is wirelessly operated by a paired personal computer (PC) with a dedicated software application.
- The stimulation device should be able to deliver electrical stimulus to multiple parts of the body (mostly to the skin, and skin overlying the joints, tendons and ligaments) with a target 'typical' impedance of 60kΩ.
- The stimulation device should not exceed a maximum current of 1mA delivered to any load impedance.
- The stimulation device should be capable of delivering noise stimulation at a range of levels which can be perceived by healthy adults with normal sensation and adults with impaired sensation due to disease e.g. people with diabetic neuropathy, stroke and multiple sclerosis.

Electrical noise specifications:

The electrical noise specifications were determined from a review of the literature, the following is the conventional approach for generating stimulus signals for SR applications.

- The noise signal should be random pseudo-white Gaussian noise.
- The amplitude of the noise signal should be zero mean with the capability to alter the maximum amplitude via adjustments to the standard deviation of the noise signal.
- The frequency range of the noise signal should be between 0 to 1000 Hz

3.2   Project Objectives

Based on the aim of the project, the requirements and specifications identified in discussion with the client and drawbacks of the previous prototype system the following project objectives were defined:

1. Design and develop electronic circuitry that enables the system to meet the specifications. The circuitry should consist of:
   - A high voltage power supply unit (HVPSU) capable of delivering at least 60V
   - A high voltage current pump (HVCP) modified from a standard Howland current pump design that can deliver a load current of 1mA.
   - A microcontroller and digital to analogue converter (DAC) combination that can drive the stimulation signal.
   - A level shifter circuit that converts the positive DAC input into an output that can swing positive or negative (necessary for the function of a Howland current pump).
   - A wireless communication module that enables communication between the device and a PC.
   - A rechargeable battery that powers the device for 8-10 hours.

2. Design and develop software consisting of two parts:
   - A GUI that enables the device to be wirelessly operated. This interface must enable the user to determine the sensory threshold of noise stimulus for a particular individual (and more specifically a particular site on the body) via an adaptive psychophysical procedure (4, 2, 1 staircase method). The GUI should be as simple as possible to facilitate ease of use.
   - Signal generation software for the microcontroller that produces electrical noise that adheres to the specifications outlined in the Identification of Design Requirements and Specifications section.

3. Test the system components (both hardware and software) to validate their functionality.

4. Assemble the system into an appropriately sized casing for a wearable device.

4   Literature Review

4.1   Introduction

This literature review will cover in more detail the following areas pertinent to the current project including a definition of SR, a brief background of SR, evidence of SR phenomenon in animal and human (physiological) systems, use and benefit of input noise to exploit SR phenomenon in human sensory systems. This will focus mainly on somatosensation and

include mechanical and electrical noise, as well as cross modal effects, evidence of increased neural activity with SR, possibility of neuroplasticity and the use and development of biomedical systems for SR applications.

4.2   Definition of Stochastic Resonance

The term SR is commonly used to describe the positive effect the presence of a non-zero level of random signal (noise) has on the performance of a particular non-linear (threshold-based) system. As such SR is a nonlinear phenomenon whereby the addition of an optimal intensity of noise can enhance the detection of weak stimuli or enhance the information content within a signal [29].

The term '*stochastic*' describes a random probability distribution that can be analysed but cannot be predicted precisely, in an SR context it relates to how the effect is achieved via a random signal [29]. '*Resonance*' was originally used because a plot depicting SNR against input noise intensity has a single maximum at a non-zero value, similar to that of frequency dependent systems that have a maximum SNR at some resonant frequency. An example of such a plot (SR curve) is shown in Figure 2 [29]. The addition of noise rapidly approaches an optimal peak value, after which further increasing the noise intensity slowly decreases performance.
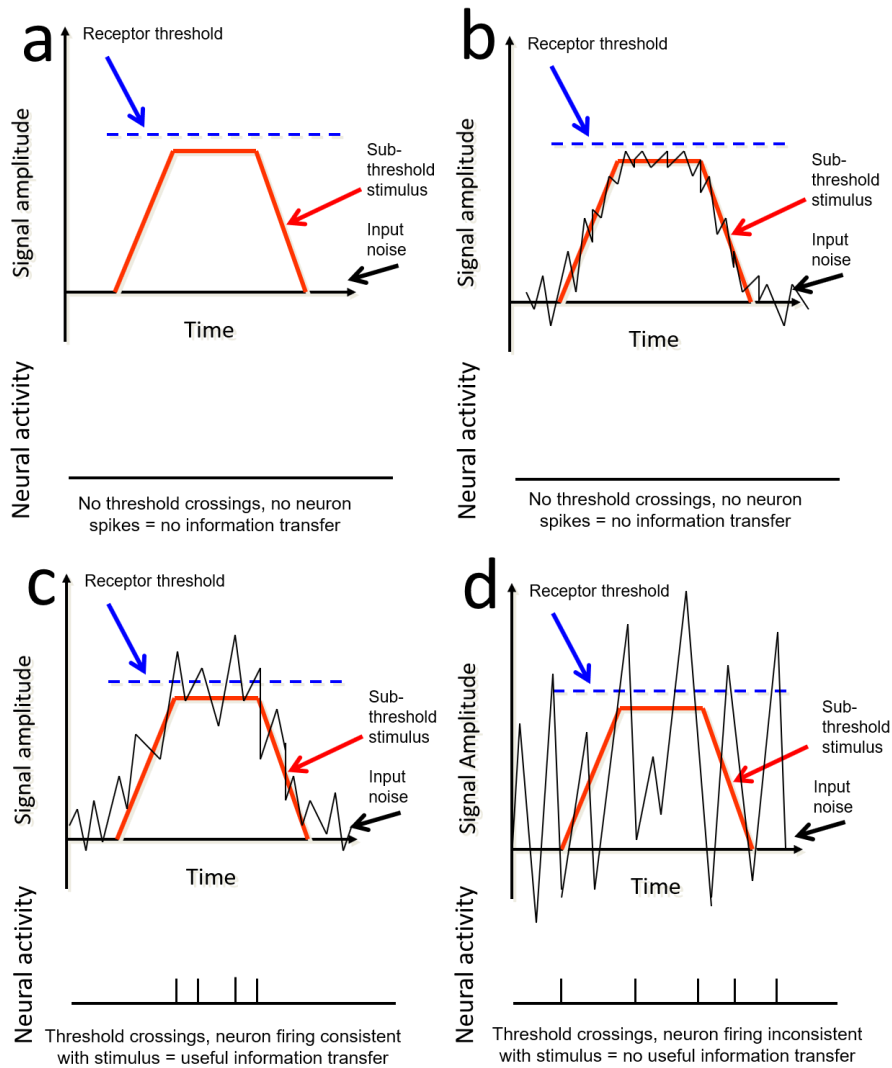
Figure 2 Input signal and various levels of added noise intensity: a) no noise, b) low noise, c) optimal noise, d) high noise. The illustration at the bottom of each panel is a schematic representation of neural firing in the nervous system which conveys information about the sub-threshold stimulus in the presence of the different levels of input noise.

Figure 2 depicts a visual representation of how SR enhances the detection of weak signals. In Figure 2a the stimulus is sub threshold, meaning no information is transferred. Figure 2b shows the addition of low level of noise, it is still not enough to cross the receptor threshold and thus still no information transfer. Figure 2c shows the optimal level of noise, the noise crosses the receptor threshold consistent with the sub threshold stimulus, resulting in a useful information transfer. Finally, in Figure 2d the additional noise intensity is higher than the optimum and the noise exceeds the receptor threshold inconsistent with the sub-threshold stimulus. There is still information transfer but it is lost or buried within the noise. Points are marked on the SR curve in Figure 3 relating to the levels of noise intensity in the sub figures of Figure 2.
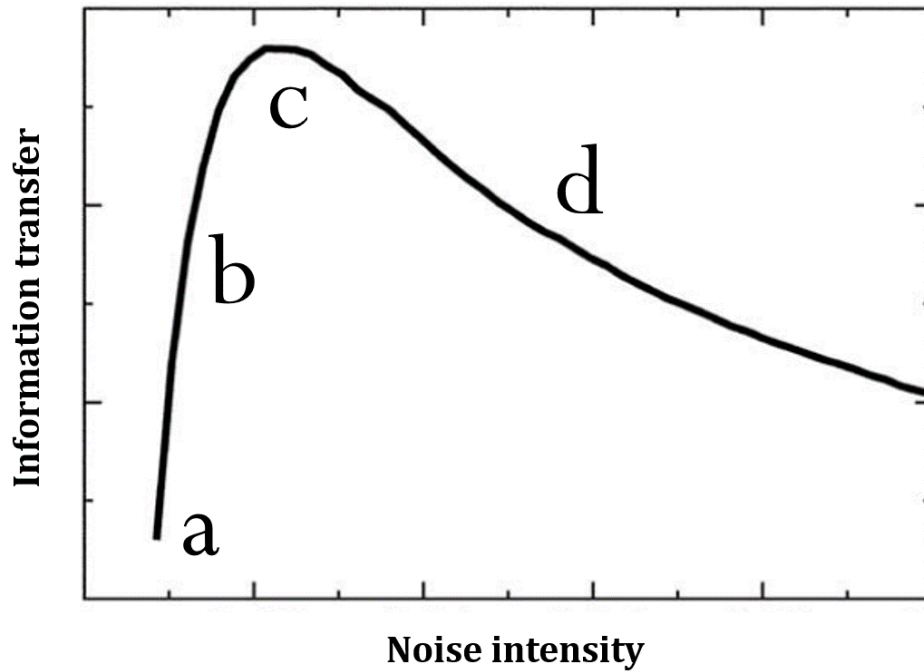
4.3 Early Demonstrations of Stochastic Resonance

The original investigations into the SR phenomenon presented a plausible explanation for the recurrence of Earth's ice ages [56-59]. These investigations constructed a theoretical model in which Earth's climate is represented by two states, one globally stable representing 'normal' climate and the other metastable, representing an ice-covered Earth. These states are separated by an energy threshold and the system is driven from random noise of the solar constant, which is the rate at which energy from the sun interacts with the earth's surface [57]. It was shown that this random noise could trigger events that switched between the two states within reasonable geological time scales. These models were only theoretical explanations. The first demonstrations of SR occurring in physical systems were made in experiments involving electronic components such as a modulated electronic Schmidt trigger [13] or bi-stable ring lasers [14, 15]. A Schmidt trigger is an electronic comparator circuit (compares two voltages and determines the bigger) that has two threshold values, if both are crossed the output value changes [60]. Ring lasers are an optical device that can trap light in a semiconductor ring, circulating indefinitely while it remains actively powered. The ring laser's state is dependent on light circulating in two directions, clockwise or counter-clockwise which switches when exceeding an acoustic frequency threshold. The introduction of a noisy electrical signal within these electrical components improved their performance by increasing the efficacy of switching between states gated by a threshold.

4.4 Stochastic Resonance in Biological Systems

The common element between each of the early examples is that the systems that display SR-type behaviour are all non-linear or threshold-based and the performance of each was improved through the addition of noise. Interestingly, a neuron can also be described as a threshold-based system. Shown in Figure 4, the charge across the membrane within a neuron cell must reach -55mV in order to excite the cell and initiate an action potential and thereby transmit information through the nervous system. If processes involved in the excitation and firing of the neuron do not achieve the necessary thresholds (e.g. stimulation of associated

receptors) then an action potential will not occur. Thus, it was proposed that SR may not be limited to artificial systems, it may also occur naturally and there is the possibility that biological systems have evolved the capability to exploit SR [5, 7].
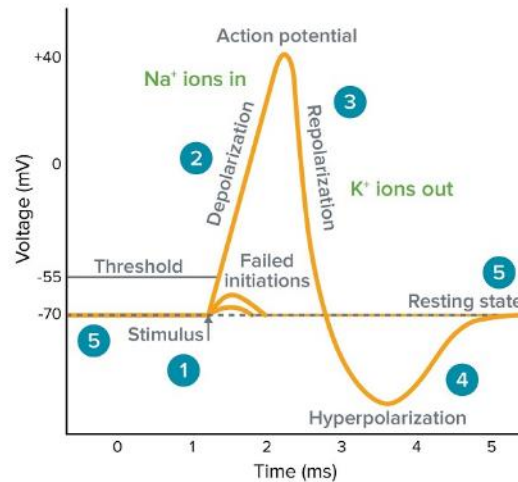
Figure 4 Action Potential, showing depolarization threshold and failed initiations (adapted from Molecular Biology [61])

Early demonstrations of the SR phenomenon in biological systems were made using animal models, with the first study investigating the use of SR to enhance the predator avoidance system of crayfish [7]. SR effects were also observed to increase the tactile sensitivity of crickets [9] and enhanced the electro sensory information that was available to a school of paddlefish's electroreceptors, enabling the small fish to feed with greater precision [6, 8]. Experiments performed on rat skin in vitro demonstrated that the ability of sensory neurons to detect peri-threshold stimulus could be enhanced by the presence of an optimal level of noise [62].

Most of the early studies involving human participants focussed on attempts to enhance somatosensation. Somatosensation includes tactile senses (e.g. fine touch and vibration) and proprioception (the sense of body or limb position) [2, 16, 18, 21-27, 39, 63]. There are a variety of receptors involved in the somatosensory system including cutaneous receptors in the skin e.g. Meissner's corpuscles (tactile), Ruffini endings (pressure/vibration), Pacinian corpuscle (pressure/ vibration plus involvement in proprioception), and receptors in the muscle and connective tissues e.g. muscle spindles (stretch/ proprioception) and the Golgi tendon organ (proprioception). Each of these receptors respond to specific stimuli (e.g. pressure, vibration, stretch) and are associated with sensory neurons, and thus may benefit from SR effects. The sensitivity of these receptors is known to deteriorate with age and this can effect an individual's functional abilities and activities of daily living [39]. This further emphasises the need for interventions or therapies which can enhance somatosensory function.

Collins et al. [2] were one of the first to investigate SR in human physiological systems. The study involved applying Gaussian 'quasi-white' mechanical noise to the fingertips of the 10 healthy young participants and then indenting the tip of each of their fingers with a known force (achieved with a force-controlled DC motor) each trial consisted of 20 presentations equally split between the presence and absence of noise [2]. The experiment was psychophysical in nature, each participant was asked if they felt a stimulus in the presence or absence of noise, quantifying the SR effect by measuring the coherence between input stimulus and % correct [2]. This study aimed to investigate whether noise could enhance sensorimotor function (i.e. touch and vibration sensation) via an SR-type effect. Results

concluded that the application of an optimal intensity of noise was increasing the participant's ability to correctly identify tactile stimulus [2].

A companion study published at the same time demonstrated that muscle spindle receptors controlling the wrist and hand extensor muscles showed enhanced responses to weak movement signals with the application of mechanical noise through the parent muscle tendon [26]. The study involved isolating a suitable afferent neuron to record neural firing using microneurography and then passively rotating the participants wrist whilst recording neural firing [26]. The results showed increased neural firing and an increase in sensitivity to stretch within the muscle spindles with the noisy stimulation of the muscle tendon [26]. Both studies showed that increasing the noise intensity rapidly increases the SNR ratio until it hits a peak performance. After this, increasing the noise intensity further slowly decreases the SNR (analogous to the plot shown in Figure 2). This is a consistent feature in SR effects and is why determining the optimal level of noise is important to maximise performance improvements. The work of Collins et al. was revisited the following year with a very similar setup and procedure [18]. Results obtained supported the earlier findings, suggesting that noise-based techniques could be used to improve the tactile sensation of humans when the stimulus is near or below threshold [18]. Further suggesting that SR could benefit individuals with elevated sensory thresholds due to age, peripheral neuropathy or other neurological related impairments such as stroke [2, 18]. However, effects across all these studies were only acute, with performance returning to baseline when the noise is removed [2, 18, 26].

4.5   Mechanical Noise

Mechanical noise has most commonly been used as an input to achieve an SR effect in physiological systems [2, 16, 18, 19, 21, 26, 28, 35]. The previously described studies involving humans were conducted using an optimal intensity of mechanical noise set by a DC controlled motor.

Vibrotactile sensitivity was shown to be enhanced by a mechanical noise stimulus applied to the sole of the foot [19, 28]. Importantly these studies also observed an SR effect in older adults, demonstrating that SR could enhance the detection of different frequencies targeted at specific receptors, 25 Hz was the target for the young group, 25 Hz and 50 Hz was the target for the older group. This information strengthens the suggestion that noise-based techniques could be used to improve tactile sensation for people regardless of their age.

Fine touch sensitivity or tactile sensation is not the only function that the SR effect can potentially enhance. Standing balance and proprioception were investigated following the demonstrations that noise could enhance the detection of stimuli that may be used in the regulation of balance (e.g. light touch and vibrations). Priplata et al. [16, 21, 35] observed that postural sway could be reduced using vibrating shoe insoles placed under foot to stimulate the mechanoreceptors in the soles of individual's feet with imperceptible levels of noisy vibrations. The noisy vibrations were controlled using a desktop signal generator and postural sway was measured by using a Vicon camera system tracking the position of a reflective marker placed on the participant's shoulders. Reductions in postural sway were consistently shown for healthy young adults, healthy older adults, patients with diabetes and patients that have suffered a stroke.

4.6   Electrical Noise

Following the initial human-based studies using mechanical noise, it was demonstrated that electrical noise can also be used to achieve an SR effect [22-25, 27, 50, 64, 65]. Electrical

noise is potentially a cheaper and more power efficient method for applying randomized noise when compared to using actuators to deliver mechanical noise.

Richardson et al. [24] was one of the earliest to demonstrate the use of electrical noise to achieve an SR effect. The experimental procedure was very similar to that of the previously described studies involving psychophysical tests of tactile sensation of the fingers. Ten healthy subjects had noise applied and then indentions were made at a known force to the right middle digit of the participants, electrical noise was introduced through the same indentor that apppied the mechanical noise in that stage of the experiment [24]. Results were comparable with the aforementioned studies using mechanical noise, where participants were able to identfy stimulus correctly with the presence of noise.

Dhruv et al. [22] also demonstrated improved tactile sensation with the application of electrical noise to the sole of the foot in older adults. The procedures involved positioning electrodes delivering imperceptible electrical noise adjacent to sites on the sole of the foot where fine nylon monofilaments of 20 different diameters (i.e. 20 different known forces) were applied to test fine touch sensation. Results from the psychophysical tests indicated signifcant improvements in fine touch sensitivty when applying random electrical noise compared to no noise, suggesting that techniques and devices based on electrical noise may enable people to overcome somatosensory deficits due to age or neuropathy-related sensory loss [22]. The final results were very similar to those observed in previous studies, suggesting that SR can improve performance even if the subject possess an elevated sensory threshold due to age, peripheral neuropathy or other neurological related impairments such as stroke [2, 18, 26]. In both studies a clear SR curve (see Figure 3) is observed, with correct identification of stimuli improved with an increasing intensity of the noise stimulus, up to a specific point, after which it slowly decreases.

Extending on the previous work using electrical noise, Gravelle et al. [27] demonstrated that random electrical noise applied to the knee has the capability to improve balance control. The experimental procedure involved balance testing of healthy older adults while they stood on one leg. Electrodes placed on the medial and lateral surfaces of the knee delivered imperceptible electrical noise (in the order of micro-amps) during the balance trials. The order of stimulation condition (i.e. with noise versus without noise) was randomised in a pairwise order. It was observed that the postural sway improved (i.e. decreased) for the trials with noise compared to the trials without noise. Another balance study demonstrated by placing electrodes on the mastoid bones (behind the ear) of young healthy subjects and applying a galvanic noise stimulus that postural sway could be reduced when compared to trials without noise [31]. It is worth emphasising that these young healthy participants had no reported balance problems, yet the noise stimulus was still able to improve their standing balance.

Several studies have identified that stimulating the ankle tendon improves proprioceptive function, reducing the perception threshold for ankle passive motion, contributing to an overall improvement in postural sway [66-68]. Combined, these studies suggest that the application of noise can enhance the detection of sensorimotor signals associated with postural stability leading to functional improvements in balance [67]. Recent studies investigating balance control also demonstrated that SR could enhance force-sense enabling the participants to better replicate the target evertor (i.e. rotating outwards) muscle tension to reduce postural sway, regardless of the presence or absence of ankle instability due to musculoskeletal injury [68]. Enhancements in proprioceptive function is believed to be related to improved encoding of information from a variety of afferent sensory neurons when

applying noise to peripheral receptors but also potentially to neurons located in higher levels of the central nervous system (CNS) [66].

4.7 Cross Modality and Versatility of SR

The SR effect is widely shown to be cross modal, that is, the medium of application for the noise need not be the same modality as the stimulus. For example, random electrical noise can enhance the detection of weak mechanical signals (e.g. vibrations). This was made apparent in the aforementioned study conducted by Richardson et al. [24] in which they directly tested cross-modality using electrical noise to enhance the detection of subthreshold mechanical stimuli, demonstrating that for SR-type effects to be observed in human sensory perception the noise and stimulus need not be of the same modality. This concept would be further studied with both sensorimotor function and balance control enhanced using mechanical and electrical noise [50]. Later studies that utilised electrical noise to improve the detection of weak mechanical stimuli further suggests the cross-modal feature of SR [22, 27].

More recent studies such as Breen et al. [23] were able to enhance the detection of weak vibrations applied to the subject's toes by delivering electrical noise to the lateral and medial plantar nerves via electrodes applied to the skin. This experiment not only demonstrates the cross modality of SR but also suggests that stimulating proximal axons may enhance somatosensory signals coming from distal regions, and therefore with electrical noise it is not necessary to apply the noise stimulation coincidental or adjacent to the site where mechanical stimuli may be present.

Additionally, it can be observed that several different bodily stimulation sites have been used in the balance control studies discussed in this literature review and all obtained consistently comparable results in reducing postural sway [16, 21, 27, 31, 67]. Human balance control being improved from a variety of stimulation sites can be explained by the human balance control system relying on feedback from the somatosensory, vestibular and visual systems [69]. This means that improving the detection of weak signals in one or more of these systems can improve balance control. Given the consistent results of these trials it is possible that SR devices delivering sub sensory noise stimulation could be utilised to enhance the balance of older adults and reduce the number of potentially harmful falls that can occur in the elderly or patients with neurological disorders.

The cross-modal effect has important implications, as electrodes are generally cheaper and more power efficient than vibrating actuators. Additionally, the ability to stimulate proximal nerves to the target region offers a versatility that enables devices to be designed with discrete and comfortable daily use in mind. These traits should be considered when designing systems that take advantage of electrical SR effects.

4.8 Neuroplasticity

It was once believed that the human brain is immutable and that any neurons damaged or destroyed would be permanent, however a paradigm shift has occurred recently with the observation that neural systems in human brains are highly plastic [70]. It is now believed that the brain is constantly changing throughout a person's lifetime, during fetal development structural changes are dominant, for adult brains the dominant type of neuroplasticity is 'functional' enabling adaptation to environment, injury or disease [71]. It has been observed that this "neural plasticity" allows neural circuits to flexibly adjust and optimise their processing in such a manner that adapts to environmental or behavioural demands of a given circumstance [72]. The molecular and cellular mechanisms at play during neural plasticity are only partially understood and are the subject of ongoing investigation [72].

The core concept of neural plasticity is well described by the phrase "neurons that fire together, wire together" (often referred to as Hebb's rule) which was originally coined by Donald Hebb in 1949 and has since gone on to influence many studies in the field of neuroscience and psychology [73]. It describes the concept that increasing neural firing associated with a particular neural pathway will act to strengthen a neural pathway and the actions which it helps control.

The introduction of external input noise to the somatosensory system has been shown to result in increased neural firing as revealed by microneurographic recordings [26, 63] of the stimulated afferent neurons. The increased neural firing has been attributed to the observed SR effects of improved somatosensory sensitivity in each case. A recent study by Ribot-Ciscar et al. [74] demonstrated that the application of mechanical noise to ankle muscle tendons improved the detection of directionally imposed movements that were initially subthreshold and imperceptible prior to the noise stimulation. Ribot-Ciscar et al. [74] also conducted a microneurographic recordings, observing increased neural activity associated with small ankle movements in the presence of the noise.

Furthermore, studies have found evidence that increased neural firing in the peripheral nervous system may elicit neuroplastic responses in the brain and spinal cord (CNS) [10, 66, 75-77]. In a study conducted by Manjarrez et al. 15 young healthy participants had a mechanical noise applied to the medial portion of the left middle fingertip and EEG recordings were obtained from the right parietal and central occipital regions of the brain [76]. Results showed that all subjects examined displayed clear SR-type behaviour in the EEG activity recorded [76]. This remarkable phenomenon suggests that SR effects can manifest both peripherally and centrally within the nervous system.

The concept of neural plasticity has become increasingly important in the application of rehabilitation therapies in individuals with functional deficits due to aging or disease. Deterioration due to aging, neurological diseases or injury to the brain can cause widespread biochemical, anatomical and physiological changes that can result in what is essentially a "new brain" [78]. In such circumstances, the brain and nervous system must re-learn behaviours lost due to injury or disease. The same neural and behavioural mechanisms that drive plasticity during learning in a healthy brain are present in a damaged or diseased brain. However more intensive practice may be necessary to establish new neural pathways. Thus the aim of intensive rehabilitation strategies is to assist in the retraining/ relearning of behaviours [78]. A number of promising neuroplasticity-based interventions and therapies have been identified and are being studied although the field is still relatively new and further investigation is necessary [79].

Evidence suggests SR effects are associated with increased neural firing and positive responses in the brain. Thus the introduction of external input noise to mediate SR effects may be another amenable technique for use in conjunction with rehabilitation therapies to strengthen or form neural pathways. This may help to achieve earlier and longer lasting rehabilitation outcomes. A study by Stein et al. investigated using rehabilitation techniques for upper limb control post-stroke in conjunction with electrical and mechanical noise on 15 subjects to determine whether SR effects from the noise stimulation led to better functional outcomes [80]. One group of participants received therapy without noise stimulation and a second group received therapy with noise stimulation. No significant differences were found between the groups, however the clinical outcome measures used to assess changes in

performance may have not been sensitive enough to reveal changes could have been attributable to the SR effects of the noise stimulation [80].

Further investigation of potential benefits from long term use of noise stimulation and exposure to SR effects in physical rehabilitation is warranted. Similar to the "carry over effect" (COE) that has been observed when using FES devices for prolonged sessions, whereby improvements in motor strength and control are retained due to neural plastic mechanisms when the stimulator is no longer in use [81-83]. It is possible prolonged exposure to SR effects associated with longer term use of noise stimulation may deliver improved somatosensory function even in the absence of the noise stimulation.
The recent advances in knowledge and understanding regarding neuroplasticity and SR could lead to SR systems being used in rehabilitation contexts for various neurological conditions that have caused significant changes to the peripheral and central nervous systems.

4.9 Stochastic Resonance Systems

Almost all experimental set-ups used in the previously discussed studies have been laboratory desktop-based systems. A limitation of using a desktop-based system is that individuals cannot reasonably take part in SR experiments for an extended period, as they are confined to the location of the system. To assess the long-term benefits of noise enhanced somatosensation it is necessary to develop portable (preferably wearable) systems that have the capability to deliver optimal levels of noise stimulation to an individual for a prolonged period with minimal functional restrictions. This is also the next logical step in progressing research into developing technology that can exploit SR effects for a therapeutic benefit.

A portable mechanical SR system that employs vibrating insoles has been proposed and developed by several research groups [32-34] based on the earlier work of Priplata et al. [16, 21, 35]. No equivalent wearable electrical system exists at the time of writing hence the focus of this project is to develop a portable and wearable electrical SR system. The exact stimulation parameters used varied somewhat in each experimental set-up and it has been recently suggested that future investigations should consider 'task-specific' (e.g. balance control, fine touch, vision, hearing etc.) effectiveness to identify optimum stimulation parameters in order to maximise functional improvements [66].

However, there are a few parameters that are quite common in electrical SR systems. They often operate using a 1kHz Gaussian (usually 'pseudo' or 'quasi' white) noise signal. The current typically has a standard deviation ranging from 15µA-1mA, any higher and it can potentially be dangerous to use (especially with higher voltages). Much lower than this and participants that have higher than normal thresholds due to age or disease may not be able to feel the noise which can compromise the setting of sensory thresholds and appropriate level of stimulation which is important to achieving SR effects [36, 37].

Typically the level of noise during use is imperceptible as it is set to just below the sensory (perception) threshold. This feature makes it suitable for long term use as the individual should not be able to feel the stimulation and thus is not a nuisance or inconvenience. In addition the randomness of stimulation signal reduces the likelihood of receptors and sensory neurons adapting to the signal during use which may otherwise happen with uniform sinusoidal signals [18]. In order to determine the optimal thresholds, most systems have a means of altering the amplitude of the noise, some used a number of pre-set levels, others utilised small 'steps' (typically reported in standard deviations of the signal) with a magnitude of micro-Amperes that can be added or subtracted from the noise [22, 23, 27].The

use of adaptive psychophysical procedures can assist with efficiently establishing sensory thresholds [84].

The design considerations for a wearable, portable system were recently reported by Karpul et al. [37]. The system was designed to deliver the SR noise as electrical stimulus applied via transcutaneous electrodes and has been tested to drive ±1mA peak to peak 1 kHz sinusoidal signal into a 60kΩ load. This circuit ensures that a safe current was being driven to the load through the implementation of a modified Howland current pump which will increase or decrease the voltage depending on the output load of the circuit, ensuring a stable current. To drive the current through high impedances like 60kΩ, which can be considered the typical load for resistance of an electrode contacting skin, the Howland current pump requires a high input voltage. This is achieved through a high voltage power supply unit made up of 4 TC962 voltage invertors. Karpul et al. [37] chose to implement the HVPSU this way because of the low quiescent current and efficacy the design offers. This was demonstrated as the overall circuit is drawing less than 21mA from a 9V source when driving the ±1mA peak to peak, 1 kHz sinusoid into the 60kΩ load. The systems circuit board was approximately 21mm × 46mm making the form factor suited for battery operated (wearable) device. Overall this system has the design features that are necessary to make a successful wearable system. It is small and lightweight and draws low power making it suitable for battery operated use. This system is still in development, as stated in Karpul et al. [37]. The next logical step is to implement the instrumentation of the circuit and provide user control, with additional low power control circuitry. Karpul et al. [37] provide a suggestion for an appropriate microcontroller (PIC24FJ128GC006) that has low power consumption and a small form factor whilst also having a built in DAC. To date they have produced no results from using this system with human participants. Adapting this circuitry and taking that next step by adding control circuitry a signal generator and a user interface would make for a robust wearable system that could be used to explore the effects of prolonged use of low-level electrical noise stimulation.

As with any electrical system being connected to a human there is a risk of sustaining minor injuries such as skin burns that must be minimised or eliminated. With the application of SR to human patients being relatively new, context specific standards or guidelines for safe use aren't available. However, there are international standards and guidelines for functional electrical stimulation (FES) devices and transcutaneous electrical nerve stimulation (TENS) to maintain patient safety [85, 86]. An example of such a standard is never placing stimulation electrodes on opposites sides of a subject's body and ensuring that current has no path through the heart. Considering that the electrical noise is applied in the same way as these FES and TENS devices (via electrodes placed onto the skin) it is reasonable to assume that those standards and guidelines are likely to be also relevant to SR devices and adhering to them will eliminate potential risks.

4.10 Applications of Stochastic Resonance Systems

As stated previously human balance control relies on feedback from the somatosensory, vestibular and visual systems [69]. This means that improving the detection of weak signals in one or more of these systems can help to improve balance control and reduce postural sway. Somatosensory systems are known to deteriorate with age and as a result balance control can decrease and risk of falling subsequently increases. Falls are a serious problem in Australia, in South Australia alone there were 22,576 people admitted to public hospitals in 2017 after a fall [87]. This is 12 times higher than the number of admissions for motor

vehicle injuries. Over 65% of these admissions were people over the age of 65 and 400 died in hospital as a result (falls account for 40% of injury-related deaths for this age group) [87, 88]. It is also estimated that the cost of falls to the Australian healthcare system will increase to $1.4 billion by 2051, making it a very serious financial as well as health problem [88]. SR systems have been shown to improve somatosensation in individuals with elevated sensory thresholds that could be due to age, peripheral neuropathy or other neurological related impairments such as stroke [2, 11, 18, 21, 22, 24-28, 30, 34, 35, 67, 68]. Previous studies based on these findings have shown SR systems can consistently produce acute improvements in the balance of individuals. With the significant consequences of poor balance in mind which are outlined above, combined with the well documented acute benefits on balance provided by SR systems, the current project will focus on assessing the effectiveness of an electrical SR system on a balance task. Neuroplastic mechanisms from prolonged use of such a system may lead to improved performance of the somatosensory system even in the absence of noise stimulation, leading to improved balance and subsequently decreasing the risk of fall related injuries. The electrical SR system that is the focus of the current project has the potential to make a positive contribution to this problem by demonstrating long-term benefits of SR.

4.11 Conclusion

Understanding of the SR phenomenon has come a long way since the original investigations in the field of climatology. It has been theoretically explored in a substantial number of models and has been observed working in many different physical and biological systems. One of the most interesting applications of SR is in improving biological systems via the introduction of external input noise. Somatosensory sensitivity and balance control can deteriorate with age or neurological pathologies and with this deterioration comes an increased risk of falls or a reduction in quality of life. Falls are a widespread and costly burden on the health system in Australia. SR effects achieved through the delivery of mechanical or electrical input noise have been shown to consistently improve balance by enhancing somatosensory function. Exploiting SR effects potentially provides an approach to improve balance and help reduce the risk of falls in individuals with balance problems. SR phenomena have been demonstrated to be cross modal, with electrical noise improving the detection of mechanical stimuli.

Through neurophysiological studies, it has been shown that SR increases neural activity which may lead to improved overall function due to neuroplasticity as has been observed during prolonged use of FES devices. No experiments to date have explored this for the long-term application of SR noise stimulation. Most of the experimental systems used to explore this phenomenon have been desktop-based systems and whilst they have been useful in demonstrating that SR has a clear and consistent effect in improving the detection of weak signals in threshold-based systems, they do have limitations in portability [2, 6, 7, 11, 19, 21-23, 26-31]. Designing a wearable system that could explore outcomes from prolonged application of sub sensory noise stimulation is the next step in researching technology that can potentially exploit SR effects for a therapeutic benefit, including enhanced rehabilitation of balance problems. At the time of writing only one mechanical system designed to be wearable has been in recent development. Regarding electrical devices, the design considerations for a portable device have been outlined [37] but no devices and no results using a portable system with human participants have been published to date. There is still a clear need to develop systems with portability in mind so that experiments involving prolonged application of low-level noise stimulation can be conducted and compared,

hopefully improving quality of life and reducing injury for those with age or disease-related deterioration of the somatosensory system.

5 Project Background

In 2017 a first prototype of a portable electrical stochastic resonance system (ESRS) (Figure 5) was completed and assembled by Shannon Deale while on placement with the Statewide Research and Teaching team within South Australian Biomedical Engineering (SA BME). This following on from the work of Daniel Ward in the development of the prototype in 2015 as part of his honours project. At the end of 2017 the device was able to produce a pseudo-white Gaussian noise signal with approximately 15V driving a maximum of 3mA through the electrodes attached to the skin. The prototype was designed around a limb resistance set at 2kΩ. This is a good approximation of the resistance of a limb but not the impedance of an electrode to skin interface) [36, 37]. The device had four independently programmable channels enabling it to stimulate four sites with different receptor thresholds at once (See Appendix A for more detailed information on this device).

Figure 5 Previous ESRS System (isometric and front face views) showing the user interface, 4 push-buttons and channel selection switches
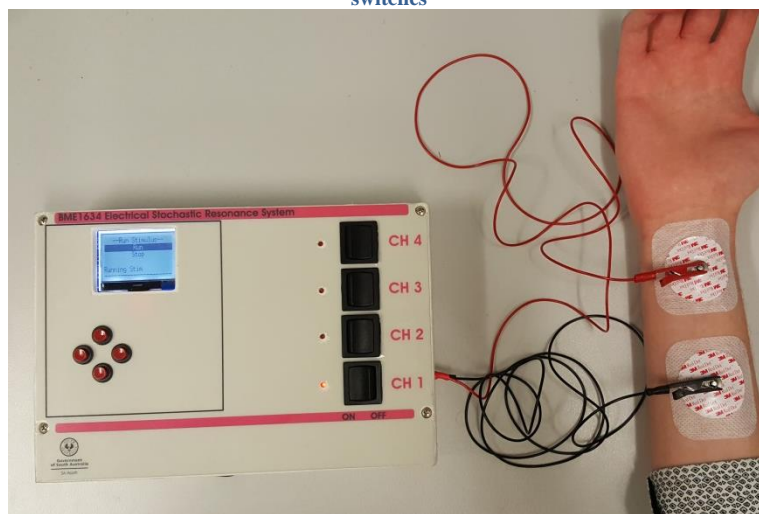
Figure 6 The previous prototype system connected to a subject's arm for scale

The internal hardware of the 2017 prototype comprised of an Arduino UNO, and custom design PCB containing a digital to analogue converter (DAC), a bi-polar voltage source and a Howland Current Pump. The user operates the system via control interfaces located on the external enclosure :

- Four push-buttons for navigating the menus.
- LCD screen for viewing the menu structure.
- Four channel switches that would hardware enable/ disable each channel.
- A power switch.
- A reset switch.

The size of the device (220mm × 150mm × 50mm) enabled portability but was not adequate for wearable applications (see Figure 6). This large size was due to the use of large components such as the Arduino UNO development kit, LCD screen plugin and button interfaces. Low output voltage was also a significant problem for this prototype as it required the individuals to rub alcohol and lightly abrade the skin to reduce skin impedance to the target 2kΩ. It has been shown that skin impedance can vary from 10kΩ to 1MΩ depending on stimulation frequency, electrode location and skin condition. Thus it was determined that the system needed to be redesigned to accommodate a more appropriate skin impedance range.[89].

When driving with ±1mA the maximum skin impedance is 6kΩ, however this is still a relatively low maximum impedance for the application. The size of the memory available to the Arduino UNO was also a constraint and as a result the software component was not able to achieve the l pulse frequency of 1kHz suggested in the literature.

Due to these limitations in hardware and software it was decided that a complete redesign of the system would be the best course of action. Using the lessons learnt from the previous device the new system would need to be much smaller, have a higher voltage output and achieve the desired output signal.

6   Project Design

The design stage of the project involved conceptualising the device, designing the circuit schematics and printed circuit boards (PCB) as well as writing pseudo-code for how the software component should work and integrate with the operation of the hardware.

6.1   Concept

The conceptualisation phase of the design identified how the system would work overall and what key design features could be implemented to improve the size and performance of this device in comparison to the previous device (see Project Background).

The Arduino UNO modules, LCD screen and button interface that were used to operate the 2017 prototype were identified as the primary constraint for the systems size. Hence these components were removed, and the device would be operated by a wirelessly linked personal computer (PC). This also aligned with the client's preference.

The wireless connection would only be necessary while the operator is using the system to determine the subject's sensory threshold. Once this is complete the device would continue to run this subthreshold stimulus until switched off. This enabled the device to be much smaller and wearable whilst also maintaining usability. The solution involved designing a PC graphical user interface (GUI) and signal generating software program implemented within a microcontroller.

A key feature of the redesign was the high voltage power supply and high voltage current pump. They enabled the device to deliver much higher voltage; at least ±60V to meet the target impedance 60kΩ whilst still delivering a ±1mA current. The device had a battery as it is intended for wearable use and the inclusion of a charging plugin port enabled convenient recharging. 7 shows a block diagram illustrating the connections between the main components of the system described here.
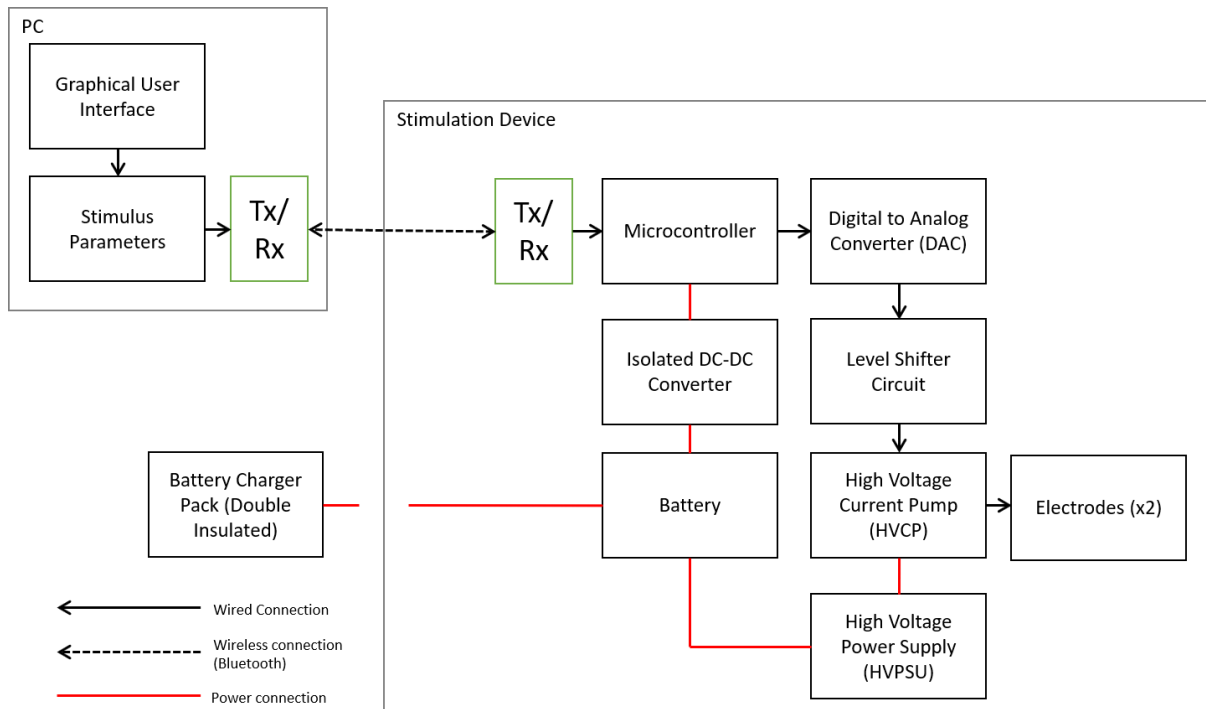
Figure 7 Concept Block Diagram of the proposed system illustrating the connections between the main components of the system including a microcontroller, DAC, level shifter, HVCP, HVPSU, GUI and a wireless transmitter/receiver.

6.2 Circuitry

As outlined in the Literature Review, the design considerations for a wearable portable system were recently reported by Karpul et al. [37]. This included the use of a high voltage power supply unit (HVPSU) and high voltage current pump (HVCP).

6.2.1 High Voltage Power Supply Unit

Karpul et al. recommended the use of a cascaded series of TC962 voltage invertors to deliver the desired ±1mA at ±60V. These voltage invertors were used to construct a HVPSU that was efficient and stable whilst able to maintain a low quiescent current to maximise battery life [37].
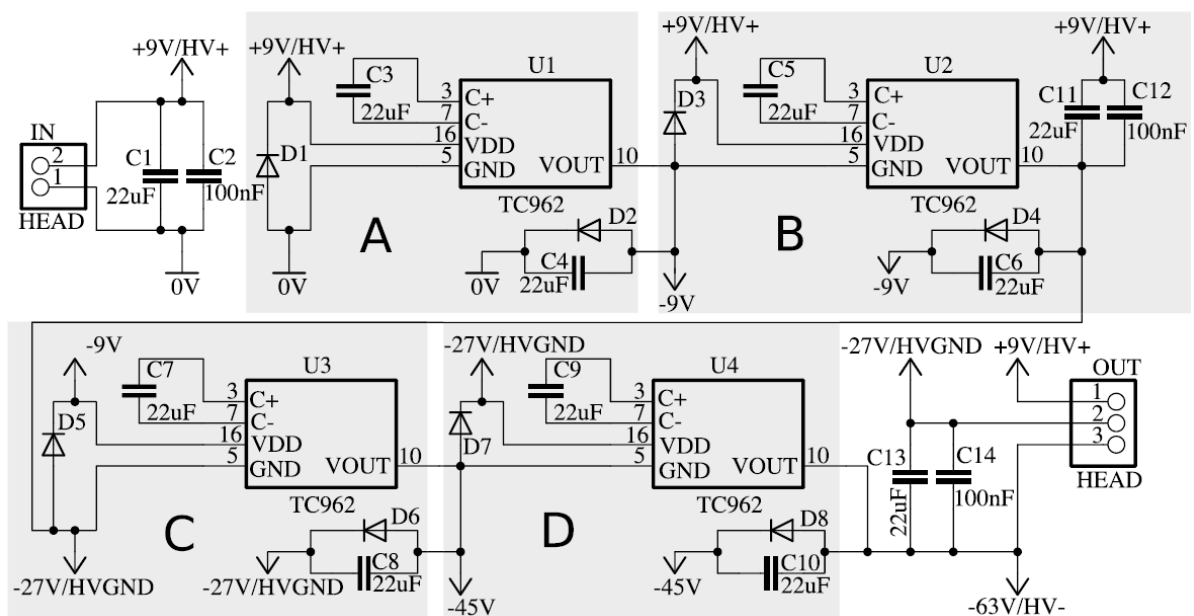
Figure 8 High Voltage Power Supply (HVPSU) from Karpul et al [37].
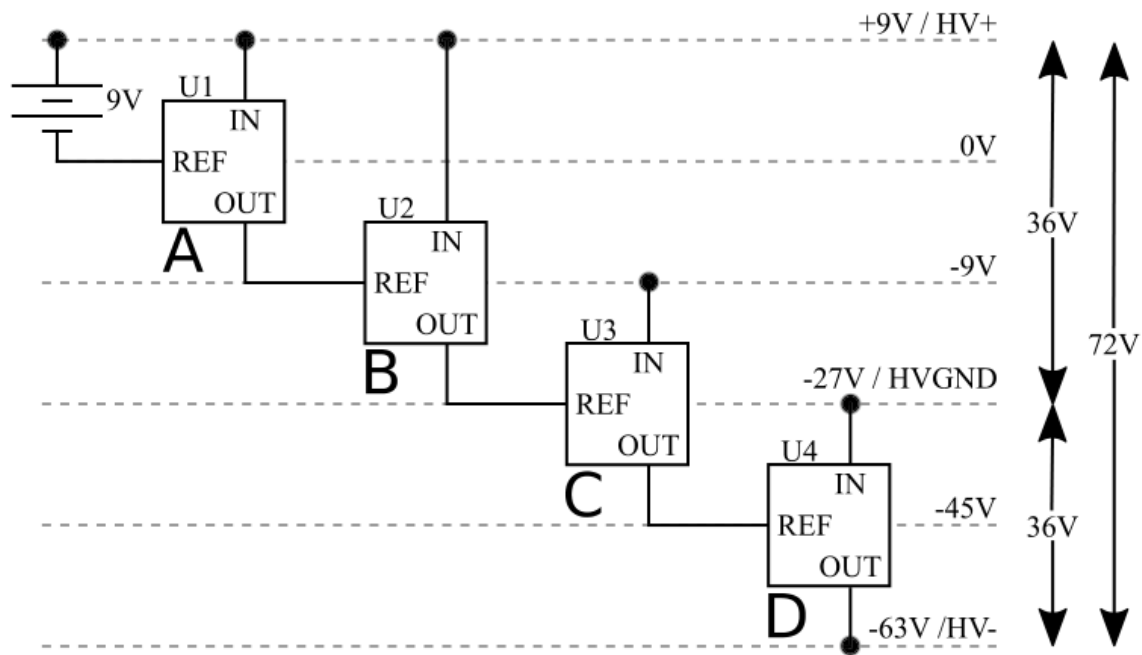
Figure 8 and Figure 9 show the circuit diagram and an explanatory diagram describing how the HVPSU functions. Briefly, each voltage invertor takes the difference between its input and reference voltages and inverts it about the reference value [37]. The first voltage invertor has an input of +9V and is referenced to 0V, producing an inverted output of -9V, the second voltage invertor again has an input of +9V but is now referenced to -9V producing an output of -27V. This repeats another two times eventually resulting in a final output of -63V which effectively provides a voltage range of 72V (+9V to -63V) [37].

The output voltage is now 8 times the value of the input voltage, this means that the current drawn from the circuit will be scaled up accordingly [37]. If 1mA is drawn from the circuit then 8mA will be drawn from the battery, hence why low quiescent current is such a critical feature of this circuit [37].

Dr Ben Patritti requested that the idea of increasing the output voltage of the HVPSU to 180V be explored, with a goal of producing ±3mA at 60kΩ rather than ±1mA. The rationale behind this was that some individuals may have elevated sensory thresholds and thus will require a higher current in order to establish their sensory threshold which determines the sub-sensory level of the stimulation necessary to achieve SR effects. However, literature regarding electrical stimulations suggest that such a large current isn't necessary achieve an SR effect [22-25, 27, 50, 64, 65], the issue of sensitivity requires a high enough voltage output so that the current can be driven through high skin impedances. Due to Ohm's law increasing the voltage further still means that ±1mA can be driven through even higher impedances. As aforementioned skin impedance can vary from 10kΩ to 1MΩ depending on stimulation frequency, bodily location and skin condition [89] so the proposal of increasing the voltage further was still explored.

Each TC962 only allows for a maximum input of 18V, thus the total voltage output can only increase in multiples of 18V. The problem is that this increases the current draw on the battery significantly. If the voltage is increased to ±144V using 8 inverters (providing ±2.4mA at 60kΩ) the current draw from the battery would be 16 times the current draw of the circuit. This issue can be resolved by using multiple batteries, however this complicates the

circuit when considering rechargeable batteries as shown in Figure 10. Certain switches would need to break the circuit at particular points to safely charge the two batteries and the device could not be operated during this time. The only other option for increasing the output voltage would be a complete redesign of the HVPSU using different components.

Considering the number of extra components needed, the increased current draw and that literature suggests ±1mA will be sufficient, it was decided that pursing an increase in output voltage to 180V in order to achieve a current output of ±3mA at 60kΩ was not worthwhile for this iteration of the prototype but may be revisited in the future.
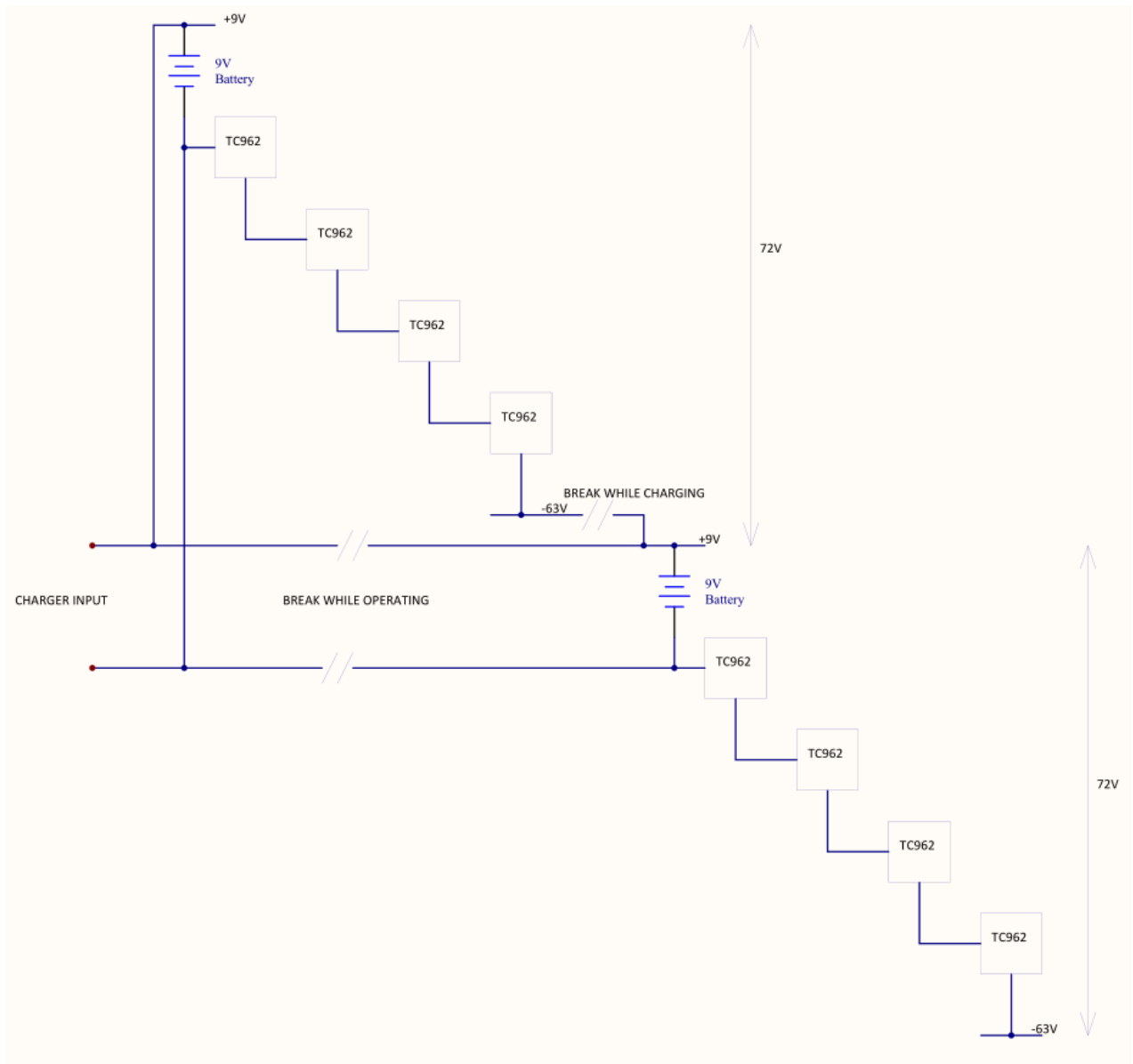
Figure 10 Cascaded power supplies diagram

6.2.2 High Voltage Current Pump

The HVCP shown in Figure 11 takes a differential input voltage and converts this to a proportional current via the gain resistor (RGain in Figure 11). The following equation describes the relationship between the load current, the differential input voltage and the value of RGain.

$$Iload = \frac{Vin_+ - Vin_-}{RGain}$$

The circuit is powered by the HVPSU outputs HV+, HV- and HVGND which are +9V, -63V and -27V respectively. This effectively means that the circuit is powered by ±36V. The T1 through T4 transistors observable in Figure 9 bootstrap the power supply for the op amp as described in [90] and [91]. This enables the power rails for the op amp to be adjusted to the portion of the power supply that is needed in that particular moment linking their output voltage to the supply voltage. This technique enables the use of low voltage op amps in high voltage applications through the addition of high voltage transistors [37].
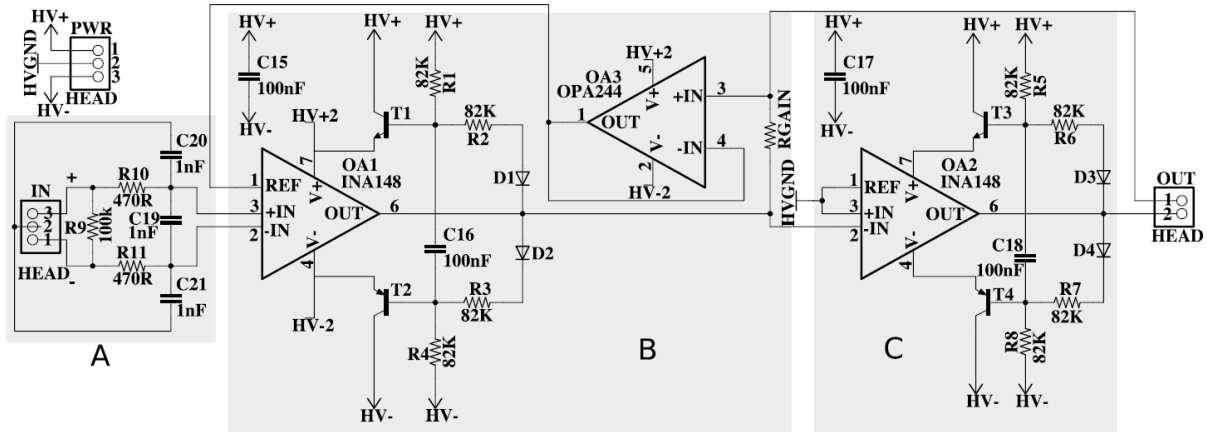
Figure 11 High Voltage Howland Current Pump (HVCP) from Karpul et al [37].

However, the bootstrapping technique does introduce one additional problem, the input values for the op amps can now fall outside the value of the power supply at any time. This means that the OA1 and OA2 in Figure 11 must be specialised differential amplifiers that are capable of handling common mode inputs that fall outside of their supply rails. Karpul identifies and suggests the Texas Instruments INA148 that can handle a common mode differential input of ±200V whilst maintaining a low quiescent current of 260μA, which is ideal for use in this project [37]. OA3 in this circuit is designed such that it provides a reference feedback voltage for the HVCP without drawing current from the load. OA3 does not require the use of the bootstrapping technique and does not need to handle a common mode differential input outside of its supply rails, its input is only slightly different from OA1's output and thus OA3 can share the floating supply for OA1 [37].

6.2.3 Control Circuitry

The design considerations for a wearable portable system outlined by Karpul et al. did not include the integration of control circuitry, a user interface or signal generation software. This project extends this work through the addition of these elements. Following is the design of control circuitry that drives the stimulation signal through the HVCP circuit.

Figure 12 Level shifter circuit that takes a 0V to 3.3V DAC input and enables a ±3.3V output

The level shifter circuit shown in Figure 12 takes the output of the DAC and enables it to swing positive and negative before being inputted into the HVCP to achieve both +60V and -60V. It contains a DC-DC isolated convertor that takes the 9V battery input and converts it to 3.3V which will also be used to power the microcontroller and the Bluetooth module (see Figure 14). The electrical isolation is critical as both the HVPSU and this level shifter circuit will be connected to the HVCP, effectively providing two different ground references (0V from the battery and -27V from the HVPSU) which will not function.

The op amp OA1 in this circuit needs to provide rail-to-rail output swings of ±3.3V. The MAX4162 was identified for use in this application as it provides rail-to-rail output voltage from a dual supply of ±1.25V to ±5V, making it suitable to provide rail-to-rail output swings of ±3.3V. To provide the -3.3V for the op amp the 3.3V from the DC to DC convertor is inverted using the same invertors from the HVPSU (TC962) because as previously mentioned this invertor provides a low quiescent current which is an important consideration in this project.

The equation describing the relationship between the input and output of the level shifter circuit is as follows.

$$Vout = 2Vin - Vref$$

Substituting simple values into this equation we can demonstrate that the level shifter circuit will function as required.

$$2(0V) - 3.2V = -3.2V$$
$$2(0.8V) - 3.2V = -1.6V$$
$$2(1.6V) - 3.2V = 0V$$
$$2(2.4V) - 3.2V = 1.6V$$
$$2(3.2V) - 3.2V = 3.2V$$

Thus, the level shifting circuit is capable of producing an output range of 3.2V to -3.2V from a DAC output between 0V and 3.2V.

The selection of a microcontroller was based on four characteristics, a built in DAC, power consumption (current draw), physical dimensions and contact pitch size (physical distance between adjacent pins).

16 bit DAC	10 Bit DAC
Typical current draw: 76mA	Typical current draw: 80µA
Dimensions: 35mm X 8mm	Dimensions: 12mm X 12mm
Contact pitch: 2.54mm	Contact pitch: 0.5mm

For the microcontroller two PICs from Microchip were identified (see Table 1) as ideal for this application, the dsPIC33FJ128GP802 and the PIC24FJ128GC010 (note, the PIC24FJ128GC006 is a chipset from this family that was recommended in Karpul et al. [37]). Whilst the PIC24F chip is superior in terms of current draw and size, initially the dsPIC33F chip was chosen due to its larger contact pitch size. The contact pitch size would enable the printed circuit board (PCB) containing the PIC to be manufactured and assembled in-house.

Figure 13 RN41 Bluetooth module

Bluetooth was chosen to implement the wireless communication component of the control circuitry as it offers lower power consumption than Wi-Fi and doesn't require line of sight such as with infra-red communication. The RN41 Bluetooth module from Microchip shown in Figure 13 was chosen, as this device is compatible with both PIC families identified as ideal for this project.

6.2.4 Overview of Circuit Interconnections

Figure 14 illustrates how all of the circuit components will connect as an overall circuit. Observing the overall connections it becomes clear why the electrical isolation is so critical. If the isolation wasn't implemented then the 0V point of the battery will connect to the reference point of the HVCP (through the inverter and level shifter circuit), simultaneously the floating ground from the HVPSU (-27V) will also be connected to be the reference point for the HVCP. The circuit cannot function like this because the 0V point of the battery is used as the reference point for the HVPSU and thus isolation must exist either in the HVPSU or in the control circuitry (via the DC-DC converter).
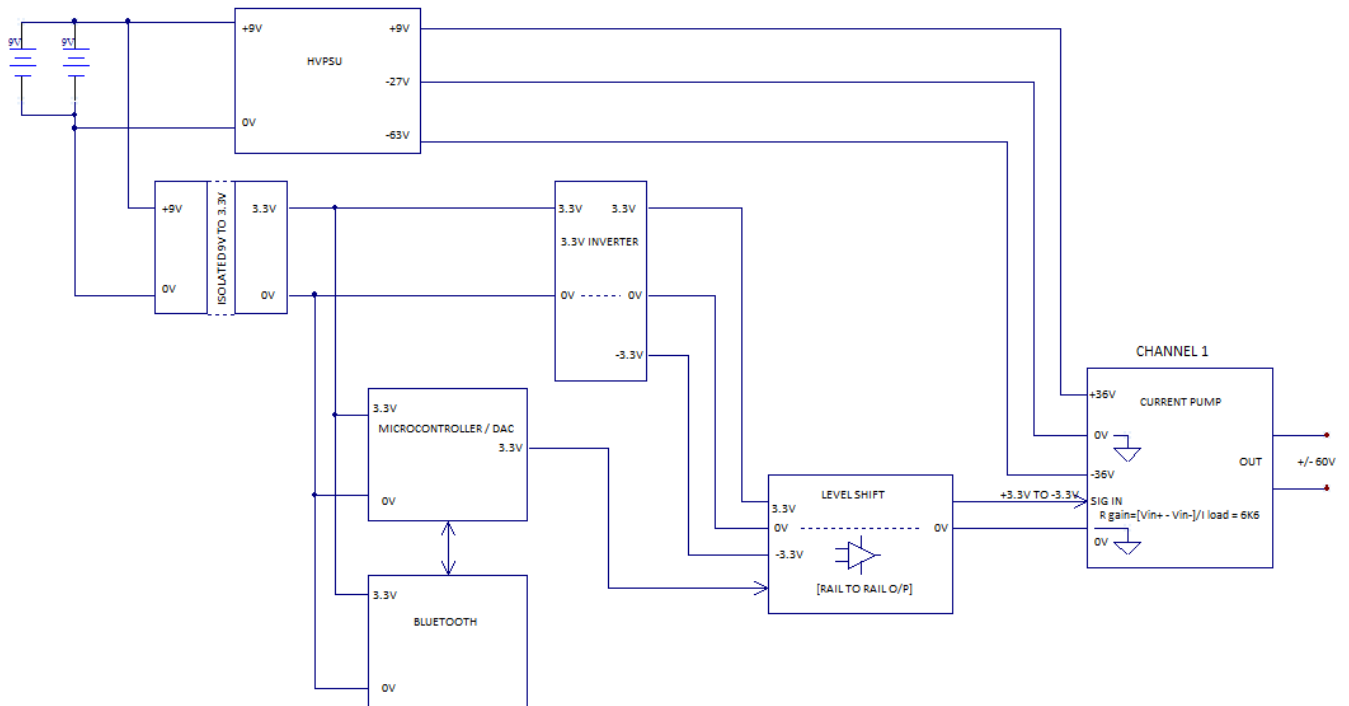
Figure 14 Overall circuit connections of the components in the system

The choice was made to implement the isolation within the control circuitry as the HVPSU and HVCP designs were being adapted from Karpul et al. [37] Changing that circuit may result in an undesirable change in performance, it was also more convenient to include isolation as part of the control circuitry design stage rather than attempting to implement it into an existing circuit design.

6.3   Software Design

The software component consists of two parts, a GUI developed for the PC that will serve as the user interface for the system and software developed and implemented in the microcontroller that will generate the desired signal. The key design decisions to be made in this stage of the project were the programming language used to develop the software components as well as the layout/ functions of the GUI.

The menu structure was loosely based on the previous prototype's menu system. However, the chosen interface of a PC enables much greater flexibility due to screen size, the option to use a mouse rather than push-buttons and access to a more powerful operating system.
The layout of the GUI is constrained by what functionality is required from the application. The main functional requirements of the GUI were:

- The user must be able to enable or disable each channel separately.
- The device must be able to be paired to the PC.
- The user must be able to run and stop the stimulation.
- The user must be able to select the stimulation current.
- The user must be able to push their selections to the device ("update the device")
- Appropriate controls should be in place to enable the user to employ the descending staircase method [92] of determining an individual's sensory threshold.
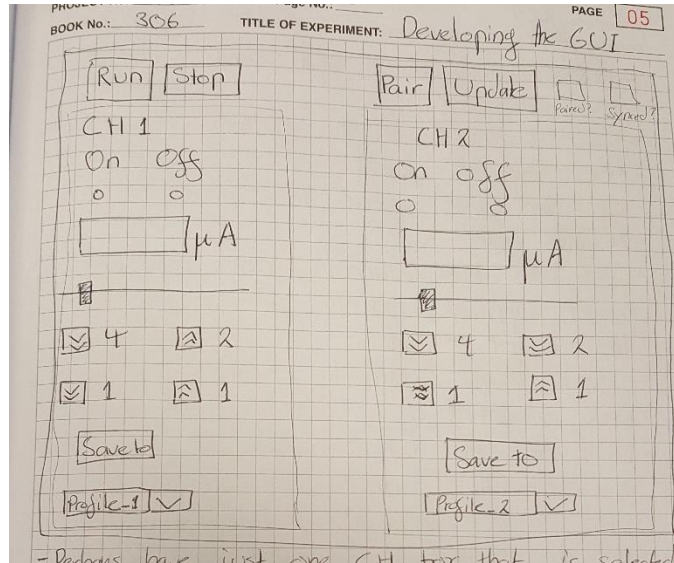
The goal with the GUI was to tailor the application towards the intentions of the client, Dr Ben Patritti. So, a plan for how the GUI would appear and function was sketched out and discussed with Dr Patritti to achieve this outcome. Figure 15 shows the sketch that was presented and agreed on as a suitable design.

The GUI functions such that the user can select the initial stimulation current either by typing it into the text box or by selecting it using the slider. The starting level may vary depending on the sensitivity of the individuals who may use the device e.g. young health adults or older adults with diminished sensation. The two channels can be switched on or off independently, the user chooses when their data is pushed to the device via the update button and the user chooses to run or stop the stimulus with their dedicated buttons. The user is then able to employ an adaptive psychophysical procedure (4, 2, 1 staircase method [92]) implemented in the software to determine the subjects threshold by changing the value of the stimulus in predefined steps of 15µA. This step size was chosen as it is the step size cited in Breen et al. [23] and it provides sufficient resolution to determine an individual's sensory threshold. The user has the options of decreasing the noise stimulus by four steps, increasing by two steps and decreasing or increasing by one step as the amplitude of the stimulus approaches the sensory threshold level of the individual. Finally, there is an option to save the current settings as a profile so that when that individual returns the user can select the last used value for that person.

Table 2 Comparisons of programming languages

Java	JavaScript	C#	C++	Python
Runs as desktop application. Easy to use and set up. Runs on most major operating systems (cross platform).	Runs in browser (does not run as a desktop application) Easy to use and set up.	Runs as a desktop application. Microsoft Visual Studio offers a drag and drop GUI editor. Can only run on windows OS.	Runs as a desktop application. Difficult programming language to use and set up. Most powerful of the selected languages.	Runs as a desktop application. Very easy to use and set up. Runs on most major operating systems (cross platform). Only suitable for small applications.

After determining the layout and function of the GUI the next decision was to identify and choose a suitable programming language for its development. The programming languages

that were considered included C#, C++, JavaScript, Java and Python (see Table 2). Python was the language decided on as it is the easiest to use and set up. The application that is being developed for this project is small and simple and Python is simple to use cross platform (in case the client switches from Windows to MAC OS in the future or decides to use a tablet/smartphone).

For the device software the use of a PIC microcontroller necessitates the software be developed in C. The software developed by students Daniel Ward, Scheina Gonzalez and Shannon Deale for the previous prototype system (written in Arduino) was planned to be adapted for use in this project (see

Appendix A
Note double click on the object below to open a pdf.

Electrical Stochastic Resonance System

Project Completion Report

Government
of South Australia

SA Health

Flinders
UNIVERSITY

BME Student
11/24/2017

Appendix B

```python
1.  #Signal Generator Code for BME 1634 ESRS
2.
3.  #GUI CODE SECTION
4.
5.  from tkinter import *
6.  from tkinter import ttk  #Importing necessary packages from tkinter
7.
8.  root = Tk() #Make the root window
9.  root.title("ESRS Control Panel") #Display title
10.
11. #VARIABLES
12. CH1IsOn = StringVar() #Device 1 enabled variable
13. CH2IsOn = StringVar() #Device 2 enabled variable
14.
15. CH1Stim = DoubleVar() #Device 1 stimulation value variable
16. CH2Stim = DoubleVar() #Device 2 stimulation value variable
17.
18.
19.
20. Run_Stop = IntVar()# Run/Stop variable
21.
22.
23. CH1Stim.set(150) #Initialise Device 1 stimulation value variable (150uA)
24. CH2Stim.set(150) #Initialise Device 2 stimulation value variable (150uA)
25. Run_Stop.set(0) #Initialise Run/Stop variable (0 = not running)
26.
27. #COMMANDS
28.
29. #######################################
30. def FourBackCH1():
31.     global CH1Stim
32.     CH1Stim.set(CH1Stim.get() - 60.0) #Decreases by 4 steps of 15uA
33.
34. def TwoForwardCH1():
35.     global CH1Stim
36.     CH1Stim.set(CH1Stim.get() + 30.0) #Increases by 2 steps of 15uA
37.
38. def OneBackCH1():
39.     global CH1Stim
40.     CH1Stim.set(CH1Stim.get() - 15.0) #Decreases by a step of 15uA
41.
42. def OneBackCH1():
43.     global CH1Stim
44.     CH1Stim.set(CH1Stim.get() + 15.0) #Increases by a step of 15uA
45.
46. #######################################
47.
48. def FourBackCH2():
49.     global CH2Stim
50.     CH2Stim.set(CH2Stim.get() - 60.0) #Decreases by 4 steps of 15uA
51.
52. def TwoForwardCH2():
53.     global CH2Stim
54.     CH2Stim.set(CH2Stim.get() + 30.0) #Increases by 2 steps of 15uA
55.
56. def OneBackCH2():
57.     global CH2Stim
58.     CH2Stim.set(CH2Stim.get() - 15.0) #Decreases by a step of 15uA
59.
60. def OneBackCH2():
61.     global CH2Stim
62.     CH2Stim.set(CH2Stim.get() + 15.0) #Increases by a step of 15uA
63.
```

```python
64. #####################################
65.
66. def Run_Stop_Func(): #toggle a Run/Stop variable
67.     global Run_Stop
68.
69.     if Run_Stop.get == 0:
70.         Run_Stop.set = 1
71.     else:
72.         Run_Stop.set = 0
73.
74.
75. #FRAMING
76. mainframe = ttk.Frame(root, padding = "9 12 9 12") #Setup initial mainframe
77. mainframe.grid(column = 0, row = 0, sticky = (N, W, E, S)) #Setup the mainframe gri
    d
78. mainframe.columnconfigure(0, weight = 1) #Configure mainframe column
79. mainframe.rowconfigure(0, weight = 1) #Configure mainframe row
80.
81. CH1frame = ttk.Frame(mainframe, borderwidth = 5, relief = 'sunken', width= 200, hei
    ght = 800 ) #Make "Device 1" a sunken frame within the mainframe
82. CH1frame.grid(column = 1, row = 3, columnspan = 3, rowspan = 9, sticky =( N, W, E,
    S))
83. CH2frame = ttk.Frame(mainframe, borderwidth = 5, relief = 'sunken', width= 200, hei
    ght = 800 ) #Make "Device 2" a sunken frame within the mainframe
84. CH2frame.grid(column = 6, columnspan = 3, rowspan = 9, row = 3, sticky = (N, W, E,
    S))
85.
86.
87. #GENERAL CONTROLS
88. ttk.Button(mainframe, text = "Update Device").grid(column = 1, row = 1, sticky = W)
     #Update Device button text
89. ttk.Button(mainframe, text = "Run/Stop", command = Run_Stop_Func).grid(column = 2,
    row = 1, sticky = E)  #Run/Stop button text
90. ttk.Button(mainframe, text = "Pair").grid(column = 8, row = 1, sticky = W)  #Pair b
    utton text
91.
92. #CH1
93. CH1checkIsOn = ttk.Checkbutton(CH1frame, text = 'Active', variable = CH1IsOn, #Chec
    kbutton that allows user to enable/disable Device 1
94.             onvalue = 'On', offvalue='Off').grid(column = 1, row = 2, sticky = W
    )
95.
96. CH1TextBox = ttk.Entry(CH1frame, textvariable = CH1Stim).grid(column = 2, row = 3,
    sticky = W) #Device 1 textbox (user can type desired stimulation value here)
97.
98. CH1Slider = ttk.Scale(CH1frame, orient=HORIZONTAL, variable = CH1Stim,
99.                     length=200, from_=1.0, to=333.0).grid(column = 1, row = 4, co
    lumnspan = 3, sticky = W) #Slider that also allows the user to change the value of
    the Device 1 textbox
100.
101.     ttk.Button(CH1frame, text = "<<", command = FourBackCH1).grid(column = 1, ro
    w = 5, sticky = W) #Button containing "<<" used for decreasing Device 1 stim value
    by four steps of 15uA
102.     ttk.Button(CH1frame, text = ">>", command = TwoForwardCH1).grid(column = 2,
    row = 5, sticky = E) #Button containing ">>" used for increasing Device 1 stim valu
    e by two steps of 15uA
103.     ttk.Button(CH1frame, text = "<", command = OneBackCH1).grid(column = 1, row
    = 6, sticky = W) #Button containing "<" used for decreasing Device 1 stim value by
     a step of 15uA
104.     ttk.Button(CH1frame, text = ">", command = OneBackCH1).grid(column = 2, row
    = 6, sticky = E) #Button containing ">" used for increasing Device 1 stim value by
     a step of 15uA
105.
106.     #CH2
107.     CH2checkIsOn = ttk.Checkbutton(CH2frame, text = 'Active', variable = CH2IsOn
    , #Checkbutton that allows user to enable/disable Device 2
```

```
108.                      onvalue = 'On', offvalue='Off').grid(column = 1, row = 2, sti
      cky = W)
109.
110.        CH2TextBox = ttk.Entry(CH2frame, textvariable = CH2Stim).grid(column = 2, ro
      w = 3, sticky = W) #Device 2 textbox (user can type desired stimulation value here)

111.
112.        CH2Slider = ttk.Scale(CH2frame, orient=HORIZONTAL, variable = CH2Stim,
113.                              length=200, from_=1.0, to=333.0).grid(column = 1, row
      = 4, columnspan = 3, sticky = W) #Slider that also allows the user to change the va
      lue of the Device 2 textbox
114.
115.        ttk.Button(CH2frame, text = "<<", command = FourBackCH2).grid(column = 1, ro
      w = 5, sticky = W) #Button containing "<<" used for decreasing Device 2 stim value
      by four steps of 15uA
116.        ttk.Button(CH2frame, text = ">>", command = TwoForwardCH2).grid(column = 2,
      row = 5, sticky = E) #Button containing ">>" used for increasing Device 2 stim valu
      e by two steps of 15uA
117.        ttk.Button(CH2frame, text = "<", command = OneBackCH2).grid(column = 1, row
      = 6, sticky = W) #Button containing "<" used for decreasing Device 2 stim value by
      a step of 15uA
118.        ttk.Button(CH2frame, text = ">", command = OneBackCH2).grid(column = 2, row
      = 6, sticky = E) #Button containing ">" used for increasing Device 2 stim value by
      a step of 15uA
119.
120.        #TEXT LABLES
121.        ttk.Label(CH1frame, text = "Device 1").grid(column = 1, row = 1, sticky = W)
      #Lable denoting Device 1 options
122.        ttk.Label(CH2frame, text = "Device 2").grid(column = 1, row = 1, sticky = W)
      #Lable denoting Device 2 options
123.
124.        ttk.Label(CH1frame, text = "uA").grid(column = 3, row = 3, sticky = W) #Disp
      lay "uA" next to the Device 1 textbox
125.        ttk.Label(CH2frame, text = "uA").grid(column = 3, row = 3, sticky = W) #Disp
      lay "uA" next to the Device 2 textbox
126.
127.        ttk.Label(CH1frame, text = "4").grid(column = 2, row = 5, sticky = W) #Displ
      ay "4" next to << in Device 1
128.        ttk.Label(CH1frame, text = "2").grid(column = 3, row = 5, sticky = W) #Displ
      ay "2" next to >> in Device 1
129.        ttk.Label(CH1frame, text = "1").grid(column = 2, row = 6, sticky = W) #Displ
      ay "1" next to < in Device 1
130.        ttk.Label(CH1frame, text = "1").grid(column = 3, row = 6, sticky = W) #Displ
      ay "1" next to > in Device 1
131.
132.        ttk.Label(CH2frame, text = "4").grid(column = 2, row = 5, sticky = W) #Displ
      ay "4" next to << in Device 2
133.        ttk.Label(CH2frame, text = "2").grid(column = 3, row = 5, sticky = W) #Displ
      ay "2" next to >> in Device 2
134.        ttk.Label(CH2frame, text = "1").grid(column = 2, row = 6, sticky = W) #Displ
      ay "1" next to < in Device 2
135.        ttk.Label(CH2frame, text = "1").grid(column = 3, row = 6, sticky = W) #Displ
      ay "1" next to > in Device 2
136.
137.        root.mainloop()
```

Appendix C

```c
/*
 * File:   main.c
 * Author: Shannon Deale
 *
 * Created on 19 September 2018, 2:32 PM
 */

#include <stdio.h>
#include <stdlib.h>
#include <xc.h>
#include <math.h>          // need this to calculate the sin function

/*
 *
 */
double User_select; //variable for storing user selected value
int random_number; // variable for storing random number
int run_stop = 1; // variable for storing run/stop information

void init(void) {
/* The following pins must be set to digital inputs to prevent damage to the LCD
 * display on the development board (as per the User Guide recommendation).
 * see Documents at:
 * "https://www.microchip.com/Developmenttools/ProductDetails/DM240015"
 * for more detailed information.
 */
//============================= PORTA =================================//

_ANSA15 = 0; // Set the function of RA15 to "digital"
_ANSA14 = 0; // Set the function of RA14 to "digital"

_ANSA10 = 0; // Set the function of RA10 to "digital"

_ANSA6 = 0; // Set the function of RA6 to "digital"
_ANSA5 = 0; // Set the function of RA5 to "digital"
_ANSA4 = 0; // Set the function of RA4 to "digital"
_ANSA2 = 0; // Set the function of RA2 to "digital"
_ANSA1 = 0; // Set the function of RA1 to "digital"

_TRISA15 = 1; // Set RA15 as "input"
_TRISA14 = 1; // Set RA14 as "input"

_TRISA10 = 1; // Set RA10 as "input"

_TRISA6 = 1; // Set RA6 as "input"
_TRISA5 = 1; // Set RA5 as "input"
_TRISA4 = 1; // Set RA4 as "input"
_TRISA3 = 1; // Set RA3 as "input"
_TRISA2 = 1; // Set RA2 as "input"
_TRISA1 = 1; // Set RA1 as "input"
_TRISA0 = 1; // Set RA0 as "input"

//============================= PORTB =================================//

_ANSB15 = 0; // Set the function of RB15 to "digital"
_ANSB14 = 0; // Set the function of RB14 to "digital"

_ANSB12 = 0; // Set the function of RB12 to "digital"
_ANSB7 = 0; // Set the function of RB7 to "digital"

_TRISB15 = 1; // Set RB15 as "input"
_TRISB14 = 1; // Set RB14 as "input"
```

```
62. _TRISB12 = 1; // Set RB12 as "input"
63. _TRISB7 = 1; // Set RB7 as "input"
64.
65. //============================= PORTC =====================================//
66. _TRISC2 = 1; // Set RC2 as "input"
67.
68. //============================= PORTD =====================================//
69. /*
70.  * Note that RD0 must remain set as a digital input only if the phototransistor
71.  * sensor and potentiometer are not used
72.  */
73. _ANSD15 = 0; // Set the function of RD15 to "digital"
74. _ANSD14 = 0; // Set the function of RD14 to "digital"
75. _ANSD13 = 0; // Set the function of RD13 to "digital"
76.
77. _ANSD11 = 0; // Set the function of RD11 to "digital"
78. _ANSD10 = 0; // Set the function of RD10 to "digital"
79. _ANSD9 = 0; // Set the function of RD9 to "digital"
80. _ANSD8 = 0; // Set the function of RD8 to "digital"
81. _ANSD7 = 0; // Set the function of RD7 to "digital"
82. _ANSD6 = 0; // Set the function of RD6 to "digital"
83.
84. _ANSD0 = 0;  // Set the function of RD0 to "digital"
85.
86. _TRISD15 = 1; // Set RD15 as "input"
87. _TRISD14 = 1; // Set RD14 as "input"
88. _TRISD13 = 1; // Set RD13 as "input"
89.
90. _TRISD11 = 1; // Set RD11 as "input"
91. _TRISD10 = 1; // Set RD10 as "input"
92. _TRISD9 = 1; // Set RD9 as "input"
93. _TRISD8 = 1; // Set RD8 as "input"
94. _TRISD7 = 1; // Set RD7 as "input"
95. _TRISD6 = 1; // Set RD6 as "input"
96.
97. _TRISD0 = 1;  // Set RD0 as "input"
98.
99. //============================= PORTE =====================================//
100.        _ANSE4 = 0; // Set the function of RE4 to "digital"
101.
102.        _TRISE8 = 1; // Set RE8 as "input"
103.
104.        _TRISE4 = 1; // Set RE4 as "input"
105.        _TRISE3 = 1; // Set RE3 as "input"
106.        _TRISE2 = 1; // Set RE2 as "input"
107.        _TRISE1 = 1; // Set RE1 as "input"
108.        _TRISE0 = 1; // Set RE0 as "input"
109.
110.        //============================= PORTF =====================================//
111.        _ANSF13 = 0; // Set the function of RF13 to "digital"
112.
113.        _ANSF8 = 0; // Set the function of RF8 to "digital"
114.
115.        _ANSF3 = 0; // Set the function of RF3 to "digital"
116.        _ANSF2 = 0; // Set the function of RF2 to "digital"
117.        _ANSF0 = 0; // Set the function of RF0 to "digital"
118.
119.        _TRISF13 = 1; // Set RF13 as "input"
120.        _TRISF12 = 1; // Set RF12 as "input"
121.
122.        _TRISF8 = 1; // Set RF8 as "input"
123.
124.        _TRISF3 = 1; // Set RF3 as "input"
125.        _TRISF2 = 1; // Set RF2 as "input"
126.        _TRISF1 = 1; // Set RF1 as "input"
```

```
127.        _TRISF0 = 1; // Set RF0 as "input"
128.
129.        //============================= PORTG ===================================
      ==//
130.        _ANSG15 = 0; // Set the function of RG15 to "digital"
131.
132.        _TRISG15 = 1; // Set RG15 as "input"
133.        _TRISG14 = 1; // Set RG14 as "input"
134.        _TRISG13 = 1; // Set RG13 as "input"
135.        _TRISG12 = 1; // Set RG12 as "input"
136.
137.        _TRISG1 = 1; // Set RG1 as "input"
138.        _TRISG0 = 1; // Set RG0 as "input"
139.
140.        }
141.
142.        void DACinit(void){
143.
144.        DAC1CONbits.DACEN = 1;// Enable DAC1 module
145.        DAC2CONbits.DACEN = 0; // Disable DAC2 module
146.
147.        DAC1CONbits.DACREF = 10;// Set reference voltage as 2*INTREF
148.
149.        DAC1CONbits.DACFM = 1;// Set data format as left justified
150.
151.        DAC1CONbits.DACTRIG = 0;// Disabling the trigger input bit
152.
153.        DAC1CONbits.DACTRIG = 0;// Disabling the trigger input bit
154.
155.        DAC1CONbits.DACSLP = 1;// Enable DAC in sleep mode
156.        DAC1CONbits.DACSIDL = 0;// Enable DAC in idle mode
157.
158.
159.
160.        _ANSG9 = 1; // Set the function of RG9 to "analog"
161.        _TRISG9 = 1; // Set RG9 as "output"
162.
163.        _ANSB13 = 1; // Set the function of RB13 to "analog"
164.        _TRISB13 = 1; // Set RB13 as "output"
165.
166.        }
167.
168.        double randn (double mu, double sigma)
169.        /* The following is from:
170.         * https://phoxis.org/2013/05/04/generating-random-numbers-from-normal-
      distribution-in-c/
171.         */
172.        {
173.          double U1, U2, W, mult;
174.          static double X1, X2;
175.          static int call = 0;
176.
177.
178.          if (call == 1)
179.            {
180.              call = !call;
181.              return (mu + sigma * (double) X2);
182.            }
183.
184.          do
185.            {
186.              U1 = -1 + ((double) rand () / RAND_MAX) * 2;
187.              U2 = -1 + ((double) rand () / RAND_MAX) * 2;
188.              W = pow (U1, 2) + pow (U2, 2);
189.            }
190.          while (W >= 1 || W == 0);
```

```c
        mult = sqrt ((-2 * log (W)) / W);
        X1 = U1 * mult;
        X2 = U2 * mult;

        call = !call;

        return (mu + sigma * (double) X1);
    }

    void DAC(void){
    random_number = (int) randn(0x7FFF,User_select/3);
    DAC1DAT = random_number;
    }

    void main(void) {
        init();
        DACinit();
        // code pulling values from the PC will go here
        while(1) {

        if (run_stop = 0)
        {
            User_select = 0x0000; // produce 0V
            DAC();
        }
        else{

            User_select = 0xFFFF; // User selected value (hard coded for now)
            DAC();
            }
        }
    }
```

for more detailed information). The basic logic structure of that code is demonstrated in the flow diagram shown in Figure 16.

To generate the random numbers from a Gaussian distribution and the user selected value the following logic based on the polar method is used [93]:

- Set up, $U1 \sim U(-1,1)$ and $U2 \sim U(-1,1)$ (where $U(-1,1)$ is the uniform distribution with range of -1 to 1)
- Generate W until $W = U1^2 + U2^2 < 1$
- Let $X1 = U1 * \sqrt{\dfrac{-2\ln(W)}{W}}$ and $X2 = U2 * \sqrt{\dfrac{-2\ln(W)}{W}}$

At this point X1 and X2 are now normal (Gaussian) random variables with a mean of 0 and a standard deviation of 1. To enable X1 and X2 to be normal random variables with a mean of μ and a standard deviation of σ the following transform is applied.

- $X_{\mu,\sigma} = \mu + \sigma X_{0,1}$ (where $X_{0,1} \sim \mathcal{N}(0,1)$ and $X_{0,1} \sim \mathcal{N}(\mu,\sigma)$

The choice was made to use the polar method to generate the pseudo-random numbers as it was simple to execute in code and is considered superior in terms of efficiency to the Box-Muller transform.
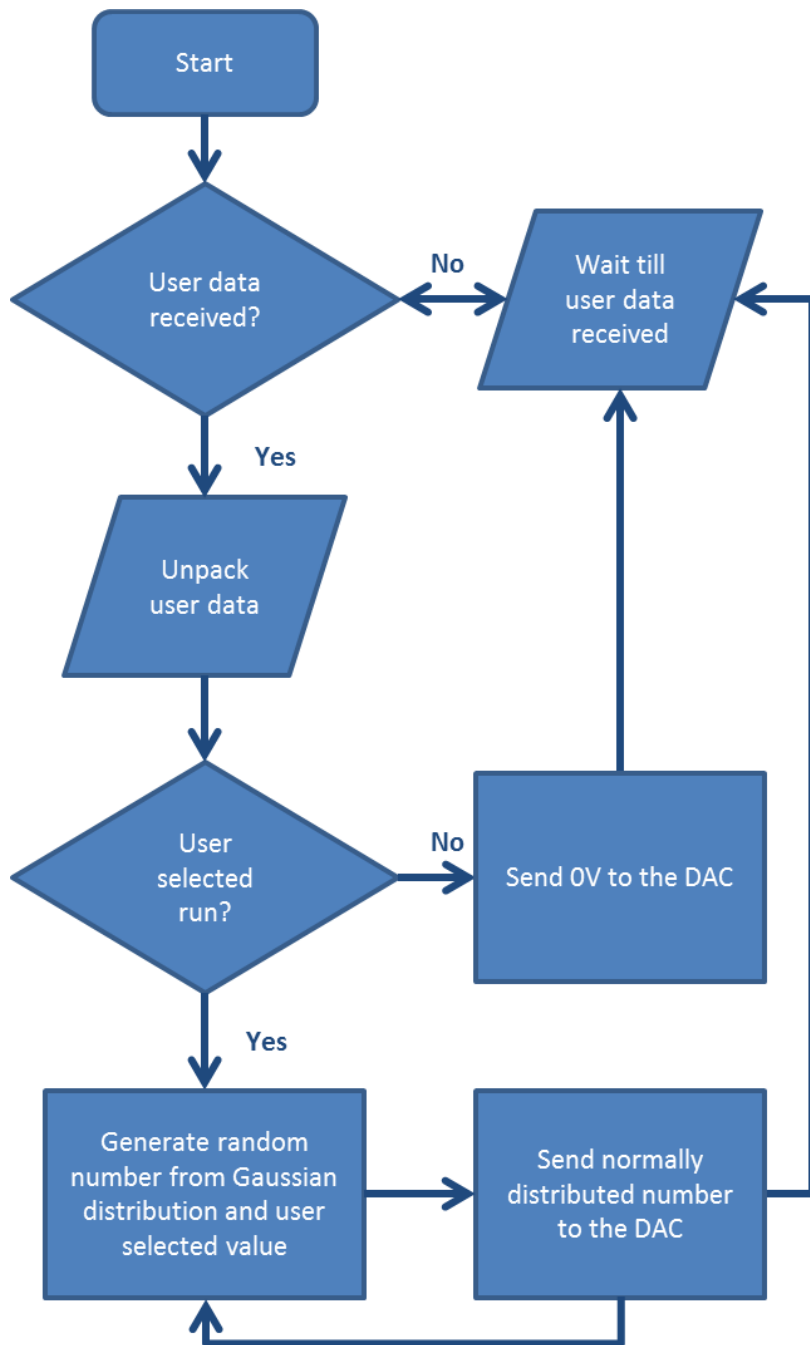
BME1634 Electrical Stochastic Resonance System

Shannon Deale

Figure 16 Flowchart describing the logic for the device software

7 Project Development

The project development stage was to involve the breadboarding and validation of the circuit designs, the manufacture and assembly of the PCBs, the development of the device software and PC GUI application as well as the assembly of the device into a case. However, due to time constraints not all of these tasks would be completed in the time available (see section Changes to Project Schedule and Scope for more information regarding this).

7.1 Breadboarding

The HVPSU and HVCP were breadboarded (shown in Figure 17) so that both circuits could be tested and validated against the results published in Karpul et al. [37]. Breadboarding enables the circuits to be set up in such a way that they can be manipulated and reconfigured with ease. This is important for the testing phase of the circuitry as it allows for the placement of temporary components such as load resistors to make measurements based on predictions.

The HVPSU was tested by measuring the voltage potential between HV+ (+9V) and HV- (-63V). First test was with no load, and then following tests involved placing load resistors of known values (27kΩ, 15kΩ, 10kΩ, 6.7kΩ, 4.6kΩ and 3.3kΩ) to increase the current draw from no load up to 20mA in increments of 2.5mA. The HVCP was similarly tested by loading with known resistor values (15kΩ, 30kΩ, 56kΩ, and 72kΩ) to simulate skin impedance and ensure that the current pump would change the voltage accordingly to deliver ±1mA through the load. A current draw of ±1mA was measured from the 9V battery when the HVPSU and HVCP are connected with no load.
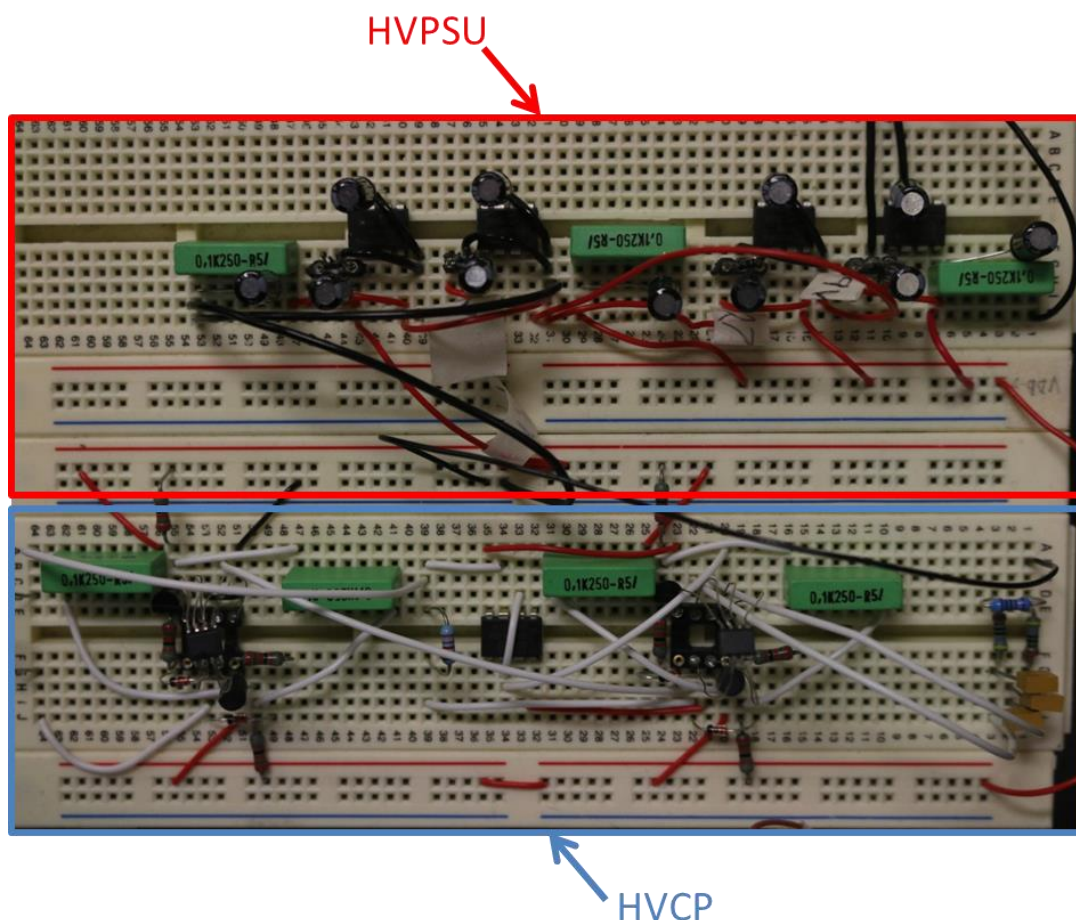

Figure 17 Breadboard of the HVPSU (red) and HVCP (blue)

BME1634 Electrical Stochastic Resonance System

Shannon Deale

The control circuitry shown in Figure 18 was also breadboarded which includes a dsPIC33FJ128GP802 microcontroller, an isolated DC-DC converter, a voltage inverter and a rail to rail op amp. The microcontroller is set up in such a way that it can be programmed from the PC via a RJ11 cable connected to an ICD3 kit. Testing for the level shifter circuit was conducted by using a desktop power supply to simulate the 0V to 3.3V DAC input and the output voltage was measured with a mustimeter.
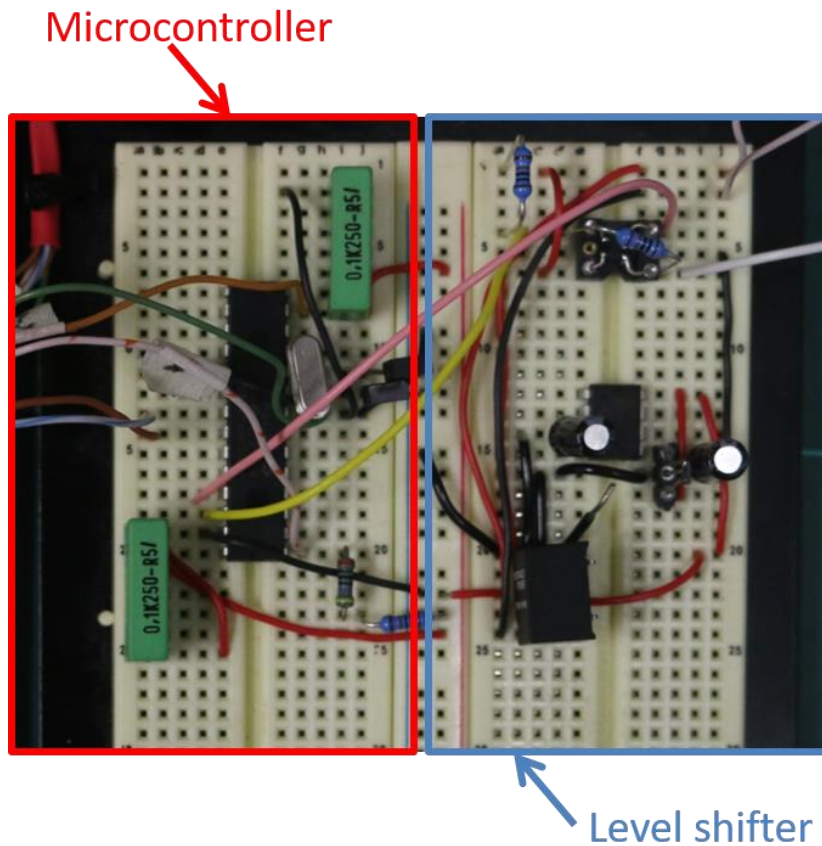
Figure 18 Breadboard of the microcontroller (red) and the level shifter circuit (blue)

Some issues were encountered during the development of the breadboarded circuits. However, as breadboard boarded circuits are easy to manipulate and modify, troubleshooting issues was reasonably simple with the only consequence being lost time. For more information regarding trouble shooting the breadboards see the Challenges section.

7.2 Printed Circuit Board Designs

A PCB was designed for both the HVPSU and the HVCP in Altium Designer 6. The electronic design software Altium Designer 6 was selected for this task and required some training from supervisors to understand the various functions and tools available. The best practices for PCB design had to be learned as the designs for each PCB were developed. Each circuit was drafted several times before resulting in the following designs.

Figure 19 and Figure 21 are the schematic drawings that were designed in Altium Designer 6; these included the footprints downloaded from Altium libraries for the specific components identified in the circuit design stage of the project. Figure 20 and **Error! Reference source not found.** are the final PCB designs designed in Altium Designer 6. The goal with these boards was to minimise the size of the boards as much as possible whilst maintaining suitable

BME1634 Electrical Stochastic Resonance System

Shannon Deale

track widths so that the boards could be manufactured and assembled within SA BME using a simple PCB milling machine.
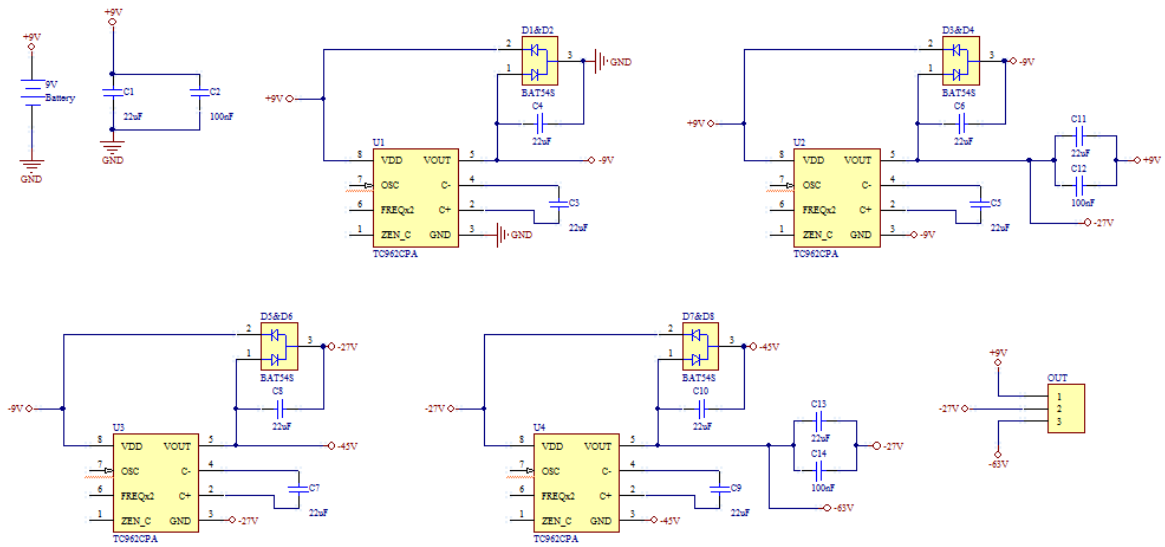
Figure 19 Altium schematic drawing for HVPSU
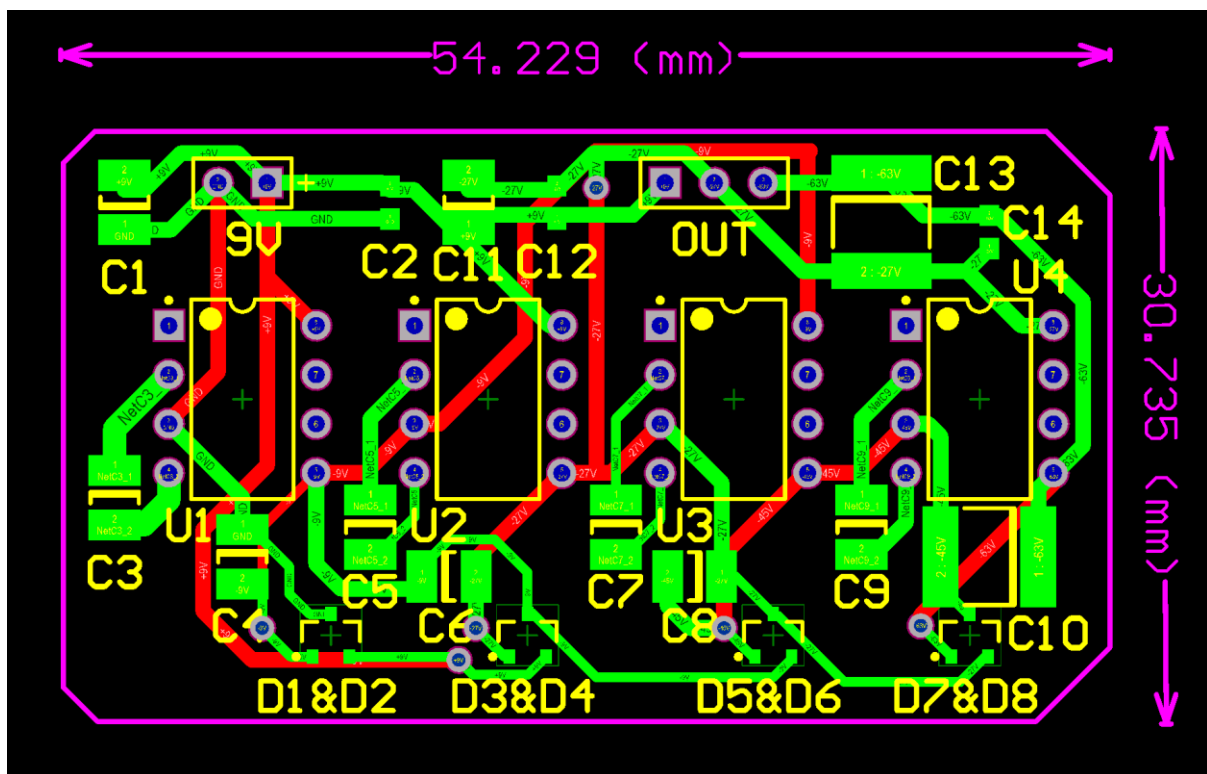
Figure 20 Altium PCB drawing for HVPSU

BME1634 Electrical Stochastic Resonance System

Shannon Deale
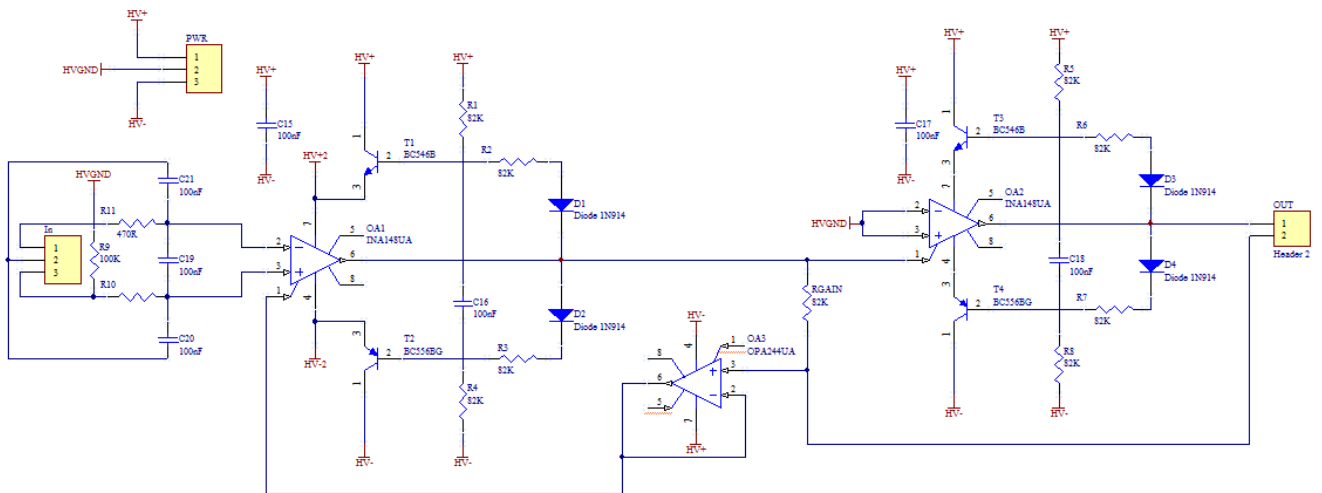
Figure 21 Altium schematic drawing for HVCP
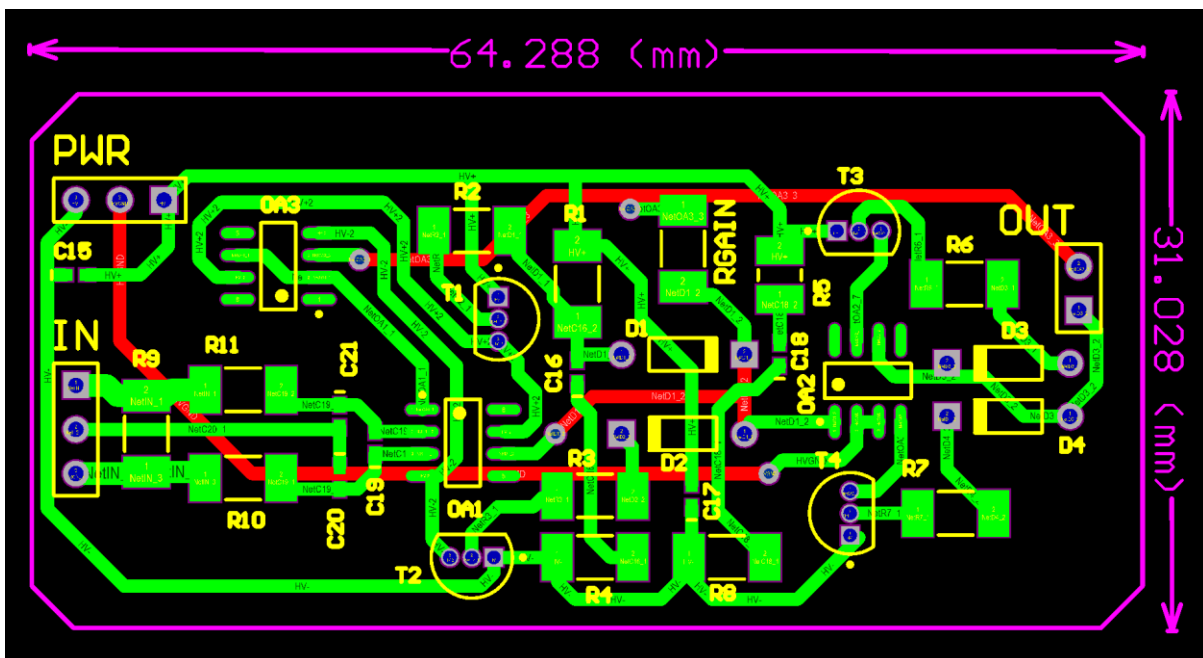
Figure 22 Altium PCB drawing for HVCP

Whilst there were no major obstacles encountered during the design of the PCBs because new skills and practices were necessary to learn in order to design acceptable PCBs and so this task required more time than originally expected. Due to the slower than expected progress a reprioritisation of the task order for the project was conducted to ensure the most critical tasks were being completed first (see the Original and Actual Schedule section for more information regarding reprioritised tasks). Designing a PCB for the control circuitry was not determined to be critical at this stage and therefore at the time of writing there are only designs for the HVPSU and the HVCP.

The PCBs that were designed did meet the criteria of being sufficiently small enough in physical dimensions to suit a wearable system whilst still having track widths large enough to be manufactured within SA BME. This means at the time of writing the HVPSU and HVCP boards are ready to be printed and have their surface components mounted.

48

7.3 Software Development

One of the tasks that was deemed a priority was the development of the software components.

Figure 23 shows the GUI developed in Python that forms the user interface for the device. The final design differs slightly from the proposed design illustrated in Figure 15. The run and stop buttons were combined into a single Run/Stop button for user convenience and the CH1 and CH2 buttons have been replaced with Device 1 and Device 2 (see Planned Scope vs Actual

BME1634 Electrical Stochastic Resonance System
Shannon Deale

Scope for more information regarding this). For the full code generating this GUI see

SA Health

Electrical Stochastic Resonance System

Project Completion Report

Government
of South Australia

SA Health

Flinders
UNIVERSITY

BME Student
11/24/2017

BME1634 Electrical Stochastic Resonance System
Shannon Deale

Appendix B.
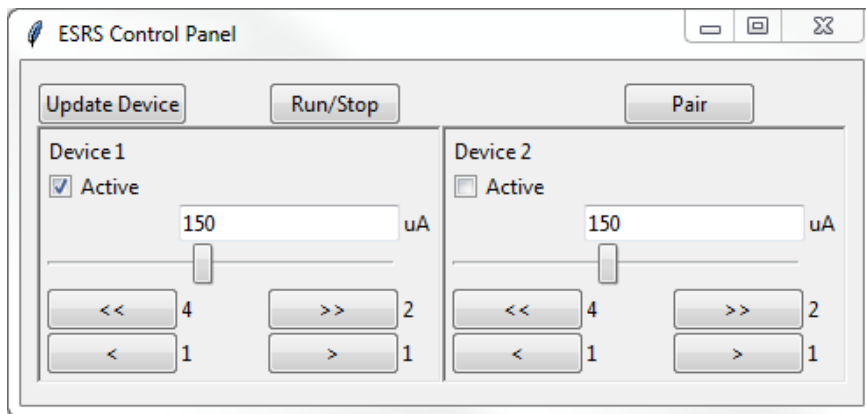
The Arduino code (mentioned in the The choice was made to implement the isolation within the control circuitry as the HVPSU and HVCP designs were being adapted from Karpul et al. [37] Changing that circuit may result in an undesirable change in performance, it was also more convenient to include isolation as part of the control circuitry design stage rather than attempting to implement it into an existing circuit design.

Software section of this document) from the previous prototype system was adapted into C

code (see

BME1634 Electrical Stochastic Resonance System
Shannon Deale

Appendix for full code listing) for the PIC microcontroller. At this stage in the project the decision was made to use a development board for the PIC24FJ128GC010 (shown in Figure 24) to simplify some of the elements of software development by removing the potential of hardware related errors and because using the dsPIC33FJ128GP802 due to contact pitch size was no longer justified (see sections Original and Actual Schedule and Resulting Changes for more information regarding this).
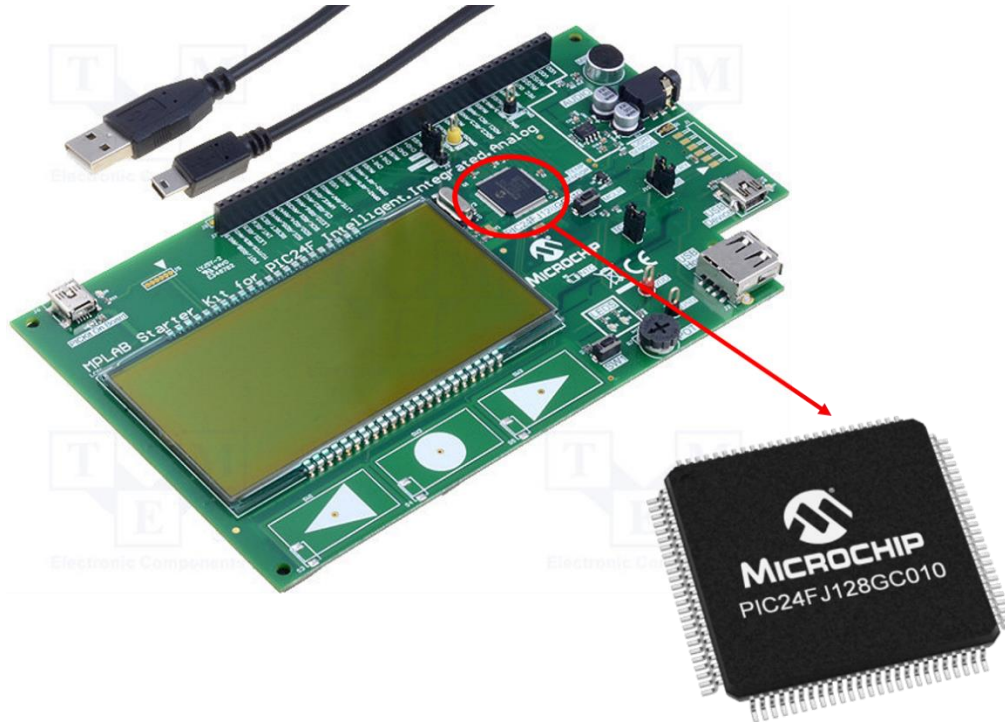
Figure 24 DM240015 development kit for the PIC24FJ128GC010 microcontroller

8   Changes to Project Schedule and Scope

Changes can happen at any point during the lifecycle of a project, often these changes are for the better after learning new information relevant to the project. In this project the original and actual schedule did not exactly match due to underestimating the time that tasks would take as well as time for troubleshooting hardware and software time. This resulted in some changes being made to the project in the interest of time.

8.1   Original and Actual Schedule

The original timeline for the project was estimated using the Gantt chart shown in Figure 25. This timeline indicates that the prototype system would be built and tested by around the 10th of August, and then simple experiments of standing balance trials with participants would be conducted in the following months. In hindsight this underestimated the time needed for troubleshooting, validation, additional tasks that were not identified in the planning stage or setbacks related to software and hardware development.
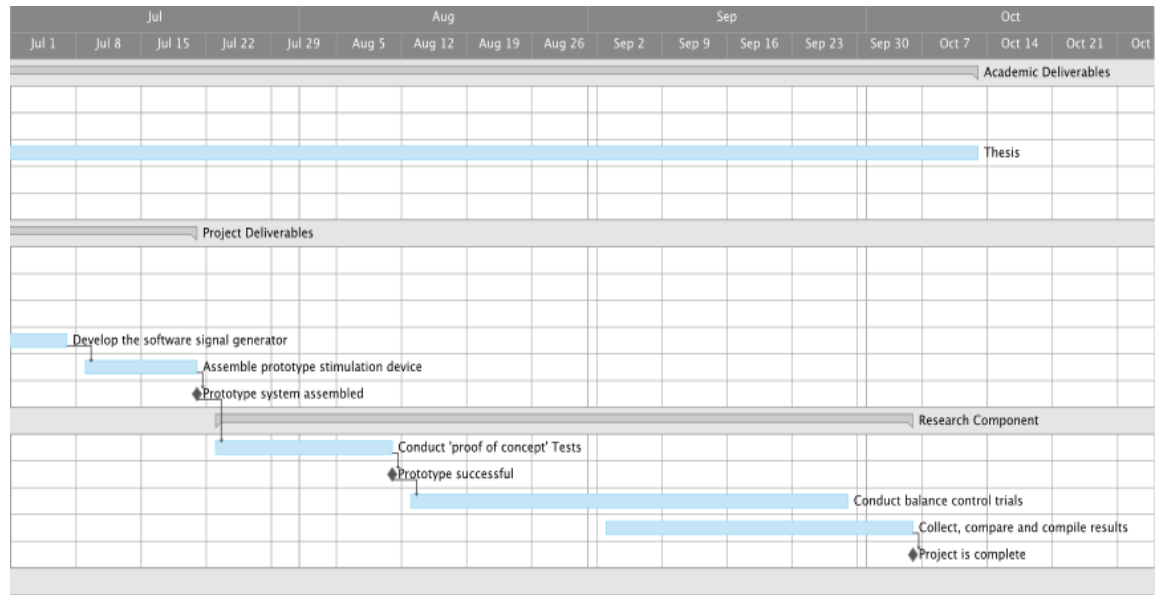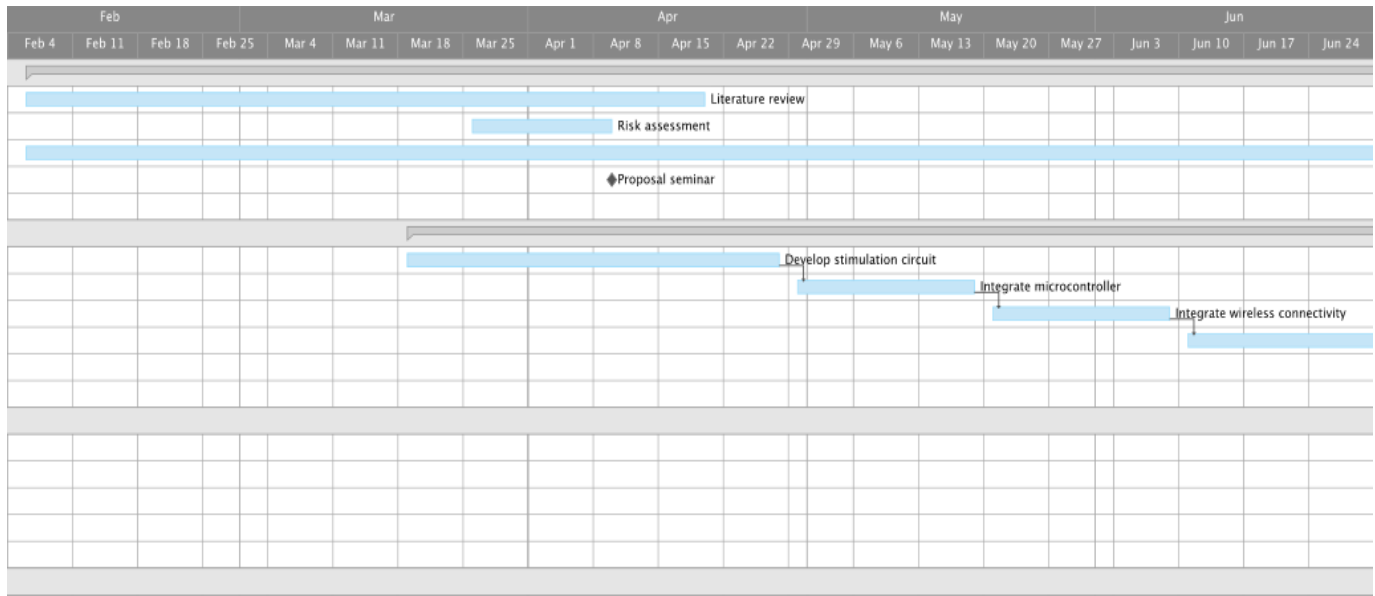
Figure 25 Original Gantt chart

BME1634 Electrical Stochastic Resonance System   Shannon Deale

At the end of July an updated Gantt chart (shown in Figure 26) was developed to best prioritise the remaining time into the most critical tasks. At this stage the PCBs were in the process of being designed, so the design of the HVPSU and HVCP PCBs were completed. The tasks deemed highest priority were the breadboarding and validation of the control circuitry as well the development of the device specific software (the GUI had been developed already at this time). These tasks were selected specifically as completing them will leave minimal design work for someone new picking up the next stage of the project. Instead the next stage will be able to focus solely on assembly and testing of the prototype system.

At the time of writing the project is on track with the updated Gantt chart, with the current task being to implement the wireless communication between the GUI and the device software. Once this task is complete the entire system can be tested and validated as a breadboarded system so that future work can focus on the manufacture and assembly of the final prototype.
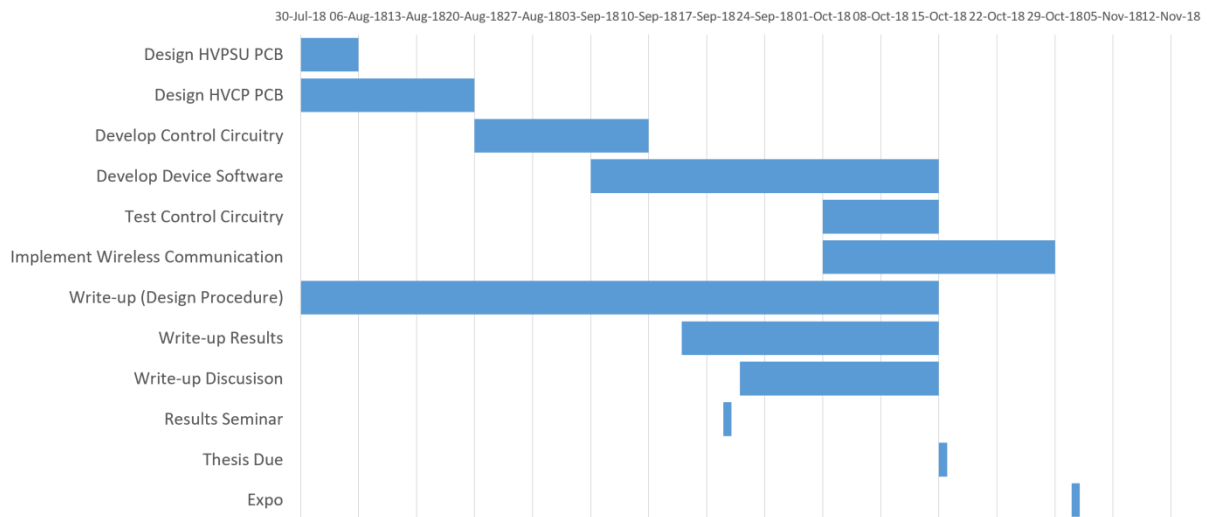
Figure 26 Updated Gantt chart (from 30th of July)

8.1.1   Resulting Changes

During the reprioritisation process it became clear that there was insufficient time remaining in the project to manufacture and assemble the PCBs. This meant that the justification for using the dsPIC33FJ128GP802 because of its larger pitch size was no longer valid. So, it was decided that the DM240015 development kit for the PIC24FJ128GC010 would be purchased and used to develop the device software. The PIC24FJ128GC010 has a much lower current draw and is smaller in physical size, making it ideal for a wearable battery-operated device. In the interest of time, the choice was made to use a development kit as it would be more efficient and eliminate potential problems with hardware when developing the software application.

8.2   Planned Scope vs Actual Scope

One notable change to the scope of the project was made during the design phase. The original specification (see Identification of Design Requirements and Specifications for more information) stated that the device should have a minimum of two stimulation channels (two electrode pairs). However, in the circuit design phase it was identified that electrical isolation would be necessary for the circuit to function, which also means that implementing two

BME1634 Electrical Stochastic Resonance System
Shannon Deale

channels would require the use of two sets HVPSU and HVCP circuits. This increases both the size and current draw of the circuit significantly.

In light of this information a change to the scope was made, instead of using two channels, multiple devices with unique identification (ID) numbers would be used. This change has advantages and disadvantages

Advantages of multiple devices:
- Failure of one device does not mean the failure of other devices connected to the subject and can be easily replaced by back up units.
- Due to safety concerns stimulation electrodes from a single device cannot be placed on the opposite sides of the subjects body [86]. If the reference voltage changes slightly a voltage potential between the two channels forms which could cause current to flow through the heart (potentially fatal if current is high enough). Multiple devices eliminate this risk entirely.
- Each individual device maintains its small size and current draw.
- The number of devices can be selected to suit the number of electrode pairs required.
- Some devices can be recharging while others are still in use.

Disadvantages of multiple devices:
- Subject must wear more than one device.
- Additional software development is required to ensure unique IDs for each device.

8.3   Challenges

The breadboard used in the project came with wires pre-soldered onto the header connections at the top of the board. These were used to implement +9V and the reference voltage for the HVPSU. At some stage before receiving this breadboard the wire soldered to the reference header had severed internally meaning that a battery or desktop power supply connected to the header would only connect the +9V side. Troubleshooting was done by splitting the HVPSU into stages and testing each one, it was observed that the first two voltage inverter stages were producing the same output which was unexpected considering they had different ground references. This prompted the testing of the ground lead connected to the header where the fault was found.

One of the diodes within a BAT54S package used in the HVPSU exploded at some stage which was difficult to determine through troubleshooting. The device is very small, so it was hard to see the rupture on the casing with the naked eye. Eventually using a multimeter the damaged component was identified and the rupture confirmed under a microscope. It was correctly configured within the circuit so the problem potentially occurred as a result of an accidental short while manipulating the circuit. Plausible but less likely is that the device malfunctioned because of a manufacturing fault. Once found the diode was replaced and the circuit functioned as expected.

The HVCP had seemingly intermittent errors during the development stage that resulted in the output voltage not changing appropriately to deliver 1mA through to the load. Troubleshooting this circuit was a challenge as it could not be broken up into stages due to the feedback loops. The cause of the problem was never identified but was eliminated through removing all components from the breadboard and reconstructing the circuit entirely.

The issue could have resulted from a number of problems including loose connections on the breadboard, damaged wiring or unintended shorts.

8.4 New Skills and Lessons Learnt

Several lessons were learned throughout the course of this project.

- First time developing in Python and thus all experience with the language was gained through this project, including how to use the tkinter packages for developing a GUI for a desktop.
- First time using Altium Designer 6 and so all experience with using the tools and techniques available has been gained through this project.
- Good practices in PCB design, including star ground, effective use of vias, minimising track lengths etc.
- Gained further experience developing software in C, particularly in programming a microcontroller through C which was a new experience.
- Gained experience with troubleshooting breadboard circuits and debugging software issues. Learning methods for finding common issues such as determining loose connections through using a mustimeter test for continuity.
- Breadboards are imperfect devices which can cause problems during testing and validating. These include current leak, loose connections, long "loopy" wires that can pick up electrical interference or produce resistance and sticky residue in the connections (from using components pulled out of cut tape) creating insulation or making it difficult to place components.
- Dr Ben Patritti is from a clinical background, this meant that discussions as a team were multi-disciplinary. Through this project understanding and experience was gained regarding discussion and finding compromises on issues as part of a multi-disciplinary team.
- Estimating the time that tasks will take to complete accurately is very difficult, extra time should be planned for troubleshooting, validation, additional tasks that were not identified in the planning stage, dead-ends in research and setbacks.

9 Cost Statement

A typical budget for an SA BME project is $1000 unless additional budget can be justified. The table in Appendix D shows the cost and quantity of all parts to be purchased, the total of which came to $344, well under the $1000 budget. Not all of the components in this list have been purchased at the time of writing, as some of the surface mount components are only necessary for the PCBs which have not been printed at the time of writing.

10 Results

Following are the results of testing the circuitry during the breadboarding stage and the software during its development. The HVPSU, HVCP and control circuitry (level shifter) were all tested as described in the Breadboarding section and the output signal generated by the device software was observed using an oscilloscope.

10.1 Circuit Testing

10.1.1 HVPSU

Figure 27 and Figure 28 show the HVPSU voltage plotted against output current. The first test was with no load and the following tests involved placing load resistors of known values (27kΩ, 15kΩ, 10kΩ, 6.7kΩ, 4.6kΩ and 3.3kΩ) to increase the current draw from no load up to 20mA in increments of 2.5mA. Karpul et al. performed a similar test loading their circuit such that it draws up to 20mA however, they did not use consistent increments instead opting to use more data points in the typical operating range (0mA – 5mA) which can be seen in Figure 27.
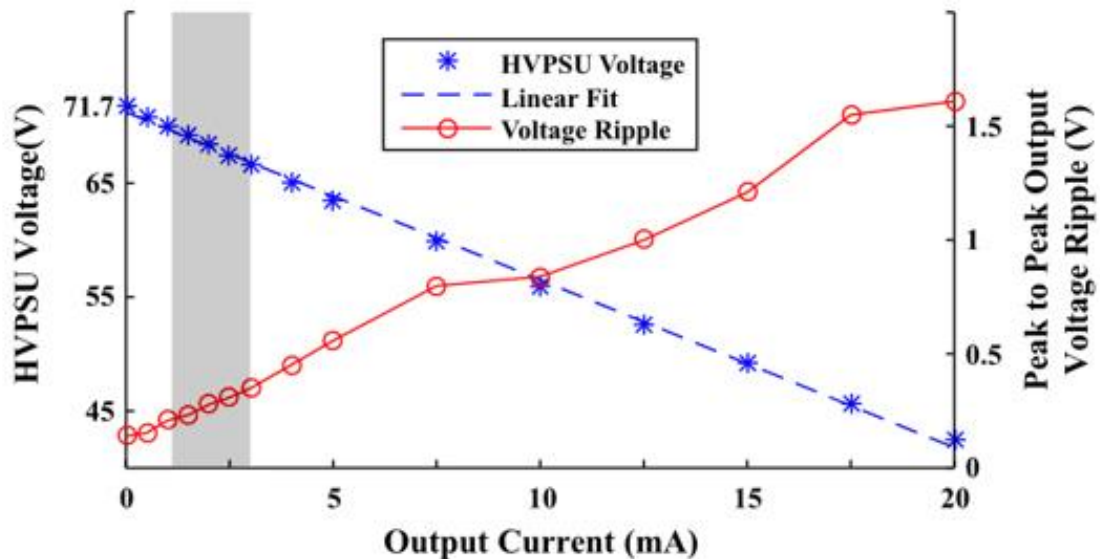
Figure 27 Results of the HVPSU from Karpul et al. [37]
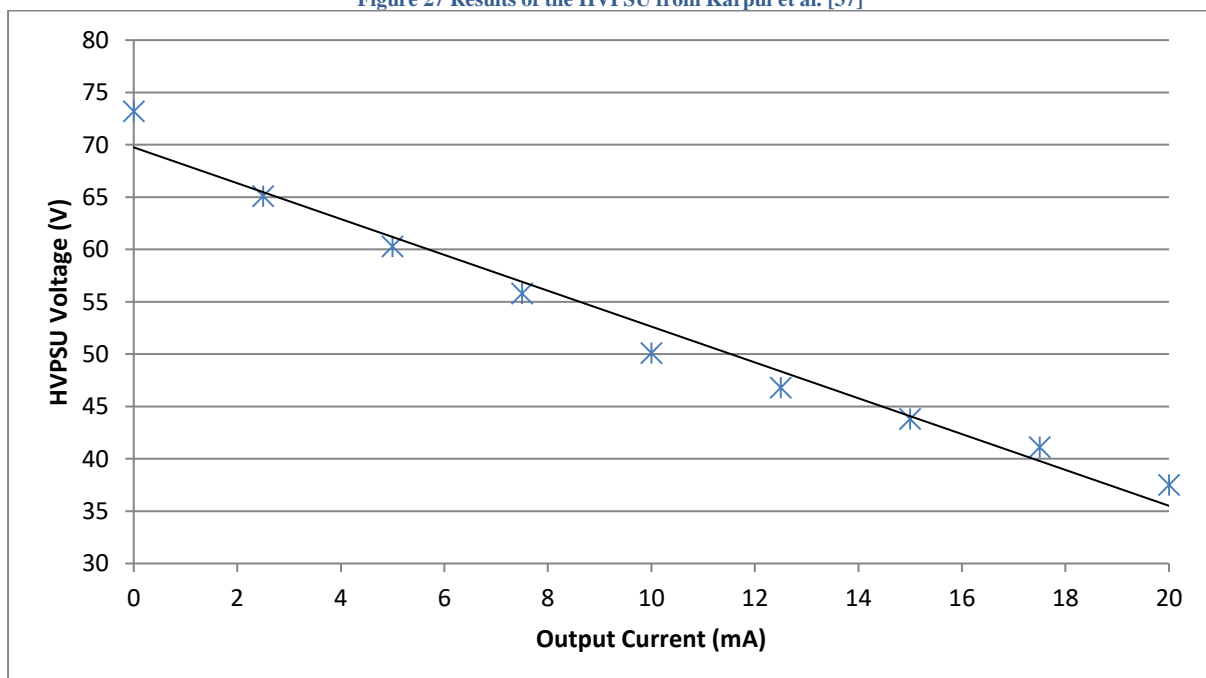
Figure 28 Results from HVPSU breadboard showing the output voltage dropping linearly with current draw.

10.1.2 HVCP

BME1634 Electrical Stochastic Resonance System

Shannon Deale

Figure 29 shows the tests of the HVCP using known resistor values of 15kΩ (a), 30kΩ (b), 56kΩ (c), and 72kΩ (d) which effectively represent load skin impedances. The voltage output across that resistor was measured using a multimeter and the resulting load current was calculated using Ohm's law.
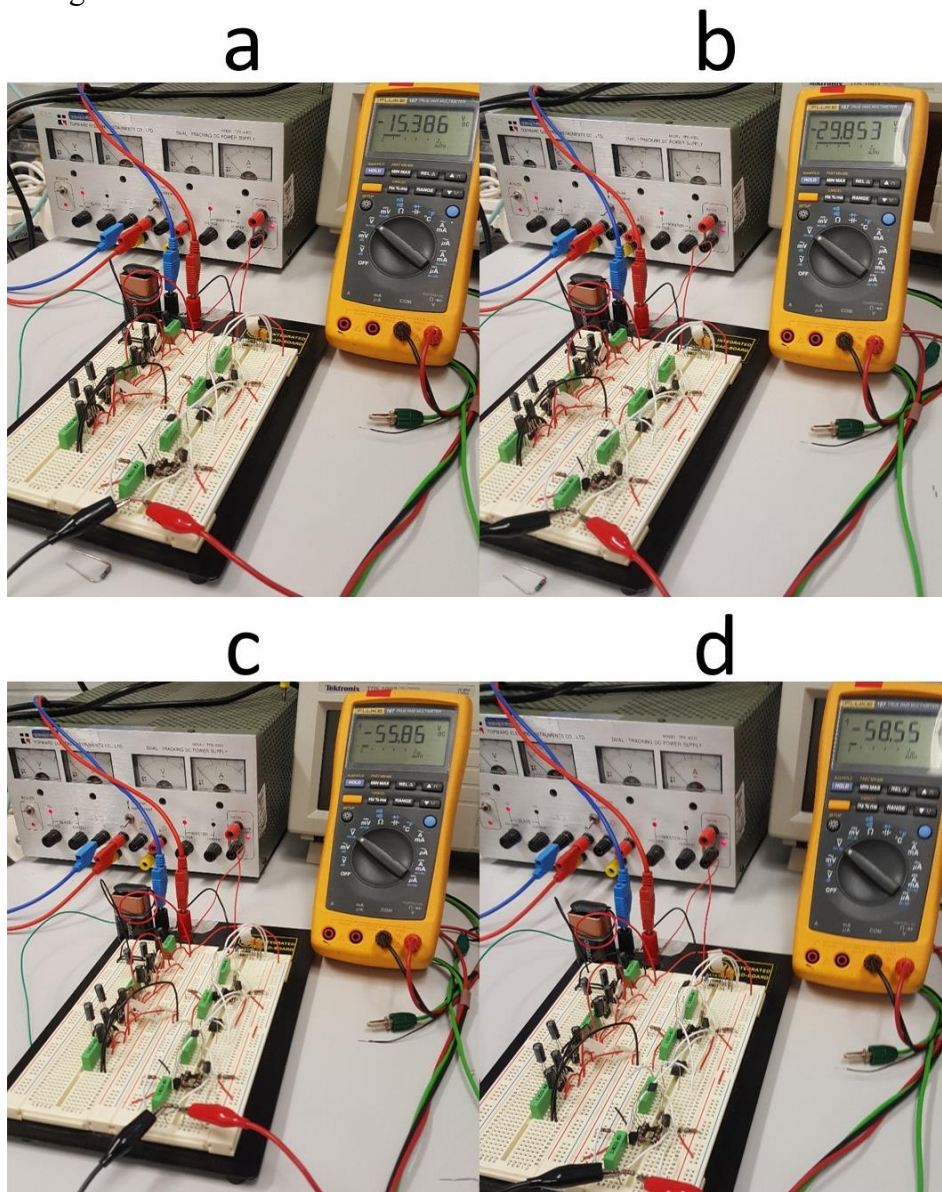
Figure 29 HVCP load current tests illustrating the setup with the HVCP breadboard circuit and multimeter voltage readings for 4 known resistor values (a) 15kΩ, (b) 30kΩ, (c) 56kΩ, and (d) 72kΩ

Table 3 shows the results calculated from the multimeter readings observable in Figure 29 a, b, c and d.

Table 3 Results from the load current tests showing the measured voltage readings for 4 known resistor values 15kΩ, 30kΩ, 56kΩ, and 72kΩ.

Load resistor (kΩ)	Measured Voltage (V)	Calculated Load Current (mA)
15	15.38	1.03
30	29.85	0.99
56	55.85	0.99
72	58.55	0.81

BME1634 Electrical Stochastic Resonance System

Shannon Deale

10.1.3 Current Draw

Table 4 summarises a comparison of the 9V supply current drawn under what can be considered "worst case" loading conditions for the circuits of the Karpul et al system and the current system. Figure 30 shows the testing used in the current project to obtain the results displayed in Table 4 for 0mA and 1mA test conditions (-1mA test condition not depicted). A 58kΩ load resistor was used to test the current system as it was the closest to the target 60kΩ that was available in the SA BME storeroom.
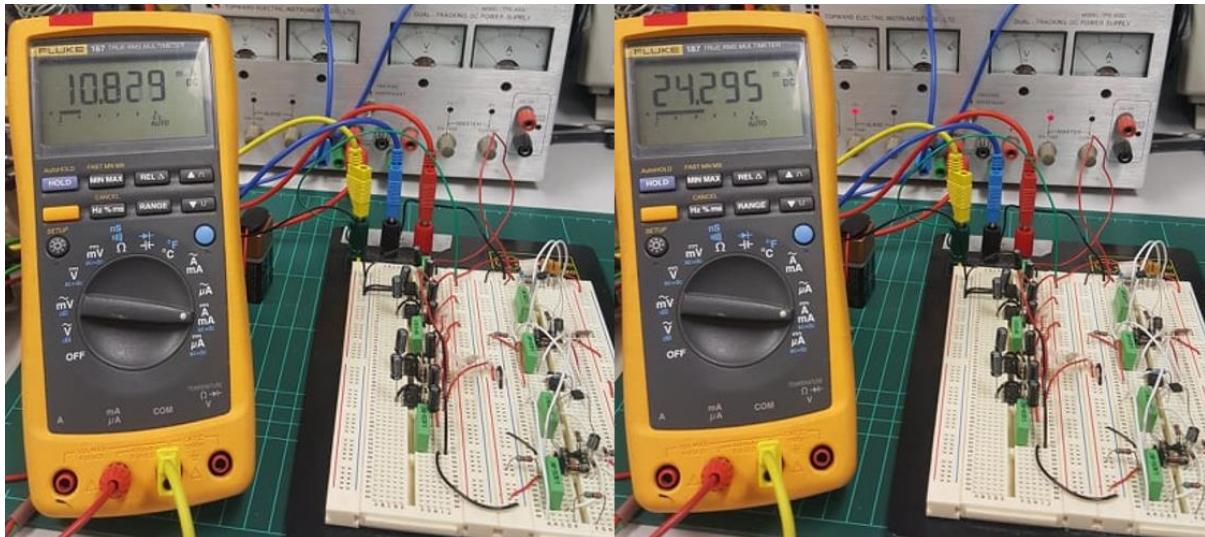
Figure 30 9V supply current draw tests with a load current of 0mA DC (left) and 1mA DC (right)

Table 4 9V supply current draw under various drive conditions for for the circuits of the Karpul et al system (load of 60kΩ) and the current system (58kΩ load).

Load Current	0mA DC	1mA DC	-1mA DC
9V supply current (mA) from Karpul et al. [37]	11.69	25.6	25.9
9V supply current (mA) from breadboard circuit	10.83	24.29	24.64

10.1.4 Control Circuitry

The level shifter circuit was tested using a desktop power supply to ensure that it could achieve ±3.3V from a 0V to 3.3V input, the results are shown in Figure 31.

BME1634 Electrical Stochastic Resonance System

Shannon Deale
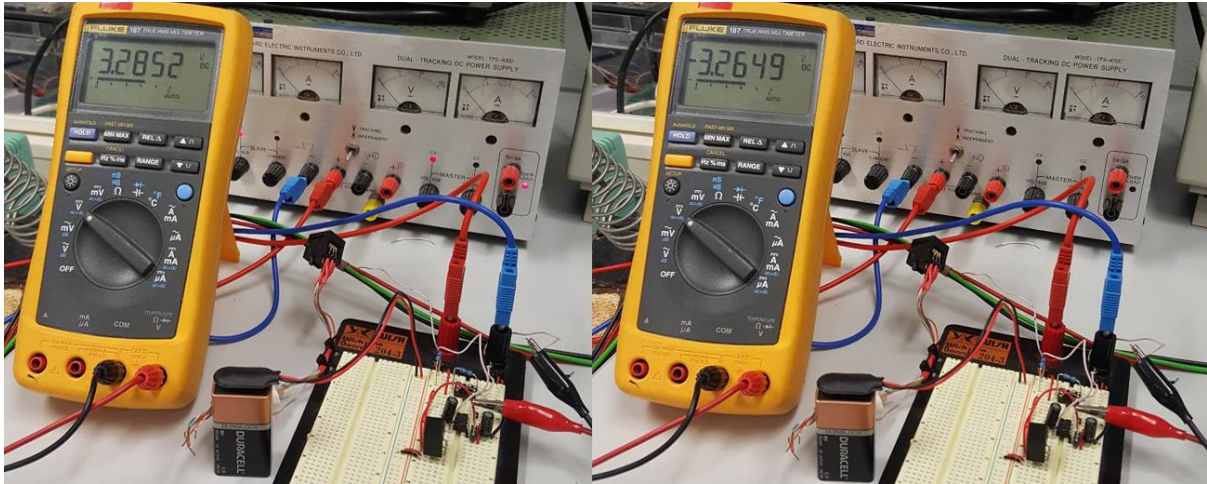
Figure 31 Testing the level shifter circuit with a 0V input (left) and a 3.2V input (right)

10.2 Software

The output signal produced by the PIC24FJ128GC010 DAC output being inputted into the level shifter circuit was measured using an oscilloscope (signal shown in Figure 32). The output signal appears to be normally distributed but at the time of writing does not achieve the ideal pulse frequency of 1kHz (current achieves approximately 6kHz).
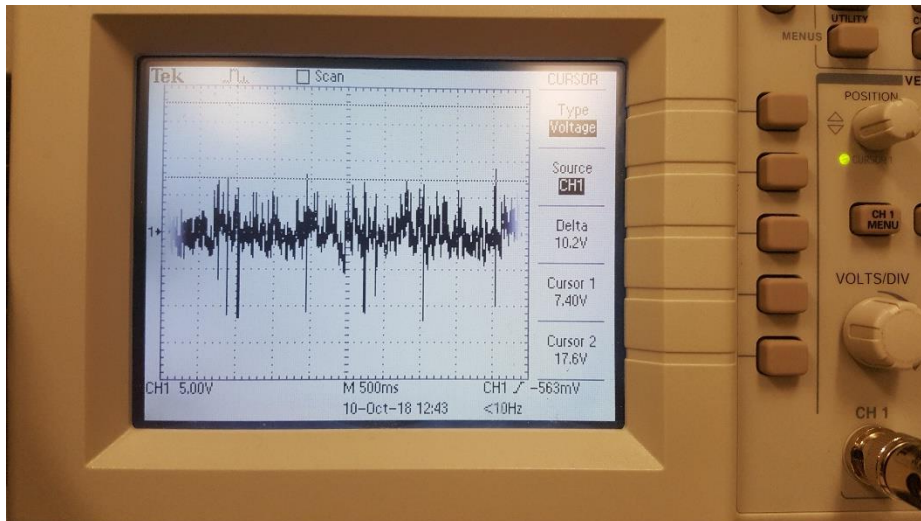
Figure 32 Output signal of PIC24FJ128GC010 and level shifter

11 Future Development

The task being undertaken at the time of writing is implementing the wireless communication between the GUI developed in Python for the PC and the device software developed in C. The plan is to have the PC push the values to the device serially via a Bluetooth connection.

Recommendations for future development on this project are as follows:

- The PCBs for each of the designed circuits should be manufactured, assembled and tested. It is recommended that a PCB for the HVPSU, HVCP and control circuitry be manufactured separately so that each circuit can be tested independently. The inclusion of test points and some light emitting diodes (LEDs) may also assist in troubleshooting and validating the PCB designs.

BME1634 Electrical Stochastic Resonance System
Shannon Deale

- The signal generation software can be improved by using interrupts to produce the DAC output, enabling precise control over the pulse frequency of the outputted signal. Also using interrupts would enable the use of the power idle mode built into the PIC24FJ128GC010, this could be implemented in such a way that when the user has set the Run/Stop variable to stop the PIC24FJ128GC010 saves power by switching to idle mode and turning off the DAC.
- The device will need a housing for the PCBs and battery, the recommendation would be to 3D print casing customised for this particular device. 3D printing suits this application as the casing size can be minimised as much as possible this way (also a smaller design means less plastic used and relatively short printing times).
- A battery needs to be selected, criteria that's important is capacity (should be between 300-500mAh) size (needs to be as small as possible) and finally the battery should be rechargeable for convenience.
- The convenience of the GUI could be improved by adding a function that saves the current stimulation settings as a profile so that it can be returned to quickly and easily when re-using it with a specific individual.
- Another convenient feature possibly worth exploring is automating the 4, 2, 1 decending staircase method [92], into a "find threshold routine" where the user is only required to hit buttons "yes" and "no" (yes meaning "yes the subject can feel the stimulus" and no meaning "no the subject does not feel the stimulus") on the GUI and then after a certain number of reversals (based on Dyck et al. [92]) the threshold is calculated and set.

In regard to this project, Dr Ben Patritti intends to test the device on individuals that have impaired balance control resulting from the deterioration of the person's somatosensation. Preliminary work would likely involve testing the system on young adults (evidence shows that the somatosensory sensitivity and balance of even young adults can benefit from input noise [16, 25, 35]), older adults and then progress to patient groups. This includes older adults and patients that suffer from neurological conditions such as diabetes, strokes, and multiple sclerosis. Dr Patritti also believes the benefit may also extend to patients with Parkinson's disease and children with cerebral palsy. Testing the device on children may be difficult as they may find the stimulation discomforting when setting thresholds but it is feasible it could improve their sense of touch.

These are only the main conditions which potentially may benefit from the effects of the stimulation but it's plausible that there may be other patient groups that could benefit if impaired somatosensation is the issue. Dr Patritti would also like to use the device to explore the possibility of also adding some sort of complimentary physical therapy to establish if any lasting benefits exist, likely facilitated by neuroplasticity (much like the '*carry over effect*' observed when applying functional electrical stimulation (FES) [81]).

The information obtained from these tests will hopefully lead to the development of devices that will operate as assistive technology in a rehabilitation setting, improving or restoring the quality of life for individuals with the aforementioned conditions. Commercial potential for the system or a future iteration of the system can be investigated with the aim of producing home-use devices that can improve the quality of life for individuals that suffer from impaired somatosensation.

BME1634 Electrical Stochastic Resonance System
Shannon Deale

12 Discussion

The objective of the project was to design and develop a prototype system that can deliver an adjustable random electrical stimulus (in the form of pseudo-white Gaussian noise) to sites on the body via electrodes. Once the desired sub-sensory level of the noise stimulus was set the system would need to continue to deliver the noise stimulus for a prolonged period of time until the device is switched off or the stimulus setting changed. The main milestones of this project were to design, develop and test various electronic circuitry and software components needed to assemble this prototype system.

It was determined that the circuitry must comprise of a HVPSU, HVCP and control circuitry that would be driven by software consisting of two parts. A GUI that enables the user to set the stimulus parameters and signal generation software to generate the pseudo-white Gaussian noise.

12.1 HVPSU

The HVPSU circuit adapted from Karpul et al. was breadboarded and tested, comparing the results to those published by Karpul et al. In both circuits the output voltage drops linearly with current draw (shown in Figure 27 and Figure 28), Karpul et al. reported that their circuit had an output impedance of 1.47kΩ and their trend line had a linear fit of $R^2 > 0.998$ [37]. By applying Thevenin's Theorem the output impedance was calculated as 1.71kΩ for the breadboarded HVPSU in this project and the trend line had a linear fit of $R^2 = 0.975$. A slightly higher output impedance is expected with a breadboarded circuit vs a PCB, overall the results of the two circuits are comparable and indicate the performance of the current circuit will fulfil the purpose of the system.

12.2 HVCP

The tests of the HVCP demonstrated it achieved the target 1mA for each of the known resistor values except the 72kΩ resistor (shown in Table 3), in this case the output voltage reached a peak of 58.5V and hence the maximum load impedance for this circuit is 58kΩ. The result is a maximum load impedance 2kΩ short of the target but this can likely be attributed to the imperfect nature of using a breadboarded system rather than a flaw of the circuit. Considering a 58kΩ resistor was used to test the circuit of this project the slightly lower values are expected. The overall result is that the current draw for the circuit from Karpul et al. and the adapted circuit in this project match closely. Karpul et al. made it clear that the 1mA and -1mA DC load currents were the best representation of a worst-case scenario.

Using the results from Table 4 it is possible to calculate the capacity required of the battery to last 8-10 hours as outlined in the specifications. The -1mA case from the published results of Karpul et al. will be used as it is the highest of all the obtained values. A worst case draw of 25.9mA necessitates the battery have at least capacity of 260mA, considering most 9V batteries typically range from 300-500mA hours a battery life of 10 hours for the entire system (including control circuitry) should be achievable.

12.3 Control Circuitry

The level shifter circuit was also breadboarded and tested. The results were as expected, the circuit functioned consistent with the following equation.

$$Vout = 2Vin - Vref$$

BME1634 Electrical Stochastic Resonance System

Shannon Deale

This circuit is necessary to achieve the desired load currents delivered by the HVCP. The level shifter takes the 0V to 3.3V DAC input and outputs ±3.3V. If the RGAIN in the HVCP is set to 3.3kΩ and the ±3.3V is connected to the Vin$_+$ input, we can calculate the resulting load current.

$$Iload = \frac{Vin_+ - Vin_-}{RGain}$$
$$\frac{\pm 3.3V - 0}{3.3k\Omega} = \pm 1mA$$

Hence the output range of the HVCP is ±1mA as was described in the Identification of Design Requirements and Specifications.

12.4 PCBs
PCBs were designed for the HVPSU and the HVCP but a PCB for the control circuitry is yet to be designed. The PCBs are yet to be manufactured but the components that will be soldered onto the boards have been identified and budgeted for which is shown in the table in Appendix D.

12.5 Software
The GUI layout shown in Figure 23 is sufficiently simple and easy to use whilst maintaining all of the required functionality described in the Identification of Design Requirements and Specifications section. The signal generation software is partially completed, the output waveform (shown in Figure 32) appears to be pseudo-white Gaussian noise. However, it does not achieve the ideal pulse frequency of 1kHz at the time of writing. Currently the system has a pulse frequency of approximately 6kHz, this could be reduced to 1kHz using delays incorporated into the current software. However, it would be more appropriate to control the pulse frequency through the use of interrupts, as this would enable precise control of the frequency that would not be affected by any additional changes to software in the future. The next steps for this project at the time of writing is to improve the software generating the stimulus to better control the pulse frequency of the stimulus signal. The implementation of Bluetooth communication in software enabling the device to communicate with the PC GUI application also needs to be developed before the system overall can be assembled. Once these steps are completed the overall combined system can be tested and validated before manufacturing the PCBs and the casing for the prototype system.

12.6 Comparisons with Previous System
The current system offers several significant improvements over the previous system described in the Project Background.

- The current system can drive ±1mA through a maximum skin impedance of 58kΩ far greater than the 2kΩ of the previous system.
- The GUI of the current system is simpler and more usable than the LCD menu navigation of the previous system.
- Component sizes are smaller, with the HVPSU PCB having the dimensions 54.229mm × 30.735mm and the HVCP having the dimensions 64.288mm × 31.028mm.

BME1634 Electrical Stochastic Resonance System
Shannon Deale

- The memory attached to the microcontroller is larger than the memory attached to the Arduino UNO of the previous system. Additionally, the GUI enables much of the program to be located on a PC rather than the device itself.

13 Conclusions

This project has achieved a number of milestones towards the objective of developing a prototype system that was capable of delivering a random electrical stimulus (in the form of white Gaussian noise) to the body via electrodes to facilitate SR effects in the sensitivity of the somatosensory system. The design of the electronic circuitry that realises the concept for the device has been completed and includes a high voltage power supply unit (HVPSU), high voltage current pump (HVCP), microcontroller, digital-to-analogue converter, level shifter and a wireless transmitter/receiver.

PCBs have been designed for the HVPSU and HVCP based on thorough breadboard testing of the two circuits, making them ready for immediate manufacture. All the components to be soldered onto the PCBs have been identified and budgeted for. The design considerations and testing for the control circuitry has also been completed and is ready for the design of a PCB. The main components of the software (namely the GUI and pseudo-white Gaussian noise) have been developed and minimal work is required to fulfil the initial specs.

Significant work has been done across all the major components within this system, all that remains is to combine them into a functioning prototype. It is envisaged that once the system is complete it will be used in a clinical research setting enabling the investigation of potential benefits from prolonged use of SR stimulation, potentially leading to improved function and quality of life.

References:

1. McDonnell, M.D. and D. Abbott, *What Is Stochastic Resonance? Definitions, Misconceptions, Debates, and Its Relevance to Biology.* PLoS Computational Biology, 2009. **5**(5): p. e1000348.

2. Collins, J.J., T.T. Imhoff, and P. Grigg, *Noise-enhanced tactile sensation.* Nature, 1996. **383**(6603): p. 770.

3. Itzcovich, E., M. Riani, and W.G. Sannita, *Stochastic resonance improves vision in the severely impaired.* Scientific Reports, 2017. **7**(1): p. 12840.

4. Morse, R.P. and E.F. Evans, *Enhancement of vowel coding for cochlear implants by addition of noise.* Nature Medicine, 1996. **2**: p. 928.

5. Wiesenfeld, K. and F. Moss, *Stochastic resonance and the benefits of noise: from ice ages to crayfish and SQUIDs.* Nature, 1995. **373**: p. 33.

6. Collins, J.J., *Fishing for function in noise.* Nature, 1999. **402**(6759): p. 241-2.

7. Douglass, J.K., et al., *Noise enhancement of information transfer in crayfish mechanoreceptors by stochastic resonance.* Nature, 1993. **365**(6444): p. 337.

8. Greenwood, P.E., et al., *Stochastic Resonance Enhances the Electrosensory Information Available to Paddlefish for Prey Capture.* Physical Review Letters, 2000. **84**(20): p. 4773-4776.

9. Levin, J.E. and J.P. Miller, *Broadband neural encoding in the cricket cereal sensory system enhanced by stochastic resonance.* Nature, 1996. **380**(6570): p. 165.

10. Manjarrez, E., et al., *Internal stochastic resonance in the coherence between spinal and cortical neuronal ensembles in the cat.* Neuroscience Letters, 2002. **326**(2): p. 93-96.

11. Priplata, A.A., et al., *Noise-Enhanced Human Balance Control.* Physical Review Letters, 2002. **89**(23): p. 238101.

12. Loader, B., et al., *Improved postural control after computerized optokinetic therapy based on stochastic visual stimulation in patients with vestibular dysfunction*. Vol. 17. 2007. 131-6.

13. Fauve, S. and F. Heslot, *Stochastic resonance in a bistable system.* Physics Letters A, 1983. **97**(1): p. 5-7.

14. Vemuri, G. and R. Roy, *Stochastic resonance in a bistable ring laser.* Physical Review A, 1989. **39**(9): p. 4668-4674.

15. McNamara, B., K. Wiesenfeld, and R. Roy, *Observation of Stochastic Resonance in a Ring Laser.* Physical Review Letters, 1988. **60**(25): p. 2626-2629.

16. Priplata, A., et al., *Noise-Enhanced Human Balance Control.* Physical Review Letters, 2002. **89**(23): p. 238101.

17. Suki, B., et al., *Life-support system benefits from noise.* Nature, 1998. **393**: p. 127.

18. Collins, J.J., T.T. Imhoff, and P. Grigg, *Noise-mediated enhancements and decrements in human tactile sensation.* Physical Review E, 1997. **56**(1): p. 923-926.

19. Liu, W., et al., *Noise-enhanced vibrotactile sensitivity in older adults, patients with stroke, and patients with diabetic neuropathy.* Archives of Physical Medicine and Rehabilitation, 2002. **83**(2): p. 171-176.

20. Mendez-Balbuena, I., et al., *Improved Sensorimotor Performance via Stochastic Resonance.* The Journal of Neuroscience, 2012. **32**(36): p. 12612.

21. Priplata, A.A., et al., *Vibrating insoles and balance control in elderly people.* The Lancet, 2003. **362**(9390): p. 1123-1124.

BME1634 Electrical Stochastic Resonance System

Shannon Deale

22. Dhruv, N., et al., *Enhancing tactile sensation in older adults with electrical noise stimulation.* Neuroreport, 2002. **13**(5): p. 597-600.

23. Breen, P.P., et al., *A new paradigm of electrical stimulation to enhance sensory neural function.* Medical Engineering & Physics, 2014. **36**(8): p. 1088-1091.

24. Richardson, K.A., et al., *Using electrical noise to enhance the ability of humans to detect subthreshold mechanical cutaneous stimuli.* Chaos: An Interdisciplinary Journal of Nonlinear Science, 1998. **8**(3): p. 599-603.

25. Collins, J.J., et al., *Noise-enhanced human sensorimotor function.* IEEE Engineering in Medicine and Biology Magazine, 2003. **22**(2): p. 76-83.

26. Cordo, P., et al., *Noise in human muscle spindles.* Nature, 1996. **383**: p. 769.

27. Gravelle, D., et al., *Noise-enhanced balance control in older adults.* Neuroreport, 2002. **13**(15): p. 1853-1856.

28. Wells, C., et al., *Touch Noise Increases Vibrotactile Sensitivity in Old and Young.* Psychological Science, 2005. **16**(4): p. 313-320.

29. Moss, F., L.M. Ward, and W.G. Sannita, *Stochastic resonance and sensory information processing: a tutorial and review of application.* Clinical Neurophysiology, 2004. **115**(2): p. 267-281.

30. Gammaitoni, L., et al., *Stochastic resonance.* Reviews of Modern Physics, 1998. **70**(1): p. 223-287.

31. Pavlik, A.E., et al., *The effects of stochastic galvanic vestibular stimulation on human postural sway.* Experimental Brain Research, 1999. **124**(3): p. 273-280.

32. Aboutorabi, A., et al., *Design and evaluation of vibratory shoe on balance control for elderly subjects: technical note*. Vol. 13. 2017. 1-5.

33. Miranda, D., et al., *Sensory Enhancing Insoles Modify Gait during Inclined Treadmill Walking with Load.* Med Sci Sports Exerc, 2016. **48**(5): p. 860-868.

34. Lipsitz, L.A., et al., *A Shoe Insole Delivering Subsensory Vibratory Noise Improves Balance and Gait in Healthy Elderly People.* Archives of Physical Medicine and Rehabilitation, 2015. **96**(3): p. 432-439.

35. Priplata, A.A., et al., *Noise-enhanced balance control in patients with diabetes and patients with stroke.* Ann Neurol, 2006. **59**(1): p. 4-12.

36. Chang, G.C. *A microprocessor-based multichannel subsensory stochastic resonance electrical stimulator*. in *2013 35th Annual International Conference of the IEEE Engineering in Medicine and Biology Society (EMBC)*. 2013.

37. Karpul, D., et al., *Low-power transcutaneous current stimulator for wearable applications.* BioMedical Engineering OnLine, 2017. **16**(1): p. 118.

38. Dunn, W., et al., *Somatosensation assessment using the NIH Toolbox*. Vol. 80. 2013. Supplement 3 S41-S44.

39. Shaffer, S.W. and A.L. Harrison, *Aging of the somatosensory system: a translational perspective*, in *Physical Therapy*. 2007. p. 193+.

40. Shaffer, S.W. and A.L. Harrison, *Aging of the Somatosensory System: A Translational Perspective.* Physical Therapy, 2007. **87**(2): p. 193-207.

41. AIHW, *Hospitalisation due to falls by older people, Australia: 2009-10*, in *Injury research and statistics series*. 2013, Australian Institute of Health and Welfare: Canberra. p. 73.

42. AIHW, *Hospitalisation due to falls by order people, Australia 2002-03 to 2012-13*, in *Injury research and statistics series*. 2017, Australian Institute of Health and Welfare: Canberra. p. 110.
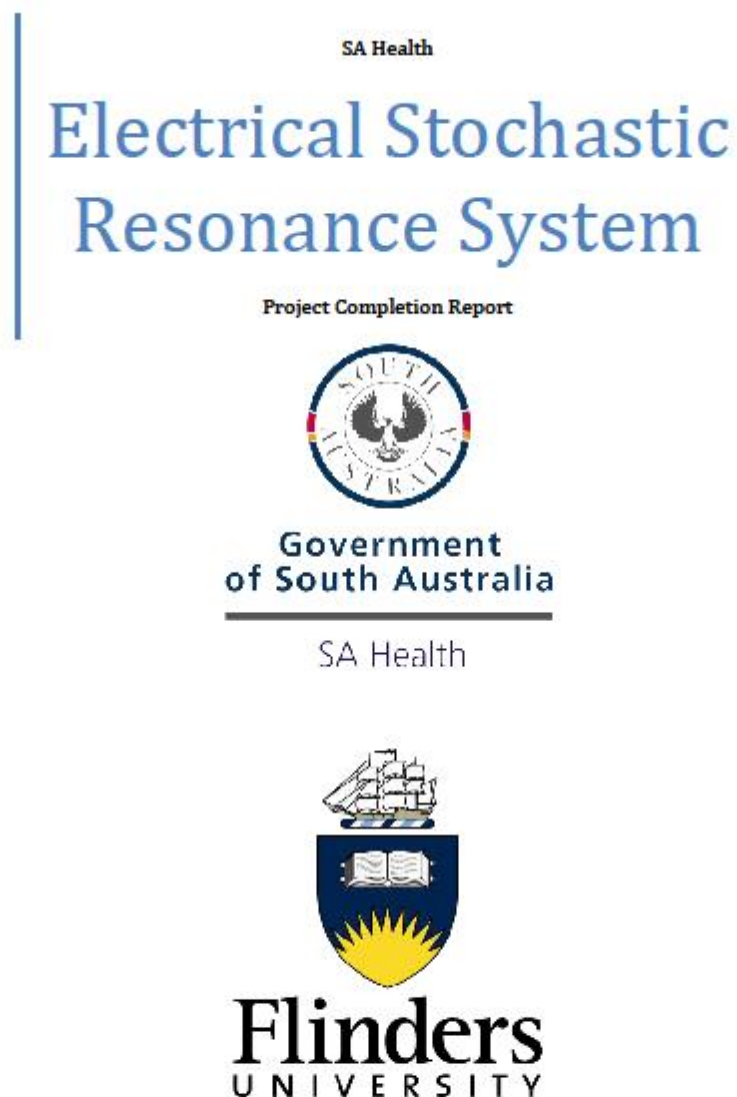
43. Watson, W.L., A.J. Clapperton, and R.J. Mitchell, *The cost of fall-related injuries among older people in NSW, 2006–07.* NSW Public Health Bulletin, 2011. **22**(4): p. 55-59.

44. Moller, J., *Projected costs of fall related injury to older persons due to demographic change in Australia*, in *Report to the Commonwealth Department of Health and Ageing under the National Falls Prevention for Older People Initiative*. 2003, National Ageing Research Institute: Canberra. p. 29.

45. GholamHosseini, H., et al. *A multifactorial falls risk prediction model for hospitalized older adults*. in *2014 36th Annual International Conference of the IEEE Engineering in Medicine and Biology Society*. 2014.

46. National Institute for Health and Care Excellence. *Falls in older people: assessing risk and prevention*. 2013.

47. Hamil, J. and A.M.K, *Biomechanical Basis of Human Movement*. 3 ed. Vol. 3. 2009: Wolters Kluwer.

48. Marieb, E.N. and K.N.H., *Human Anatomy & Physiology*. P.N.I. ed. Vol. 9. 2013: Pearson Education Limited.

49. Abrahamová, D. and F. Hlavacka, *Age-Related Changes of Human Balance during Quiet Stance.* Physiological Research, 2008. **57**(6): p. 957-64.

50. Collins, A.T., et al., *Stochastic resonance electrical stimulation to improve proprioception in knee osteoarthritis.* The Knee, 2011. **18**(5): p. 317-322.

51. Bronstein, A.M. and M. Pavlou, *Balance, in Handbook of Clinical Neurology*, P.B. Michael and C.G. David, Editors. 2013, Elsevier.p. p. 189-208.

52. Nardone, A. and M. Schieppati, *Group II spindle fibres and afferent control of stance. Clues from diabetic neuropathy.* Clinical Neurophysiology, 2004. **115**(4): p. 779-789.

53. Carey, L.M., T.A. Matyas, and L.E. Oke, *Sensory loss in stroke patients: Effective training of tactile and proprioceptive discrimination.* Archives of Physical Medicine and Rehabilitation. **74**(6): p. 602-611.

54. Australian Bureau of Statistics, *4364.0.55.001 - National Health Survey: First Results, 2014-15* 2015: Canberra

55. Australian Institute of Health and Welfare, *Australia's health 2008*. 2008, AIHW: Canberra.

56. Nicolis, C., *Stochastic aspects of climatic transitions—response to a periodic forcing.* Tellus, 1982. **34**(1): p. 1-9.

57. Nicolis, C. and G. Nicolis, *Stochastic aspects of climatic transitions–Additive fluctuations.* Tellus, 1981. **33**(3): p. 225-234.

58. Benzi, R., et al., *Stochastic resonance in climatic change.* Tellus, 1982. **34**(1): p. 10-16.

59. Benzi, R., et al., *A Theory of Stochastic Resonance in Climatic Change.* SIAM Journal on Applied Mathematics, 1983. **43**(3): p. 565-578.

60. Otto, H.S., *A thermionic trigger.* Journal of Scientific Instruments, 1938. **15**(1): p. 24.

61. Molecular Devices. *What is an action potential?* 2017 [cited 2018 11/07]; Available from: https://www.moleculardevices.com/applications/patch-clamp-electrophysiology/what-action-potential.

62. J Collins, J., T. T Imhoff, and P. Grigg, *Noise-enhanced information transmission in rat SA1 cutaneous mechanoreceptors via aperiodic stochastic resonance*. Vol. 76. 1996. 642-5.

63. Breen, P.P. and V.G. Macefield. *Proximally applied subsensory electrical noise stimulation reduces variance in action potential timing and enhances sensory*

BME1634 Electrical Stochastic Resonance System

Shannon Deale

perception. in *2013 6th International IEEE/EMBS Conference on Neural Engineering (NER)*. 2013.

64. Collins, A.T., et al., *The effects of stochastic resonance electrical stimulation and neoprene sleeve on knee proprioception.* Journal of Orthopaedic Surgery and Research, 2009. **4**: p. 3-3.

65. Iliopoulos, F., T. Nierhaus, and A. Villringer, *Electrical noise modulates perception of electrical pulses in humans: sensation enhancement via stochastic resonance.* Journal of Neurophysiology, 2013. **111**(6): p. 1238-1248.

66. Toledo, D.R., J.A. Barela, and A.F. Kohn, *Improved proprioceptive function by application of subsensory electrical noise: Effects of aging and task-demand.* Neuroscience, 2017. **358**: p. 103-114.

67. Ross, S.E., *Noise-enhanced postural stability in subjects with functional ankle instability.* British Journal of Sports Medicine, 2007. **41**(10): p. 656.

68. Ross, S.E., et al., *Noise-Enhanced Eversion Force Sense in Ankles With or Without Functional Instability.* Journal of Athletic Training (Allen Press), 2015. **50**(8): p. 819-824.

69. Grace Gaerlan, M., et al., *Postural balance in young adults: The role of visual, vestibular and somatosensory systems.* Journal of the American Academy of Nurse Practitioners, 2012. **24**(6): p. 375-381.

70. Kaas, J.H., *Neural Plasticity*, in *International Encyclopedia of the Social & Behavioral Sciences (Second Edition)*, J.D. Wright, Editor. 2015, Elsevier: Oxford. p. 619-622.

71. Demarin, V., *Neuroplasticity in neurodegenerative diseases and stroke.* Journal of the Neurological Sciences, 2013. **333**: p. e199.

72. Buonomano, D.V. and H.A. Johnson, *Cortical Plasticity and Learning: Mechanisms and Models*, in *Encyclopedia of Neuroscience*, L.R. Squire, Editor. 2009, Academic Press: Oxford. p. 183-188.

73. Hebb, D.O., *The Organization of Behavior : A Neuropsychological Theory*. 2005, Mahwah, UNITED STATES: Taylor & Francis Group.

74. Ribot-Ciscar, E., V. Hospod, and J.-M. Aimonetti, *Noise-enhanced kinaesthesia: a psychophysical and microneurographic study.* Experimental Brain Research, 2013. **228**(4): p. 503-511.

75. Manjarrez, E.a., et al., *Stochastic Resonance within the Somatosensory System: Effects of Noise on Evoked Field Potentials Elicited by Tactile Stimuli.* The Journal of Neuroscience, 2003. **23**(6): p. 1997.

76. Manjarrez, E., et al., *Stochastic resonance in human electroencephalographic activity elicited by mechanical tactile stimuli.* Neuroscience Letters, 2002. **324**(3): p. 213-216.

77. Seo Na, J., et al., *Effect of imperceptible vibratory noise applied to wrist skin on fingertip touch evoked potentials – an EEG study.* Physiological Reports, 2015. **3**(11): p. e12624.

78. Kleim, J.A., *Neural plasticity and neurorehabilitation: Teaching the new brain old tricks.* Journal of Communication Disorders, 2011. **44**(5): p. 521-528.

79. Cramer, S.C., et al., *Harnessing neuroplasticity for clinical applications.* Brain, 2011. **134**(6): p. 1591-1609.

80. Stein, J., et al., *Stochastic Resonance Stimulation for Upper Limb Rehabilitation Poststroke*. Vol. 89. 2010. 697-705.

81. Rushton, D.N., *Functional Electrical Stimulation and rehabilitation—an hypothesis.* Medical Engineering & Physics, 2003. **25**(1): p. 75-78.

BME1634 Electrical Stochastic Resonance System

Shannon Deale

82. Subramanya, K.B., A.K.M. Kanakabettu, and M. Mahadevappa, *Functional electrical stimulation for stoke rehabilitation.* Medical Hypotheses, 2012. **78**(5): p. 687.

83. Yan, T., et al., *Functional Electrical Stimulation Improves Motor Recovery of the Lower Extremity and Walking Ability of Subjects With First Acute Stroke: A Randomized Placebo-Controlled Trial.* Stroke, 2005. **36**(1): p. 80-85.

84. Ehrenstein, W.H. and A. Ehrenstein, *Psychophysical Methods*, in *Modern Techniques in Neuroscience Research*, U. Windhorst and H. Johansson, Editors. 1999, Springer Berlin Heidelberg: Berlin, Heidelberg. p. 1211-1241.

85. Karleen, A., *Using Electrical Stimulation*, in *A Guideline for Allied Health Professionals*, D.A. McCluskey, Editor. 2014, Sydney Local Health District and Royal Rehabilitation Centre; Sydney, Australia.

86. Biopac Systems Inc, *App Note 257: Safe Use of Electrical Stimulators*. 2008: Goleta. p. 1-5.

87. SA Health. *South Australia Falls Prevention*. [Infographic] 2017 [cited 2018 18/07]; Available from: http://www.sahealth.sa.gov.au/wps/wcm/connect/dbb7840047d3aef8a1d6a5fc651ee2b2/2018+Falls+Month+STATE+STAFF+Infographic.pdf?MOD=AJPERES&CACHEID=ROOTWORKSPACE-dbb7840047d3aef8a1d6a5fc651ee2b2-m9gfocW.

88. Australia & New Zealand Falls Prevention Society. *Info about falls*. 2006 [cited 2018 18/07]; Available from: http://www.anzfallsprevention.org/.

89. Rosell, J., et al., *Skin impedance from 1 Hz to 1 MHz.* IEEE Trans Biomed Eng, 1988. **35**(8): p. 649-51.

90. King, G. and T. Watkins, *Bootstrapping your op amp yields wide voltage swings*, in *EDN*. 1999. p. 117.

91. Caldwell J, *A high-voltage bidirectional current source*. Texas Instruments: Dallus.

92. Dyck, P.J., et al., *A 4, 2, and 1 stepping algorithm for quick and accurate estimation of cutaneous sensation threshold.* Neurology, 1993. **43**(8): p. 1508.

93. Phoxis. *Generating random numbers from Normal distribution in C*. 2013; Available from: https://phoxis.org/2013/05/04/generating-random-numbers-from-normal-distribution-in-c/.

Appendix A
Note double click on the object below to open a pdf.

SA Health

Electrical Stochastic Resonance System

Project Completion Report

**Government
of South Australia**

SA Health

Flinders
U N I V E R S I T Y

BME Student
11/24/2017

BME1634 Electrical Stochastic Resonance System
Shannon Deale

Appendix B

```
138.        #Signal Generator Code for BME 1634 ESRS
139.
140.        #GUI CODE SECTION
141.
142.        from tkinter import *
143.        from tkinter import ttk  #Importing necessary packages from tkinter
144.
145.        root = Tk() #Make the root window
146.        root.title("ESRS Control Panel") #Display title
147.
148.        #VARIABLES
149.        CH1IsOn = StringVar() #Device 1 enabled variable
150.        CH2IsOn = StringVar() #Device 2 enabled variable
151.
152.        CH1Stim = DoubleVar() #Device 1 stimulation value variable
153.        CH2Stim = DoubleVar() #Device 2 stimulation value variable
154.
155.
156.
157.        Run_Stop = IntVar()# Run/Stop variable
158.
159.
160.        CH1Stim.set(150) #Initialise Device 1 stimulation value variable (150uA)
161.        CH2Stim.set(150) #Initialise Device 2 stimulation value variable (150uA)
162.        Run_Stop.set(0) #Initialise Run/Stop variable (0 = not running)
163.
164.        #COMMANDS
165.
166.        #######################################
167.        def FourBackCH1():
168.            global CH1Stim
169.            CH1Stim.set(CH1Stim.get() - 60.0) #Decreases by 4 steps of 15uA
170.
171.        def TwoForwardCH1():
172.            global CH1Stim
173.            CH1Stim.set(CH1Stim.get() + 30.0) #Increases by 2 steps of 15uA
174.
175.        def OneBackCH1():
176.            global CH1Stim
177.            CH1Stim.set(CH1Stim.get() - 15.0) #Decreases by a step of 15uA
178.
179.        def OneBackCH1():
180.            global CH1Stim
181.            CH1Stim.set(CH1Stim.get() + 15.0) #Increases by a step of 15uA
182.
183.        #######################################
184.
185.        def FourBackCH2():
186.            global CH2Stim
187.            CH2Stim.set(CH2Stim.get() - 60.0) #Decreases by 4 steps of 15uA
188.
189.        def TwoForwardCH2():
190.            global CH2Stim
191.            CH2Stim.set(CH2Stim.get() + 30.0) #Increases by 2 steps of 15uA
192.
193.        def OneBackCH2():
194.            global CH2Stim
195.            CH2Stim.set(CH2Stim.get() - 15.0) #Decreases by a step of 15uA
196.
197.        def OneBackCH2():
198.            global CH2Stim
199.            CH2Stim.set(CH2Stim.get() + 15.0) #Increases by a step of 15uA
```

BME1634 Electrical Stochastic Resonance System

Shannon Deale

```
200.
201.        ##########################################
202.
203.        def Run_Stop_Func(): #toggle a Run/Stop variable
204.            global Run_Stop
205.
206.            if Run_Stop.get == 0:
207.                Run_Stop.set = 1
208.            else:
209.                Run_Stop.set = 0
210.
211.
212.        #FRAMING
213.        mainframe = ttk.Frame(root, padding = "9 12 9 12") #Setup initial mainframe
214.        mainframe.grid(column = 0, row = 0, sticky = (N, W, E, S)) #Setup the mainfr
   ame grid
215.        mainframe.columnconfigure(0, weight = 1) #Configure mainframe column
216.        mainframe.rowconfigure(0, weight = 1) #Configure mainframe row
217.
218.        CH1frame = ttk.Frame(mainframe, borderwidth = 5, relief = 'sunken', width= 2
   00, height = 800 ) #Make "Device 1" a sunken frame within the mainframe
219.        CH1frame.grid(column = 1, row = 3, columnspan = 3, rowspan = 9, sticky =( N,
    W, E, S))
220.        CH2frame = ttk.Frame(mainframe, borderwidth = 5, relief = 'sunken', width= 2
   00, height = 800 ) #Make "Device 2" a sunken frame within the mainframe
221.        CH2frame.grid(column = 6, columnspan = 3, rowspan = 9, row = 3, sticky = (N,
    W, E, S))
222.
223.
224.        #GENERAL CONTROLS
225.        ttk.Button(mainframe, text = "Update Device").grid(column = 1, row = 1, stic
   ky = W) #Update Device button text
226.        ttk.Button(mainframe, text = "Run/Stop", command = Run_Stop_Func).grid(colum
   n = 2, row = 1, sticky = E)   #Run/Stop button text
227.        ttk.Button(mainframe, text = "Pair").grid(column = 8, row = 1, sticky = W)
   #Pair button text
228.
229.        #CH1
230.        CH1checkIsOn = ttk.Checkbutton(CH1frame, text = 'Active', variable = CH1IsOn
   , #Checkbutton that allows user to enable/disable Device 1
231.                        onvalue = 'On', offvalue='Off').grid(column = 1, row = 2, sti
   cky = W)
232.
233.        CH1TextBox = ttk.Entry(CH1frame, textvariable = CH1Stim).grid(column = 2, ro
   w = 3, sticky = W) #Device 1 textbox (user can type desired stimulation value here)
234.
235.        CH1Slider = ttk.Scale(CH1frame, orient=HORIZONTAL, variable = CH1Stim,
236.                        length=200, from_=1.0, to=333.0).grid(column = 1, row
   = 4, columnspan = 3, sticky = W) #Slider that also allows the user to change the va
   lue of the Device 1 textbox
237.
238.        ttk.Button(CH1frame, text = "<<", command = FourBackCH1).grid(column = 1, ro
   w = 5, sticky = W) #Button containing "<<" used for decreasing Device 1 stim value
   by four steps of 15uA
239.        ttk.Button(CH1frame, text = ">>", command = TwoForwardCH1).grid(column = 2,
   row = 5, sticky = E) #Button containing ">>" used for increasing Device 1 stim valu
   e by two steps of 15uA
240.        ttk.Button(CH1frame, text = "<", command = OneBackCH1).grid(column = 1, row
   = 6, sticky = W) #Button containing "<" used for decreasing Device 1 stim value by
    a step of 15uA
241.        ttk.Button(CH1frame, text = ">", command = OneBackCH1).grid(column = 2, row
   = 6, sticky = E) #Button containing ">" used for increasing Device 1 stim value by
    a step of 15uA
```

BME1634 Electrical Stochastic Resonance System

Shannon Deale

```python
242.
243.        #CH2
244.        CH2checkIsOn = ttk.Checkbutton(CH2frame, text = 'Active', variable = CH2IsOn
    , #Checkbutton that allows user to enable/disable Device 2
245.                        onvalue = 'On', offvalue='Off').grid(column = 1, row = 2, sti
    cky = W)
246.
247.        CH2TextBox = ttk.Entry(CH2frame, textvariable = CH2Stim).grid(column = 2, ro
    w = 3, sticky = W) #Device 2 textbox (user can type desired stimulation value here)

248.
249.        CH2Slider = ttk.Scale(CH2frame, orient=HORIZONTAL, variable = CH2Stim,
250.                        length=200, from_=1.0, to=333.0).grid(column = 1, row
    = 4, columnspan = 3, sticky = W) #Slider that also allows the user to change the va
    lue of the Device 2 textbox
251.
252.        ttk.Button(CH2frame, text = "<<", command = FourBackCH2).grid(column = 1, ro
    w = 5, sticky = W) #Button containing "<<" used for decreasing Device 2 stim value
    by four steps of 15uA
253.        ttk.Button(CH2frame, text = ">>", command = TwoForwardCH2).grid(column = 2,
    row = 5, sticky = E) #Button containing ">>" used for increasing Device 2 stim valu
    e by two steps of 15uA
254.        ttk.Button(CH2frame, text = "<", command = OneBackCH2).grid(column = 1, row
    = 6, sticky = W) #Button containing "<" used for decreasing Device 2 stim value by
     a step of 15uA
255.        ttk.Button(CH2frame, text = ">", command = OneBackCH2).grid(column = 2, row
    = 6, sticky = E) #Button containing ">" used for increasing Device 2 stim value by
     a step of 15uA
256.
257.        #TEXT LABLES
258.        ttk.Label(CH1frame, text = "Device 1").grid(column = 1, row = 1, sticky = W)
    #Lable denoting Device 1 options
259.        ttk.Label(CH2frame, text = "Device 2").grid(column = 1, row = 1, sticky = W)
    #Lable denoting Device 2 options
260.
261.        ttk.Label(CH1frame, text = "uA").grid(column = 3, row = 3, sticky = W) #Disp
    lay "uA" next to the Device 1 textbox
262.        ttk.Label(CH2frame, text = "uA").grid(column = 3, row = 3, sticky = W) #Disp
    lay "uA" next to the Device 2 textbox
263.
264.        ttk.Label(CH1frame, text = "4").grid(column = 2, row = 5, sticky = W) #Displ
    ay "4" next to << in Device 1
265.        ttk.Label(CH1frame, text = "2").grid(column = 3, row = 5, sticky = W) #Displ
    ay "2" next to >> in Device 1
266.        ttk.Label(CH1frame, text = "1").grid(column = 2, row = 6, sticky = W) #Displ
    ay "1" next to < in Device 1
267.        ttk.Label(CH1frame, text = "1").grid(column = 3, row = 6, sticky = W) #Displ
    ay "1" next to > in Device 1
268.
269.        ttk.Label(CH2frame, text = "4").grid(column = 2, row = 5, sticky = W) #Displ
    ay "4" next to << in Device 2
270.        ttk.Label(CH2frame, text = "2").grid(column = 3, row = 5, sticky = W) #Displ
    ay "2" next to >> in Device 2
271.        ttk.Label(CH2frame, text = "1").grid(column = 2, row = 6, sticky = W) #Displ
    ay "1" next to < in Device 2
272.        ttk.Label(CH2frame, text = "1").grid(column = 3, row = 6, sticky = W) #Displ
    ay "1" next to > in Device 2
273.
274.        root.mainloop()
```

Appendix C

```
224.        /*
225.         * File:   main.c
226.         * Author: Shannon Deale
227.         *
228.         * Created on 19 September 2018, 2:32 PM
229.         */
230.
231.        #include <stdio.h>
232.        #include <stdlib.h>
233.        #include <xc.h>
234.        #include <math.h>          // need this to calculate the sin function
235.
236.        /*
237.         *
238.         */
239.        double User_select; //variable for storing user selected value
240.        int random_number; // variable for storing random number
241.        int run_stop = 1; // variable for storing run/stop information
242.
243.        void init(void) {
244.        /* The following pins must be set to digital inputs to prevent damage to the
    LCD
245.         * display on the development board (as per the User Guide recommendation).
246.         * see Documents at:
247.         * "https://www.microchip.com/Developmenttools/ProductDetails/DM240015"
248.         * for more detailed information.
249.         */
250.        //============================ PORTA ===================================
    ==//
251.        _ANSA15 = 0; // Set the function of RA15 to "digital"
252.        _ANSA14 = 0; // Set the function of RA14 to "digital"
253.
254.        _ANSA10 = 0; // Set the function of RA10 to "digital"
255.
256.        _ANSA6 = 0; // Set the function of RA6 to "digital"
257.        _ANSA5 = 0; // Set the function of RA5 to "digital"
258.        _ANSA4 = 0; // Set the function of RA4 to "digital"
259.        _ANSA2 = 0; // Set the function of RA2 to "digital"
260.        _ANSA1 = 0; // Set the function of RA1 to "digital"
261.
262.        _TRISA15 = 1; // Set RA15 as "input"
263.        _TRISA14 = 1; // Set RA14 as "input"
264.
265.        _TRISA10 = 1; // Set RA10 as "input"
266.
267.        _TRISA6 = 1; // Set RA6 as "input"
268.        _TRISA5 = 1; // Set RA5 as "input"
269.        _TRISA4 = 1; // Set RA4 as "input"
270.        _TRISA3 = 1; // Set RA3 as "input"
271.        _TRISA2 = 1; // Set RA2 as "input"
272.        _TRISA1 = 1; // Set RA1 as "input"
273.        _TRISA0 = 1; // Set RA0 as "input"
274.
275.        //============================ PORTB ===================================
    ==//
276.        _ANSB15 = 0; // Set the function of RB15 to "digital"
277.        _ANSB14 = 0; // Set the function of RB14 to "digital"
278.
279.        _ANSB12 = 0; // Set the function of RB12 to "digital"
280.        _ANSB7 = 0; // Set the function of RB7 to "digital"
281.
282.        _TRISB15 = 1; // Set RB15 as "input"
```

BME1634 Electrical Stochastic Resonance System

Shannon Deale

```
283.        _TRISB14 = 1; // Set RB14 as "input"
284.
285.        _TRISB12 = 1; // Set RB12 as "input"
286.        _TRISB7 = 1; // Set RB7 as "input"
287.
288.        //============================ PORTC ===================================//
289.        _TRISC2 = 1; // Set RC2 as "input"
290.
291.        //============================ PORTD ===================================//
292.        /*
293.         * Note that RD0 must remain set as a digital input only if the phototransistor
294.         * sensor and potentiometer are not used
295.         */
296.        _ANSD15 = 0; // Set the function of RD15 to "digital"
297.        _ANSD14 = 0; // Set the function of RD14 to "digital"
298.        _ANSD13 = 0; // Set the function of RD13 to "digital"
299.
300.        _ANSD11 = 0; // Set the function of RD11 to "digital"
301.        _ANSD10 = 0; // Set the function of RD10 to "digital"
302.        _ANSD9 = 0; // Set the function of RD9 to "digital"
303.        _ANSD8 = 0; // Set the function of RD8 to "digital"
304.        _ANSD7 = 0; // Set the function of RD7 to "digital"
305.        _ANSD6 = 0; // Set the function of RD6 to "digital"
306.
307.        _ANSD0 = 0;  // Set the function of RD0 to "digital"
308.
309.        _TRISD15 = 1; // Set RD15 as "input"
310.        _TRISD14 = 1; // Set RD14 as "input"
311.        _TRISD13 = 1; // Set RD13 as "input"
312.
313.        _TRISD11 = 1; // Set RD11 as "input"
314.        _TRISD10 = 1; // Set RD10 as "input"
315.        _TRISD9 = 1; // Set RD9 as "input"
316.        _TRISD8 = 1; // Set RD8 as "input"
317.        _TRISD7 = 1; // Set RD7 as "input"
318.        _TRISD6 = 1; // Set RD6 as "input"
319.
320.        _TRISD0 = 1;  // Set RD0 as "input"
321.
322.        //============================ PORTE ===================================//
323.        _ANSE4 = 0; // Set the function of RE4 to "digital"
324.
325.        _TRISE8 = 1; // Set RE8 as "input"
326.
327.        _TRISE4 = 1; // Set RE4 as "input"
328.        _TRISE3 = 1; // Set RE3 as "input"
329.        _TRISE2 = 1; // Set RE2 as "input"
330.        _TRISE1 = 1; // Set RE1 as "input"
331.        _TRISE0 = 1; // Set RE0 as "input"
332.
333.        //============================ PORTF ===================================//
334.        _ANSF13 = 0; // Set the function of RF13 to "digital"
335.
336.        _ANSF8 = 0; // Set the function of RF8 to "digital"
337.
338.        _ANSF3 = 0; // Set the function of RF3 to "digital"
339.        _ANSF2 = 0; // Set the function of RF2 to "digital"
340.        _ANSF0 = 0; // Set the function of RF0 to "digital"
341.
342.        _TRISF13 = 1; // Set RF13 as "input"
```

BME1634 Electrical Stochastic Resonance System

Shannon Deale

```
343.        _TRISF12 = 1; // Set RF12 as "input"
344.
345.        _TRISF8 = 1; // Set RF8 as "input"
346.
347.        _TRISF3 = 1; // Set RF3 as "input"
348.        _TRISF2 = 1; // Set RF2 as "input"
349.        _TRISF1 = 1; // Set RF1 as "input"
350.        _TRISF0 = 1; // Set RF0 as "input"
351.
352.        //============================= PORTG =================================
    ==//
353.        _ANSG15 = 0; // Set the function of RG15 to "digital"
354.
355.        _TRISG15 = 1; // Set RG15 as "input"
356.        _TRISG14 = 1; // Set RG14 as "input"
357.        _TRISG13 = 1; // Set RG13 as "input"
358.        _TRISG12 = 1; // Set RG12 as "input"
359.
360.        _TRISG1 = 1; // Set RG1 as "input"
361.        _TRISG0 = 1; // Set RG0 as "input"
362.
363.        }
364.
365.        void DACinit(void){
366.
367.        DAC1CONbits.DACEN = 1;// Enable DAC1 module
368.        DAC2CONbits.DACEN = 0; // Disable DAC2 module
369.
370.        DAC1CONbits.DACREF = 10;// Set reference voltage as 2*INTREF
371.
372.        DAC1CONbits.DACFM = 1;// Set data format as left justified
373.
374.        DAC1CONbits.DACTRIG = 0;// Disabling the trigger input bit
375.
376.        DAC1CONbits.DACTRIG = 0;// Disabling the trigger input bit
377.
378.        DAC1CONbits.DACSLP = 1;// Enable DAC in sleep mode
379.        DAC1CONbits.DACSIDL = 0;// Enable DAC in idle mode
380.
381.
382.
383.        _ANSG9 = 1; // Set the function of RG9 to "analog"
384.        _TRISG9 = 1; // Set RG9 as "output"
385.
386.        _ANSB13 = 1; // Set the function of RB13 to "analog"
387.        _TRISB13 = 1; // Set RB13 as "output"
388.
389.        }
390.
391.        double randn (double mu, double sigma)
392.        /* The following is from:
393.         * https://phoxis.org/2013/05/04/generating-random-numbers-from-normal-
    distribution-in-c/
394.         */
395.        {
396.          double U1, U2, W, mult;
397.          static double X1, X2;
398.          static int call = 0;
399.
400.
401.          if (call == 1)
402.            {
403.              call = !call;
404.              return (mu + sigma * (double) X2);
405.            }
```
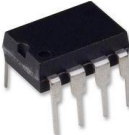
BME1634 Electrical Stochastic Resonance System

Shannon Deale

```
406.
407.         do
408.           {
409.             U1 = -1 + ((double) rand () / RAND_MAX) * 2;
410.             U2 = -1 + ((double) rand () / RAND_MAX) * 2;
411.             W = pow (U1, 2) + pow (U2, 2);
412.           }
413.         while (W >= 1 || W == 0);
414.
415.         mult = sqrt ((-2 * log (W)) / W);
416.         X1 = U1 * mult;
417.         X2 = U2 * mult;
418.
419.         call = !call;
420.
421.         return (mu + sigma * (double) X1);
422.       }
423.
424.       void DAC(void){
425.       random_number = (int) randn(0x7FFF,User_select/3);
426.       DAC1DAT = random_number;
427.       }
428.
429.       void main(void) {
430.           init();
431.           DACinit();
432.           // code pulling values from the PC will go here
433.           while(1) {
434.
435.           if (run_stop = 0)
436.           {
437.               User_select = 0x0000; // produce 0V
438.               DAC();
439.           }
440.           else{
441.
442.               User_select = 0xFFFF; // User selected value (hard coded for now)
443.               DAC();
444.               }
445.           }
446.           }
```

BME1634 Electrical Stochastic Resonance System

Shannon Deale

Appendix D

Parts for HVPSU and Modified Howland Current Pump							
Part Number	**Manufacturer**	**Price**	**Packaging**	**Suplier/ Order Number**	**Image**	**Qty**	**Cost**
TC962CPA/EPA	MICROCHIP	$4.17	DIP	Element 14 / 1467788		5.00	20.85
BAT54S	DIODES INC	$0.08	Surface Mount	Element 14 / 9526510		10.00	0.79
50ZL22MEFC5X11	RUBYCON	$0.17	Through Hole	Element 14 / 1144712		15.00	2.55
OPA244UA	TEXAS INSTRUMENTS	$2.23	DIP	Element 14 / 1097475		1.00	2.23
INA148UA/2K5	TEXAS INSTRUMENTS	$7.54	Surface Mount	Element 14 / 2782756		2.00	15.08

BME1634 Electrical Stochastic Resonance System   Shannon Deale

BC546BTF	ON SEMICONDUCTOR	$0.08	Through Hole	Element 14 / 2453787		0.00	0.00
1N914	ON SEMICONDUCTOR	$0.02	Through Hole	Element 14 / 9843817		10.00	0.23
BC556BTF	ON SEMICONDUCTOR	$0.07	Through Hole	Element 14 / 2453802		5.00	0.34
ERJ12ZYJ823U	PANASONIC ELECTRONIC COMPONENTS	$0.50	Surface Mount	Element 14 / 2323999		10.00	5.01
ERJ12ZYJ471U	PANASONIC ELECTRONIC COMPONENTS	$0.50	Surface Mount	Element 14 / 2323976		5.00	2.51
ERJ12SF1003U	PANASONIC ELECTRONIC COMPONENTS	$0.75	Surface Mount	Element 14 / 2324372		2.00	1.50
ERJ12SF3301U	PANASONIC ELECTRONIC COMPONENTS	$0.75	Surface Mount	Element 14 / 2324405		2.00	1.50

BME1634 Electrical Stochastic Resonance System   Shannon Deale

Part Number	Manufacturer	Price	Packaging	Suplier/ Order Number	Image	Qty	
C1608X5R1H104K080AA	TDK	$0.10	Surface Mount (1608)	Element 14 / 2211177		15.00	1.55
GRM1555C1H102JA01D	MURATA	$0.03	Surface Mount (1005)	Element 14 / 8819556		5.00	0.17
CKG57NX5R1H226M500 JH	TDK	$5.28	Surface Mount 5750	Element 14 / 2210741		5.00	26.40
C2012X5R1E226M125AC	TDK	$1.56	Surface Mount (2012)	Element 14 / 2525137		10.00	15.60
Total					_		$96.31
Parts for Control Circuitry (Microcontroller and Bluetooth Module)							
Part Number	Manufacturer	Price	Packaging	Suplier/ Order Number	Image	Qty	
DSPIC33FJ128GP802-E/SP	MICROCHIP	$ 6.01	DIP	Element 14 / 1676257		1	$ 6.01

BME1634 Electrical Stochastic Resonance System   Shannon Deale

Part Number	Manufacturer	Price	Mount	Suplier/ Order Number	Image	Qty	
PIC24FJ128GC006-I/MR	MICROCHIP	$ 6.92	Surface Mount	Element 14 / 2355355		1	$ 6.92
RN41-I/RM630	MICROCHIP	$ 31.06	Surface Mount	Element 14 / 2678456		1	$ 31.06
DM240015	MICROCHIP	$ 169.79	Development Kit	Mouser / 579-DM240015		1	$ 169.79
Total					–		$213.78
Parts for Control Circuitry (Isolator and Level Shift Circuitry)							
Part Number	**Manufacturer**	**Price**	**Mount**	**Suplier/ Order Number**	**Image**	**Qty**	

TRN 1-0510SM	TRACOPOWER	$28.27	Surface Mount	Element 14 / 2829856		1	$28.27
MAX4162EUK+T	Maxim	$5.92	Surface Mount	RS / 7327908		1	$5.92
Total							$34.19
Grand Total							$344.28